UNIT HYDROGRAPH ESTIMATION USING DIGITAL DRAINAGE MODEL FOR APPLICABLE TEXAS WATERSHEDS

A Thesis

Presented to

the Faculty of the Interdisciplinary Graduate Program

in Environmental Engineering

University of Houston

In Partial Fulfillment

of the Requirements for the Degree

Doctor of Philosophy

in Environmental Engineering

by

Xin He

December 2007

UNIT HYDROGRAPH ESTIMATION USING DIGITAL DRAINAGE MODEL FOR APPLICABLE TEXAS WATERSHEDS

_____

Xin He

Approved:

_____

Chairman of the Committee
Theodore Cleveland, Associate Professor,
Civil and Environmental Engineering

Committee Members:

_____

K.H. Wang, Professor,
Civil and Environmental Engineering

_____

William Dupre, Associate Professor,
Department of Geosciences

_____

Jerry R. Rogers, Associate Professor,
Civil and Environmental Engineering

_____

C. Richard Liu, Professor,
Electrical and Computer Engineering

_____

Larry C. Witte, Associate Dean,
Cullen College of Engineering

_____

C. Vipulanandan, Professor and Chairman,
Civil and Environmental Engineering

ACKNOWLEDGEMENTS

This research was funded by the Texas Department of Transportation (TxDOT), I am grateful for their cooperation and the financial support. Also I want to thank the other members in the research group, Texas Tech University, Lamar University, and U.S. Geological Survey (USGS), especially thanks to Dr. William Asquith, Meghan Roussel, and Amanda Garcia all at the U.S. Geological Survey, Texas Water Science Center, Austin, Texas.

I would like to thank my professor Dr. Cleveland without whom I couldn't even stand here. He has always given me ideas and encouragement for my work, and he has been such a wonderful professor to work with. I would also like to extend my thanks to Dr. Dupre, Dr. Liu, Dr. Wang and Dr. Rogers for taking time from their busy schedules to serve on the committee.

Six years ago, the same time, I came to USA, knowing nothing about hydrology, and having no idea of what I want to be. It was Dr. Cleveland who taught me so much, and gave me the opportunity to learn. In china we have an old saying that, "He who teaches me may be considered my father-figure for life". Soon I will leave this school, becoming a real engineer. I hope I can be one of the students he will feel proud of.

Also, I extent my thanks to all the teachers and professors I have met from my elementary school till my graduate school. Without their patience and guidance, I would not achieve my doctoral degree today. I want to include some names here: Wenhong Deng, Mingying Wang, Haihui Yang, Guifang Li, and Dr. Cleveland, who have always inspired me to go for my dream.

I want to thank to my colleges, Thuy, Abhijeet, Williams, and the previous students worked here: Edd, Kp, Ioana, Matt, Robert and Samuel, everyone I met in our lab, they always keep me accompany, give me advices, encouragement and who also teach me how to understand and make American jokes. It's been really nice to work with all of them.

Finally I want to dedicate this thesis to my dear parents. My dad Guohua He, and my mom Xiufen Gu who gave me the most support, and always set me good examples in my life. They gave me the best love of the world. They are the best parents, my best teachers and best friends forever.

UNIT HYDROGRAPH ESTIMATION USING DIGITAL DRAINAGE MODEL FOR APPLICABLE TEXAS WATERSHEDS

A Thesis

Presented to

the Faculty of the Interdisciplinary Graduate Program

in Environmental Engineering

University of Houston

In Partial Fulfillment

of the Requirements for the Degree

Doctor of Philosophy

in Environmental Engineering

by

Xin He

December 2007

ABSTRACT

Surface runoff and streamflow along with groundwater are the components of the hydrologic cycle that are typically of the most interest to water resources engineers. Watershed models are mathematical representations of hydrologic processes which partition precipitation into abstractions and runoff to streams. Such modeling requires the estimation of specific time-response characteristics of watershed. In the absence of observations, these characteristics are estimated from watershed physical characteristics. An exploratory assessment of a particle-tracking approach for parameterizing unit hydrographs from topographic information for applicable Texas watersheds is presented.

The study examined 92 watersheds in Texas, for which rainfall and runoff data were available. Drainage areas ranged from approximately 0.25 to 150 square miles; main channel lengths ranged from approximately 1 to 50 miles; and dimensionless main channel slopes ranged from approximately 0.0002 to 0.02.

Unit hydrographs based entirely on topographic information were generated and used to simulate direct runoff hydrographs from observed rainfall events. These simulated results were compared to observed results to assess method performance. Unit hydrographs were also generated by a conventional analysis (of the observed data) approach to provide additional performance comparison.

Three loss models were selected to produce the effective runoff. They are the

fractional loss model (FRAC), the initial abstraction constant loss model (IACL) and the Green-Ampt infiltration loss model(GAIN). The results show that loss models have minor effects on the timing parameters of hydrograph.

The final results demonstrate that the procedure is a reasonable approach to estimate unit hydrograph parameters from a relatively minimal description of watershed properties, in this case elevation and a binary development classification. The method produced unit hydrographs comparable to those determined by conventional analysis and is a useful synthetic hydrograph approach.

TABLE OF CONTENTS

LIST OF FIGURES

FIGURES **Page**

LIST OF TABLES

TABLES **Page**

LIST OF SYMBOLS

A Area

CHAPTER 1

INTRODUCTION

1.1. Background

Estimation of representative runoff hydrographs from design storms is an important component of hydrologic engineering. The goal is important because these "design hydrographs," in general, and the peak stream flow of a design hydrograph, in particular, are critical for cost-effective, risk-mitigated design of drainage structures such as bridges, culverts, roadways, and other infrastructure.

From 2001–2007, the University of Houston, Texas Tech University, Lamar University, and the U.S. Geological Survey (USGS), in cooperation with the Texas Department of Transportation (TXDOT) in a peer-to-peer association (TXDOT Research Projects 0–4193, 0-4696, and 0-5822) investigated rainfall and runoff behavior from 92 USGS streamflow-gaging stations (watersheds) to enhance design hydrograph estimation for applicable watersheds in Texas. The locations of the stations are shown in Figure 1.1. In the figure, the stations in Houston have been studied but were not studied by the remainder of the research team (other institutions). Appendix 1, Table 1 lists the station's identification code, common name, latitude, longitude, and total drainage area as reported in Asquith and others (2004) for the central Texas stations and from Liscum (1998) for the Houston stations.

Design hydrographs ideally should mimic the general volume, peak streamflow, and shape of observed runoff hydrographs. Design hydrographs often are produced using unit hydrographs. Among some other concepts, runoff hydrograph estimation by the unit

hydrograph method requires (1) a rainfall hyetograph that represents rainfall intensity of a storm over time on a watershed and (2) a method to convert this hyetograph into an appropriate excess rainfall hyetograph. This conversion from rainfall to excess rainfall is made by a watershed-loss model. There are two general classes of watershed-loss model: non-time and time distributed. A non-time distributed model is appropriate when only total runoff volume and not an actual runoff hydrograph is required for a particular circumstance. This class effectively is not considered further in this dissertation other then its mention in the literature review.

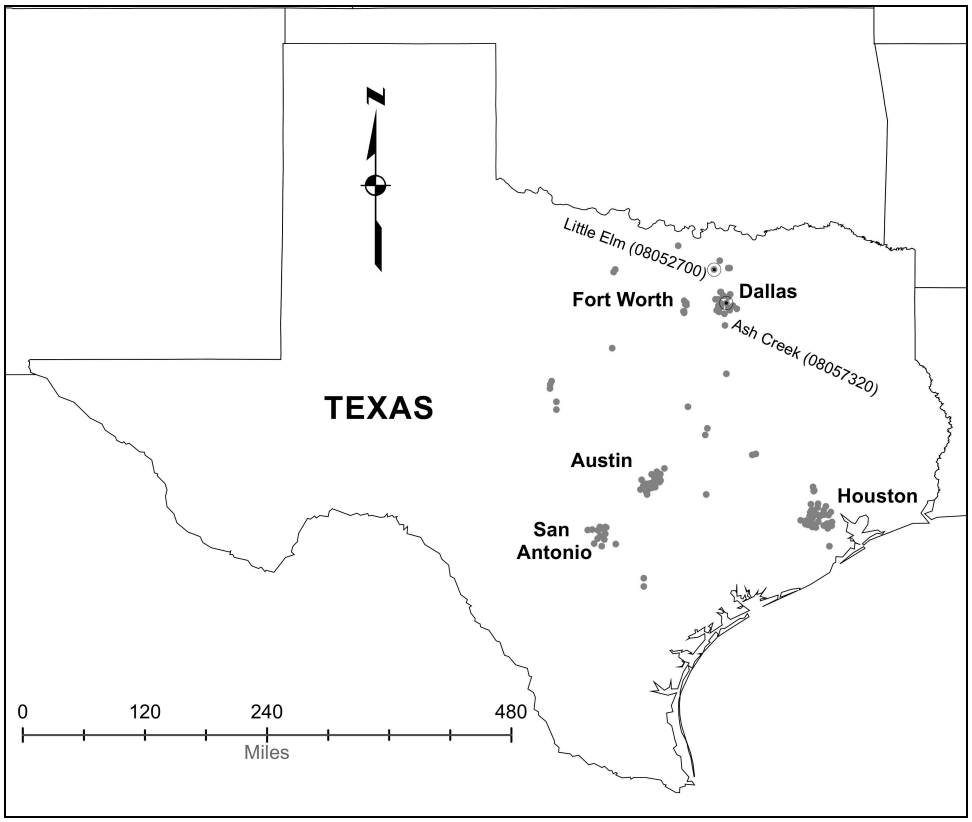

Figure 1.1 Locations of U.S. Geological Survey streamflow-gaging stations in Texas used in analysis of unit hydrographs, and loss models

(from Cleveland, He, Thompson, Fang, 2007).

Time-distributed, watershed-loss models on the other hand are required when an analyst requires a design hydrograph. When the design storm hyetograph is combined with a time-distributed watershed-loss model, an excess rainfall hyetograph results. When the resulting design excess rainfall hyetograph is "convolved" with the unit hydrograph, the runoff hydrograph of the design storm is produced. In particular, the time-distributed, watershed-loss model should be mathematically consistent in structure or general form with hypothesized processes it should also be at about the same level of complexity as the unit hydrograph model.

Figure 1.2 is a schematic of the modeling approach just described. In the figure the watershed of interest is the elongated ellipse just above the outflow hydrograph. Above this watershed are two ovals that represent, in a signal processing context, two filters.

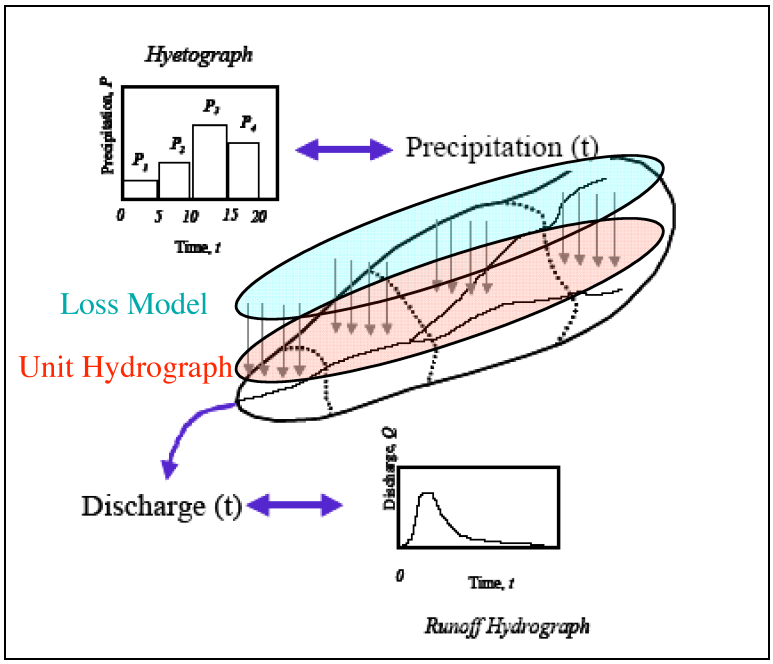

Figure1.2. Schematic of Rainfall-Runoff Modeling

(from Cleveland and Asquith, 2007)

From the top down, the filters are the loss model and the unit hydrograph model; the loss model accounts for the proportion of the rainfall that is lost and the proportion that becomes available for runoff and the unit hydrograph model redistributes in time, that incoming proportion of rainfall that is available for runoff.

1.2. Purpose and Scope

Unit hydrographs are developed for a specific watershed using two basic approaches. If unit rainfall-runoff data are available, then numerous techniques can be applied to estimate a unit hydrograph from the data. If no data are available, then methods of synthetic hydrology must be applied. Current practice is regionalization of measured behavior. Methods of regionalization are used to transfer known hydrographs (or other hydrologic entities) from a location where measurements are available to unmonitored watersheds. The regionalization involves determining time parameters for the unit hydrograph procedure, and time parameters may include time to peak, time base, or time of concentration. It also involves development of regional regression equations for time parameters, watershed and/or rainfall characteristics.

The principal elements required for the approach are the determination of characteristic loss features (loss model) and characteristic response time (unit hydrograph model). Even the temporal redistribution is performed using hydraulic models, which is certainly feasible and often the most appropriate approach, there is still the need to understand how to convert the rainfall signal into an excess rainfall signal, and this will be accomplished with some kind of loss model. In the collective research as well as in the literature the losses are correlated with watershed soil properties, while the

characteristic response time is associated with physical characteristics such as areas, slopes, characteristic lengths, and characteristic velocities.

The objective in this dissertation is to examine a unit hydrograph parameterization method based on topographic information, a simple motion equation, and correspondingly simple loss models to predict the runoff volume, rate and timing with minimal watershed characterization using data readily available to drainage engineers, and compare the performance of this approach to the current practice.

1.3. Dissertation Structure

This dissertation, in addition to presenting the exploratory work based on terrain modeling and the examination of three loss models, also summarizes nearly five years of effort by the research team, including significant involvement by the author. As such, the dissertation contains several major, but co-dependent, elements:

1. A summary of the conventional unit hydrograph approach used in the research that both to supports the TxDOT funded research goals as well as provides the comparative behavior to evaluate the terrain-model approach. The summary includes discussion of the timing parameter that contains all the information of watershed response; its computation and estimation are vital to the use of unit hydrographs.
2. A summary of the loss modeling approach used in the research, both in the context of the TxDOT funded research and its eventual application in synthetic hydrograph generation.

3. A description of the digital terrain runoff model (DTRM) that is the principal exploratory component of the research. This model attempts to determine the watershed timing parameter from elevation arrays only and minimal other watershed description. The DTRM is an alternative to conventional single-metric based unit hydrographs and its performance is evaluated in the context of the conventional unit hydrograph approach.
4. A statistical analysis of DTRM performance as compared to the conventional approach as well as suggestions for future modifications to improve the DTRM as a research tool.
5. Appendices that present supporting details regarding the dissertation.

1.4. Contents of the Dissertation

The remainder of this dissertation is outlined as follows. Chapter 2 is a literature review related to unit hydrographs and the importance of timing parameters. Chapter 3 is a review of prior studies related to loss modeling as well as the selection of the simplified loss models chosen for this research. Chapter 4 presents a description of the conventional analysis used in this research where a particular loss model is combined with the unit hydrograph model for the study watersheds and the underlying parameters are estimated. Regionalization results are presented in this chapter. Chapter 5 provides the detailed description of digital terrain runoff model (DTRM) as an alternative to regionalization for the unit hydrograph portion of rainfall-runoff modeling, and presents the results and comparison with conventional unit hydrographs. Finally, the conclusions and future study was summarized in Chapter 6.

CHAPTER 2

UNIT HYDROGRAPHS AND TIMING

Practical runoff prediction using hydrological concepts has been practiced for at least a century. The approach is to determine the runoff hydrograph from a precipitation hyetograph for a specific watershed. The procedures used prior to the 1940's were largely empirical ad-hoc models of the rainfall runoff process. It was recognized in the 1850's that runoff was related to rainfall intensity, rainfall duration (i.e. the hyetograph), and to the time required for runoff to leave a watershed. Furthermore at that time it was also recognized that the watershed's "time" characteristic was related to its slope, area, and shape. J.C.I. Dooge, who established the basis for application of linear systems theory to hydrograph analysis, and was the first to establish the theoretical basis for unit hydrographs, credits this early understanding of runoff behavior and the subsequent development of the rational method to T.J. Mulvaney in 1851 (Dooge, 1959; 1973). To date, the focus of runoff prediction has been to determine how to relate morphological and topographic characteristics to watershed response. It is as yet a largely unsolved problem (in the practical sense); yet good simple approximations are available.

In this chapter, there is a literature review about unit hydrographs, from the definitions to the factors which affect the shape of hydrograph, and the estimations of timing parameters. Also this chapter will discuss the previous study about geomorphic unit hydrograph (GUH), which leads to the concept of the digital terrain runoff model (DTRM) used in this research.

2.1 Unit Hydrograph

Unit hydrograph (UH) is the hydrograph resulting from the unit excess rainfall uniformly over the watershed at a uniform rate during a given period of time. The definition was first proposed by Sherman in 1932, up till today it is still considered as a standard-of-practice in hydrologic engineering. The major advantage in unit hydrograph theory is the linearity, when a unit hydrograph is determined for a basin, thus the response to any other storm can be obtained by linear combinations. The basic assumptions of unit hydrograph theory are:

- Effective rainfall or rainfall excess has a constant intensity within the effective duration,
- Effective rainfall is uniformly distributed spatially,
- Time base of runoff (period of time that direct runoff exceeds zero) resulting from an effective rainfall of specific duration is constant,
- The ordinates of direct runoff of a constant base time are directly proportional to the total amount of direct runoff represented by the hydrograph (linearity), and
- For a particular watershed, the size of the direct runoff hydrograph for two effective rainfall pulses is in direct proportion to the relative size of the pulses.

In fact, these assumptions are often not true, particularly for small watersheds, which have a strong tendency towards non-linear response. However, the unit hydrograph approach is usually good enough to obtain engineering estimates for design purposes with circumstances. Sherman's unit hydrograph procedure should be used with

watershed drainage areas that are less than about 2,000 square miles. For larger area, the UH can still be applied by subdividing the watershed into smaller sub-watersheds and each of those subjected to a hydrograph analysis. UH can be expressed as:

$$q(t) = \int_0^T r(\tau) f(t-\tau) d\tau \qquad (2.1)$$

Where *q(t)* is unit discharge from a basin at time t, *r(t)* is an input function that represents either rainfall or excess rainfall, $f(t-\tau)$ is a response function (the unit hydrograph), and *T* is the duration of the input. Equation 2.1 assumes that basins respond as linear systems and this assumption is the main criticism of unit hydrograph theory. Despite this criticism, unit hydrographs are used to estimate streamflow from relatively small basins, typically for engineering purposes and often produce reasonable results. With the linearity assumption, the response $f(t-\tau)$, has the same properties as a probability density function. Specifically, it integrates to unity on the range $(-\infty,\infty)$, and $f(t-\tau) \geq 0$ for any values of $(t-\tau)$.

2.2. Factors Affecting Hydrographs

Before time parameters are examined, it is informative to briefly discuss the factors affecting hydrograph components such as shape and peak discharge. The factors that affect hydrograph shape can generally be grouped into climatic factors and physiographical factors. Each of the groups contains a host of factors and the important ones are discussed below:

1. Size of the basin: Small basins behave differently from the large basins in terms of the relative importance of various phases of the runoff phenomenon. In small

basins the overland flow phase is predominant over the channel flow. Hence the land use and intensity of rainfall have important role on the peak discharge. In large basins these effects are suppressed as the channel flow phase is more important (Subramanya, 1984).

2. Slope of the channel and slope of basin: The slope of the main stream controls the average velocity of flow. As the recession limb of the hydrograph represents the depletion of storage, the channel slope has a pronounced effect on this part of the hydrograph. Larger channel slopes give rise to quicker depletion of storage and hence result in steeper recession limbs of hydrographs. This results in smaller time bases. The basin slope is important in small catchments where the overland flow is relatively more important. In such cases the steeper slope of the catchment results in larger peak discharges (Subramanya, 1984).

3. Shape of the basin: The shape of the basin influences the time required for water to travel from the distant parts of the basin to the outlet of a basin. Thus the occurrence of the peak and hence the shape of the hydrograph are affected by the basin shape. Fan shaped or nearly semi-circular shaped catchments give high peak and narrow hydrographs while elongated catchments give low-peaked and broad hydrographs (Subramanya, 1984).

4. Drainage density: The drainage density is defined as the ratio of the total channel length to the total drainage area. A large drainage density creates a situation conducive for quick disposal of localized runoff down the channels. This fast response is reflected in a pronounced peak discharge. In basins with smaller

drainage densities, the overland flow is predominant and the resulting hydrograph is squat with a slowly rising limb (Subramanya, 1984).

5. Land use: Vegetation and forests increase the infiltration and storage capacities of the soils. Further, each causes considerable retardance to the overland flow. Thus, vegetative cover reduces peak discharge. This effect is usually very pronounced in small catchments of areas less than 150 km^2 (58 $mile^2$). Further, the effect of the vegetative cover is prominent in small storms. In general, for two catchments of equal area, other factors being identical, the peak discharge is higher for a catchment that has a lower density of vegetative cover (Subramanya, 1984).

6. Intensity of rainfall: Among the climatic factors, intensity, duration and direction of rainfall movement are the three important ones affecting the shape of hydrograph. For a given duration, peak and volume of the surface runoff are essentially proportional to the intensity of rainfall. Rain intensity has substantial influence on runoff. If the intensity of rain increases, the runoff increases rapidly (Subramanya, 1984).

7. Duration of rainfall: The duration of rainfall of given intensity also has a direct proportional effect on the volume of runoff. The effect of duration is reflected in the rising limb and peak discharge (Subramanya, 1984).

8. Rainfall movement: If the rainfall moves from upstream of the catchment to the downstream end, there will be the quicker concentration of flow at the basin outlet. This results in a peaked hydrograph. Conversely, if the storm movement is up the catchment, the resulting hydrograph will have a lower peak and longer time base (Subramanya, 1984).

2.3 Hydrograph Timing Parameters

Some of the timing parameters for the unit hydrograph are travel time, time of concentration and time to peak. However there is a difficulty in defining and quantifying the timing parameters for unit hydrograph, and sometimes the same parameter may have different definitions or multiple meanings, and this increases confusion for applying it in hydrologic design definitions.

Travel Time

The conceptual definition is that travel time (T_t) is the time a water parcel takes to travel from one location in a watershed to another location downstream. The travel may occur on the ground surface or below it or in a combination of the two (Kent, 1972). This definition implicitly assumes that the two points are hydraulically connected. The travel time is expected to be a function of positions of two points in a watershed (NRCS, 1972; Viessman and Lewis 2002; Garg, 2001). T_t is affected by storage, hydraulic factors, flow paths, and flow types (overland flow or channel flow).

Time of Concentration

The conceptual definition for the time of concentration (T_c) is the time it takes a water parcel to travel from the hydraulically most distant part of the watershed to the outlet or reference point downstream. This definition has been used for many hydrologic studies and applications (NRCS, 1972; Kirpich, 1940; USCE, 1966; Bell and Kar, 1969; Schultz and Lopez, 1974; McCuen et al., 1984; Subramanya, 1984; Garg, 2001; Ben-Zvi, 1984; Huber, 1984; McCuen, 1998).

In hydrograph analysis, the time of concentration is the time difference between the end of rainfall excess and the inflection point of a hydrograph where the recession curve begins as shown in Fig. 2.1 (NRCS, 1972; Kirpich, 1940; USCE, 1966; McCuen et al., 1984; Bell and Kar, 1969; Schultz and Lopez, 1974). The inflection point is the point on the hydrograph recession limb that directs runoff ceases (Fig. 2.1). Another slightly different definition uses the time from the centroid of rainfall excess to the inflection point of the hydrograph (Fig. 2.1). The definition in this context is an "analysis based" approach and has been used for many hydrologic studies and applications (McCuen et al., 1984; Subramanya, 1984; Garg, 2001; Huber, 1984; McCuen, 1998). These analysis based definitions are useful to quantify T_c when rainfall-runoff data are available.

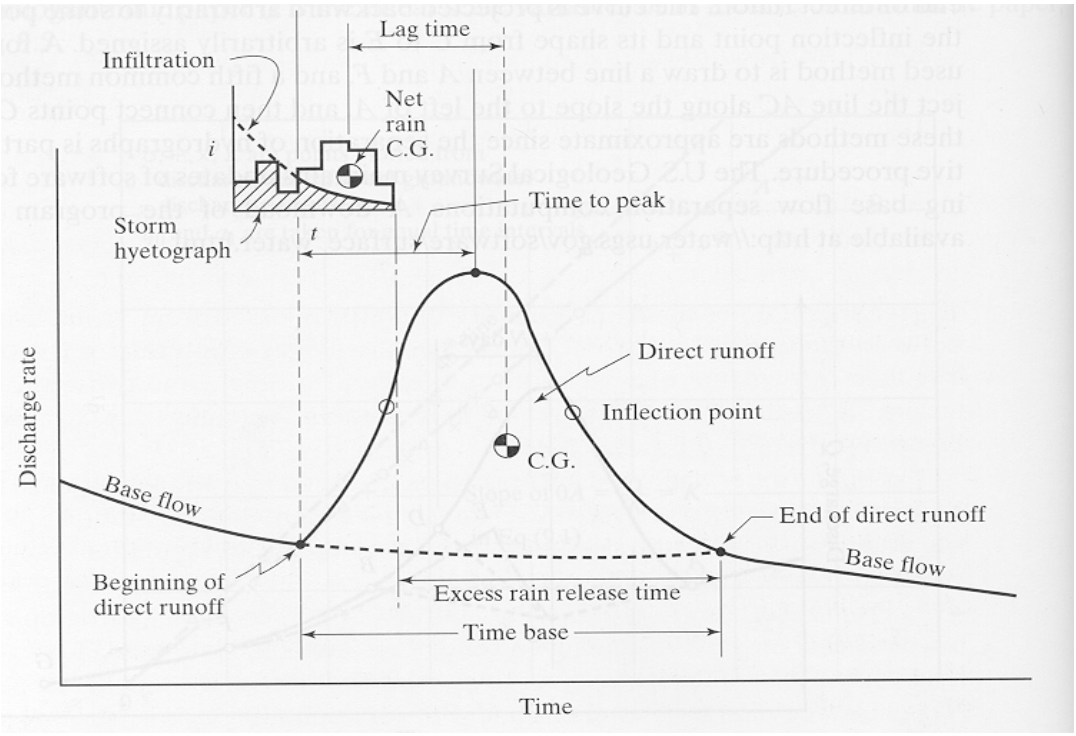

Figure 2.1. Hydrograph time relationships and time parameters of hydrograph (from Viessman and Lewis, 2002).

Excess-Rainfall Release Time

The excess-rainfall release time (T_e) is defined as the time required for the last, most hydraulically remote drop of excess rain that fell on the watershed to pass the outlet, signaling the cessation of direct runoff. T_e can be easily determined as the time interval between the end of rainfall and the end of direct runoff as the excess-rainfall release time (Fig. 2.1). This definition is often preferred because few storm durations (especially for large watersheds) exceed the time of concentration, making determination of T_c possible only by examination excess rain recession (Viessman and Lewis, 2002).

The time of concentration is often equated with the excess-rainfall release time because the time for runoff to arrive at the outlet from the most hydraulically remote point after rain ceases is assumed to be indicative of the time required for 100 percent contribution from all points during any uniform storm having sufficient duration (Viessman and Lewis, 2002). It is worth to point out that the definition of T_c for hydrograph analysis (end of excess to inflection point) contradicts to the definition of T_c as the excess-rainfall release time. Excess-rainfall release time as estimation of T_c is always longer than time to inflection as T_c since the end point of the excess-rainfall release time is always later.

Wave Travel Time

The wave travel time (T_w) is the time it takes a shallow wave in the channel to propagate from one location to another. This surface wave celerity is faster than the average flow velocity and varies with channel shapes and other factors. For rectangular channel, the wave travel time is approximately 5/3 of the average velocity of flow

(Viessman and Lewis, 2002). This parameter is important to hydrograph routing in streams.

For hydrograph analysis, Viessman and Lewis (2002) point out that the last drop of direct runoff to pass the outlet, conceptually travels over the surface at the speed of a small surface wave, rather than a speed equal to the average velocity of flow. They also stated that both wave travel time and excess-rainfall release time are often used synonymously with time of concentration.

Time to Equilibrium

If an inflow of excess rainfall continues at a steady rate for an indefinite period of time the outflow continues to increase and its value asymptotically approaches the value of the inflow. The time elapsing before there is no significant difference between inflow and outflow (usually less than 3%) is called the "time to equilibrium" (Bell and Kar, 1969). Even though these conditions rarely occur in nature and it is not usually possible to determine the time of equilibrium (T_{eq}) form rainfall-runoff data, the concept has been found useful, for example, in deriving S-hydrographs (Viessman and Lewis, 2002). The time to equilibrium (maximum discharge of S-hydrograph in Fig. 2.2) is equal to the time base of the unit hydrograph (T_b) minus the duration of the unit hydrograph (D) (Viessman and Lewis, 2002).

$$T_{eq} = T_b - D = T_e \qquad (2.2)$$

This is the same as the excess-rainfall release time shown in Fig. 2.1. When kinematic wave theory is used to model overland flow over planes or different shapes of watersheds, the maximum discharge equals rainfall intensity times plan or watershed area

to indicate 100 percent contribution of runoff to the outlet, therefore, time to equilibrium was treated as synonymous with time of concentration (Overton and Meadows, 1976). Based on above definition, for turbulent flow, Overton and Meadows (1976) stated that

$$T_c = 1.6T_L\,(lag\ time) \tag{2.3}$$

In which is close to NRCS relationship. Izzard (1946) defined the equilibrium time as the time interval required for the runoff rate to become equal to the supply rate. This definition was also used by Morgali and Linsley (1965) and Wei and Larson (1971).

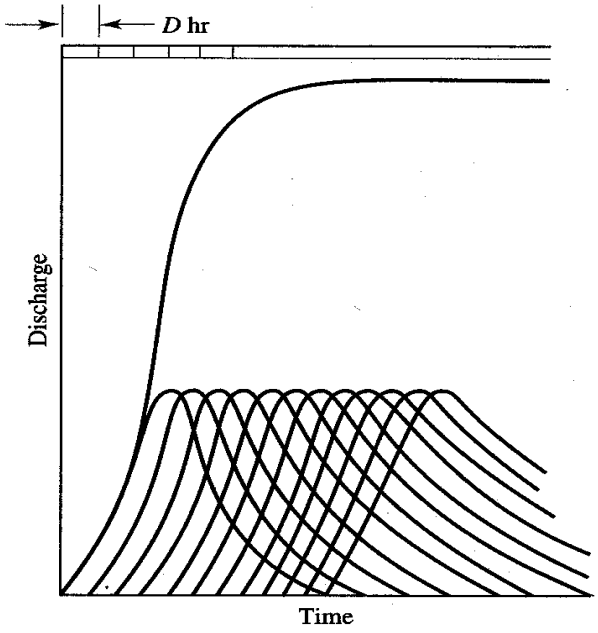

Figure 2.2. S-hydrograph developed by lagging of known *D* hour UH for infinite times (from Viessman and Lewis, 2002).

Lag Time

Though direct runoff begins with the commencement of excess rainfall (Fig. 2.1), the largest portion of runoff generally lags the rainfall because it takes time for runoff to

travel from any location within the watershed to the outlet. The lag time has been used widely for many hydrological studies and applications; there are several definitions used to develop different hydrological procedures (Rao and Delleur, 1973).

The basin lag time is most often defined as the difference in time from the center of mass of rainfall excess to the center of mass of direct runoff produced by the net rain (Carter, 1961; Espey et al., 1966; Viessman and Lewis, 2002), and it is shown in Fig. 2.1 and as T_4 in Fig. 2.3. This definition is used for many hydrological studies and applications (Horner and Flynt, 1936; Mitchell, 1948; Bell and Kar, 1969; Askew, 1970; McCuen, NRCS, 1972; Schulz and Lopez, 1974; Subramanya, 1984; Wong and Rawls, 1984; Simas and Hawkins, 1996; Viessman and Lewis, 2002). The single linear reservoir theory (Chow, 1964) indicated that the reservoir constant K should be equal to the lag time (T_4).

The second definition of the basin lag time is the time from the center of mass of the rainfall excess to the peak discharge rate on the hydrograph (T_1 in Fig. 2.3) and used by Eagleson (1962), Bell and Kar (1969), Rao and Delleur (1973), and Schulz and Lopez (1974). The third definition is the time interval from the maximum rainfall rate to the peak rate of runoff (Viessman and Lewis, 2002). USBR (1965) and Wilson (1972) defined the lag time as the centroid of rainfall excess and the time when 50 percent of the direct runoff has passed the gaging station (T_5 in Fig. 2.3). Wilson (1972) also defined the lag time as the time interval between the beginning of rainfall excess and the centroid of direct runoff hydrograph.

Linsley et al. (1958) used the average lag time T_3 (Fig. 2.3) starting from the beginning to the centroid of the direct runoff and related it to the length of the main

stream (L), the distance along the main stream from the basin outlet to a point opposite the centre of the gravity of the basin in miles (L_{ca}), and the mean basin slope S: $T_3 \sim a(L L_{ca} / \sqrt{S})^b$.

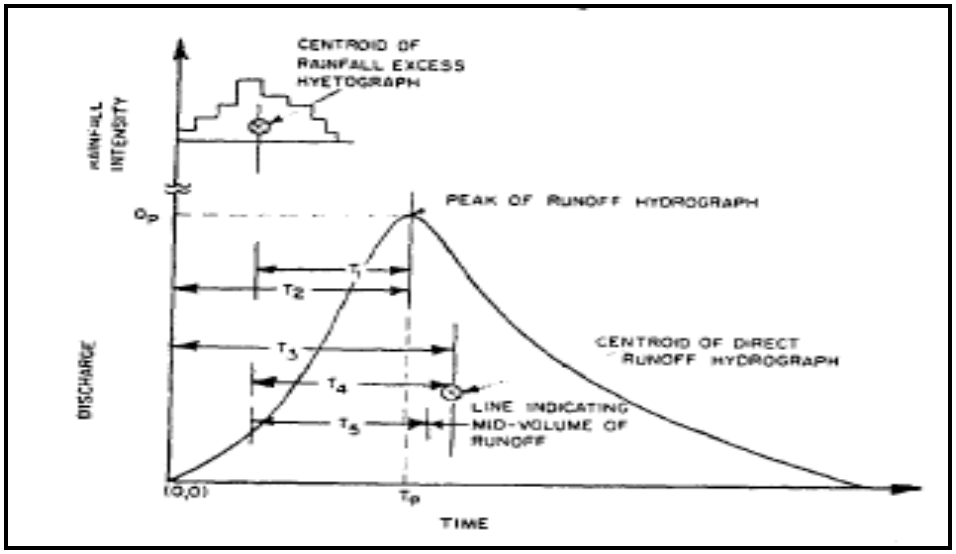

Figure 2.3. Different lag time definitions (adopted from Rao and Delleur, 1973).

Time to Peak

The time to peak is the time from the beginning of direct runoff (or rainfall excess) to the peak discharge in a simple (single peak) hydrograph (Fig. 2.1 and T_2 in Fig. 2.2), and is used in many hydrologic applications (Linsley et al., 1958; Askew, 1970; NRCS, 1972, Schulz and Lopez, 1974; McCuen et al., 1984). Sometimes it is called the rise time of the hydrograph (Ramser, 1927; Kirpich, 1940; Gray, 1961; Wu, 1963; Bell and Kar, 1969). It is also defined as the time interval between the centroid of rainfall excess and the peak of the direct runoff as depicted as T_1 in Fig. 2.2 (Snyder, 1938; Taylor and Schwarz, 1952; Eagleson, 1962; Schulz and Lopez, 1974). Lopez (1973) used the time interval between the beginning of rainfall and the peak discharge of the

direct runoff as the time to peak. Time to peak and peak discharge are two most significant parameters we exam in this research.

Duration of Excess Precipitation

The duration of rainfall excess (D) is the time from beginning to end of an excess precipitation during a rainfall event. This duration is typically used as the duration of a unit hydrograph, and is always shorter than the duration of a storm due to initial rainfall abstraction as indicated in Fig. 2.1.

Time Base of a Runoff Hydrograph

The time base of a runoff hydrograph (T_b) is the elapsed time from the beginning of direct runoff until the return to baseflow (the direct-runoff component reaches zero) (Fig. 2.1). Time base for a unit hydrograph becomes important for some synthetic UH procedures (e.g. Snyder, 1938).

2.4 Previous Study

Given a record of storm rainfall and runoff, a "traditional method" (Viessman and Lewis, 2003) can be applied to the whole storm to extract the unit hydrograph of the watershed for that storm. The traditional method does not use the sophisticated mathematics like Gamma unit hydrograph or Rayleigh Unit hydrograph. The traditional method is an approach used by analysts prior to development of more computationally sophisticated techniques for computing unit hydrographs from observed rainfall and runoff data for a watershed. It usually comprises three steps:

1. Base flow was abstracted from the runoff hydrograph to produce the direct runoff hydrograph. Base flow generally is small in comparison to total direct runoff.
2. The area under the direct runoff hydrograph is numerically integrated using the trapezoid rule to compute the total direct runoff.
3. Each ordinate of the direct runoff hydrograph is divided by the total direct runoff. A hydrograph with unit depth is produced-the unit hydrograph.

Traditionally, as suggested by Sherman (1932) and explained in many references, the UH of a watershed is derived from observed runoff and rainfall records. For ungaged watersheds, such data are unavailable, and synthetic methods are used to infer the unit hydrograph. These methods vary in how the geomorphic information from the watershed is incorporated to produce estimates of the unit hydrograph.

Several methods have been developed for estimating synthetic unit hydrographs for locations where observations of input and response are lacking. Chow (1988) grouped synthetic unit hydrographs into three types: (1) those relating hydrograph characteristics (peak flow, time to peak, base time, etc.) to watershed characteristics (Synder, 1983; Gray, 1961); (2) those based on conceptual models of watershed storage (Clark, 1943; Nash 1957); and (3) those based on a dimensionless unit hydrograph (DUH) (Soil Conservation Service 1972). Type 1 and 2 involve empirical coefficients whose validity is limited to a particular watershed or region. Type 3 is based on the expectation that, by selecting proper dimensionless ratios, all individual unit hydrographs can be transformed into a more-or-less universally applicable DUH.

Clark (1945) developed a method for generating unit hydrographs for a watershed based on routing a time-area relationship through a linear reservoir. Excess rainfall covering a watershed to some unit depth is released instantly and allowed to traverse the watershed and the time-area relation represents the translation hydrograph. The time-area relationships are usually inferred from a topographic map. The linear reservoir is added to reflect storage effects of the watershed. Clark's method clearly attempts to relate geomorphic properties to watershed response.

Leinhard (1964) derived a unit hydrograph model using a statistical-mechanical analogy and two important assumptions. The first is that the travel time taken by an excess raindrop landing on the watershed to the outlet is proportional to the pathline distance that the raindrop must travel. The second assumption is that the area swept by any characteristic distance is proportional to some power of that characteristic distance. Dimensionally, the ratio of the travel time to path length would be a characteristic velocity. Lienhard's derivation did not attempt to relate watershed properties that might appear on a map to the hydrologic response, but the connection was implied.

Rodriguez-Iturbe and Valde (1979) and Gupta and others (1980) examined the structure of unit hydrographs conceptualized as residence time distributions from a geomorphic perspective and provided guidance to parameterize the hydrographs in terms of Horton's bifurcation ratio, stream length ratio, and stream area ratio and an independently specified basin lag time. In those works the result was called a geomorphic unit hydrograph (GUH). Like Leinhard's derivation the relationships of path, path length, and travel time are fundamental in the development of the unit

hydrographs. Furthermore, all these derivations rely on the concept of representing the excess rainfall as an ensemble of particles distributed on the watershed.

Kirshen and Bras(1982) developed a watershed discharge hydrograph simulation model based on the hydraulically based geomorphologic instantaneous unit hydrograph. The IUH is interpreted as the probability density function (PDF) of the travel time that a drop of water, landing anywhere in the watershed, takes to reach the outlet. Kirshen and Bras (1983) investigated the assumption of the exponential travel-time distribution and proposed instead a time distribution based upon the linearization of equations of motion, the solution of which was developed by Harely (1967).

Jin(1992) developed a GUH based on a gamma-distribution and suggested a way to parameterize the distribution based on path types and a streamflow velocity. Like the prior work, the concept of distance, velocity and time was crucial. In Jin's GUH the initial estimate of velocity was based on a peak observed discharge for a basin, thus some kind of streamflow record was required, or some estimate of bankflow discharge would be required.

Maidment (1993) developed a GIS-based approach using the classical time-area method and GIS scripts. Muzik (1996) approached the time-area modeling in a similar fashion. These works used flow routing based on a constant velocity or subjectively predetermined velocity map independently incorporating concepts of a GUH.

Kull and Feldman (1998) assumed that travel time for each cell in the watershed was simply proportional to the time of concentration scaled by the ratio of travel length of the cell over the maximum travel length. Thus the velocity from any point to the outlet is uniform and constant. Each cell's excess rainfall is lagged to the outlet based on the

travel distance from the cell. Travel time in overland and channel flow are determined beforehand. This approach is essentially a version of Clarks (1945) methodology and is implemented in HEC-GEOHMS (HEC 2000).

Saghafian and Julien (1995) derived a GIS-based time-to-equilibrium approach for any location on a watershed based on a uniform overland flow model, which incorporated elevation information. Saghafian and others (2002) used this concept to develop a time-variable isochrones GIS technique to generate runoff hydrographs for non-uniform hyetographs (non-uniform in space and time).

Lee and Yen (1997) recognized that a kinematic-wave model could be used to estimate travel times over a path to the watershed outlet and developed a procedure to parameterize a GUH by relating slope along a set of planes defined by stream order that are linked to each other at the watershed outlet.

Oliver and Maidment (1999) developed a raster-based, spatially distributed routing technique based on a first-passage-time response function (a gamma-type unit hydrograph at the cell scale).

Common to all these methods is the use of spatially distributed topology, but they all require some independent evaluation of overland versus channel flow to route from cell to cell. For example, HEC-HMS modelers will need to determine a time-of-concentration value; Olivera and Maidment (1999) work appears to need response function parameters in advance of analysis, Saghafian and others (2002) require regression equations to relate channel geometry to flow for the channel routing component of their analysis. Also common to these methods is the concept of

accumulating flows cell-by-cell and determining the travel time from the outlet back to the contributing area.

In all these previous studies it is clear that the time-area relationship is incorporated either directly as a hydraulic relationship (constant velocity, CN-based velocity, kinematic-wave) or indirectly as a ratio of grid travel time to time of concentration. Thus it is concluded that specification of some meaningful grid kinematics based on hydraulic considerations can provide a technique to directly determine T_c and T_p.

The literature review on regionalization of timing parameters was important to develop timing parameters of ungaged watersheds. Many empirical equations have been developed from various databases and watersheds to estimate timing parameters. These equations are based on correlations with various watershed and/or rainfall characteristics. Some investigators also developed equations to compute timing parameters from other timing parameters. The particle tracking method proposed in this research uses the digital elevation model and provides an independent verification on computation of time of concentration.

CHAPTER 3

LOSS MODELS

3.1 Introduction

The physical loss processes include evaporation (as well as evapotranspiration) and infiltration into the soil. The physical storage processes include storage in a thin layer of water covering a watershed (that eventually evaporates), as well as water sequestered in ponds, lakes, reservoirs, potholes, and so forth. In the regulating structures (ponds, detention basins, reservoirs) changes in storage can be measured and quantified. Pothole storage and similar mechanisms are at best a guess. For hydrologic response prediction at the storm-length temporal scale, these two components are often lumped into a single loss term; this aggregation is a simplification that makes data management simpler in the context of design, however this loss term is significant because it is the term in the volume balance that actually governs (mathematically) the runoff component. This chapter we will discuss the procedure of loss phase and the selection of infiltration models applied for the study.

3.2 Excess Precipitation

The excess precipitation is the fraction of actual precipitation that appears as direct runoff (after base flow separation). Typically the precipitation signal (the hyetograph) is separated into three parts, the initial abstraction, the losses, and the excess precipitation.

Initial abstraction is the fraction of rainfall that occurs before direct runoff. Operationally several methods are used to estimate the initial abstraction. One method is to simply censor precipitation that occurs before direct runoff is observed. A second method is to assume that the initial abstraction is some constant volume (Viessman, 1968). The NRCS method assumes that the initial abstraction is some fraction of the maximum retention that varies with soil and land use (essentially a CN based method).

3.3 Rainfall Loss Models

Since 1890 the infiltration theory was developed into three major directions: empirical, approximate and physical, starting with Briggs (1897). For the empirical models, first presented by Kostiakov (1932), then Lewis (1935), Horton (1940), Holtan (1960), then Fok (2-D) (1970). For approximate loss models, it was first revised from Green-Ampt(1911), then Philip (1957), Bouwer (non-uniform,1968), Mein-Larson (steady rain, 1972), Moral-Seytoux (unsteady rain, 1975) and Chu (unsteady rain, 1979). Up today most of the interest is focusing on the direction of physical loss models.

The basis for the recent physical based infiltration models in hydrology is the Richards equation. However, few watershed models have used the Richards equation because of its complexity. Another additional observation is that most empirical and approximate models view infiltration in the "Hortonian" sense. The soil is treated as a semi-infinite media and the soil saturates from the surface down. The physical models specify the appropriate boundary conditions. In both cases, surface ponding starts when the surface application rate exceeds the soil surface infiltration rate.

Losses after initial abstraction are the fraction of precipitation that is stored in the watershed (depression, interception, soil storage) that does not appear in the direct runoff hydrograph. Typically depression and interception storage are considered part of the initial abstraction, so the loss term essentially represents infiltration into the soil in the watershed. Several methods to estimate the losses include: Phi-index method, Constant fraction method, and infiltration capacity approaches (Horton's curve, Green-Ampt model).

Phi-index Model

The ϕ-index is a simple infiltration model used in hydrology. The method assumes that the infiltration capacity is a constant ϕ(in/hr). With corresponding observations of a rainfall hyetograph and a runoff hydrograph, the value of ϕ can in many cases be easily guessed. Field studies have shown that the infiltration capacity is greatest at the start of a storm and that it decreases rapidly to a relatively constant rate. The recession time of the infiltration capacity may be as short as 10 to 15 minutes. Therefore, it is not unreasonable to assume that the infiltration capacity is constant over the entire storm duration. When the rainfall rate exceeds the capacity, the loss rate is assumed to equal the constant capacity, which is called the phi (ϕ) index. When the rainfall is less than the value of ϕ, the infiltration rate is assumed to equal to the rainfall intensity.

Mathematically, the phi-index method for modeling losses is described by

$$F(t)= I(t), \text{ for } I(t) < \phi \quad (3.1)$$

$$F(t)= \phi \text{ ,for } I(t)> \phi, \quad (3.2)$$

where F(t) is the loss rate, I(t) is storm rainfall intensity, t is time, and ϕ is a constant.

If measured rainfall-runoff data are available, the value of ϕ can be estimated by separating base flow from the total runoff volume, computing the volume of direct runoff, and then finding the value of ϕ that results in the volume of effective rainfall being equal to the volume of direct runoff. A statistical mean phi-index can then be computed as the average of storm event phi values. Where measured rainfall-runoff data are not available, the ultimate capacity of Horton's equation, f_c, might be considered.

Kostiakov's Model

Kostiakov proposed a simple infiltration model relating the infiltration rate f_p to time t, which was presented by Skaggs and Khaleel (1982) as

$$f_p = K_k t^{-\alpha} \qquad (3.3)$$

where K_k and α are constants which depend on the soil and initial conditions and may be evaluated using the observed infiltration rate-time relationship. The limitations of using Kostiakov's model are its need for a set of observed infiltration data for parameter evaluation; thus, it cannot be applied to other soils and conditions which differ from the conditions for which parameters K_k and α were determined. The Kostiakov model has primarily been used for irrigation applications. This model is equivalent to the exponential model in HEC-HMS software.

Horton's model

A three-parameter empirical infiltration model was presented by Horton (1940) and has been widely used in hydrologic modeling. He found that the infiltration capacity f_p to time t relationship may be expressed as

$$f_p = f_c + (f_0 - f_c)e^{-\beta t} \qquad (3.4)$$

Where f_0 is the maximum infiltration rate at the beginning of a storm event and reduces to a low and approximately constant rate of f_c as the infiltration process continues and the soil becomes saturated. The parameter β controls the rate of decrease in the infiltration capacity. Horton's equation is applicable only when effective rainfall intensity i_e is greater than f_c. Parameters f_c, f_0, and β must be evaluated using observed infiltration data.

Factors assumed to be influencing infiltration capacity, soil moisture storage, surface-connected porosity and effect of root zone paths follow the equation

$$f = aS_a^{1.4} + f_c, \tag{3.5}$$

Where f = infiltration capacity (in/hr),

a = infiltration capacity of available storage ((in/hr)/(in)) (Index of surface connected porosity),

S_a = available storage in the surface layer in inches of water equivalent (A-horizon in agricultural soils - top six inches),

Factor f_c = constant after long wetting (in/hr).

The modified Holton equation used by US Agricultural Research Service is

$$f = GIa\ Sa^{1.4} + f_c, \tag{3.6}$$

where GI = Growth index - takes into consideration density of plant roots which assist infiltration (0.0 - 1.0). Wide-scale application of this model is limited because of the dependence of the parameters on specific soil and moisture conditions, although these parameters can be related to the physically based parameters of the Green-Ampt equation. The model is criticized.

Constant Fraction Model

The constant fraction model simply assumes that some constant ratio of precipitation becomes runoff; the fraction is called a runoff coefficient. At first glance it appears that it is a rational method disguise, but the rational method does not consider storage and travel times. Thus in the rational method, if one doubles the precipitation intensity, and halved the duration, one would expect the peak discharge to remain unchanged, while in a unit hydrograph such changes should have a profound effect on the hydrograph. As a model, the method is simple to apply, essentially

$$\begin{aligned} p_e(t) &= crp * p_{raw}(t) \\ \int A p_e(t)dt &= \int DRH(t)dt \end{aligned} \qquad (3.8)$$

where crp = the runoff coefficient,

p_e = the effective precipitation,

p_{raw} = the raw precipitation,

A = drainage area.

The first equation states that the effective precipitation is a fraction of the raw precipitation, while the second states that the total effective precipitation volume should equal the total direct runoff volume.

Holtan Model

Holtan (1961) developed an empirical equation on the premise that soil moisture storage, surface-connected porosity, and the effect of root paths are the dominant factors influencing the infiltration capacity. Holtan and Lopez modified the Horton equation to be:

$$f = GI\, A\, S_a^{1.4} + f_c \qquad (3.9)$$

Where f is the infiltration rate (in/h), GI is the growth index of crop in percent maturity varying from 0.1 to 1.0 during the season, A is the infiltration capacity (in h^{-1}) per (in) of available storage and is an index representing surface-connected porosity and the density of plant roots which affect infiltration, S_a is the available storage in the surface layer (A horizon) in inches, and f_c is the constant infiltration rate when the infiltration curve reaches the asymptote (steady infiltration rate). Holtan model computes the infiltration rate based on the actual available storage of the surface layer (A horizon). This equation is easy to use for prediction of rainfall infiltration and the values for the input parameters can be obtained from the tables for known soil types and land use. The major difficulty for using the Holtan equation is the evaluation of the depth of the top layer (control layer). Huggins and Monk (1966) showed that the control depth is highly dependent on cultural practices and surface conditions.

Others Infiltration Models Study

Diaz-Granados et al (1983) used the physically based infiltration and exfiltration models, developed by Eagleson (1978), with exponential distribution presentation of three relevant independent climatic random variables-rainfall intensity, rainfall duration and time between storms to simulate the soil moisture. Philip's expression (1969) is developed as a function of soil parameters. Diaz-Granados et al. (1983) proposed an empirical equation for soil moisture computation based on long-term averages of climatological and soil parameters. They grouped the watershed area into two portions: mountainous and alluvial areas. For the mountainous area, a linear rainfall-runoff relationship is utilized. The resultant surface runoff is regarded as a water depth on the

alluvial area. The effective rainfall on the alluvium is computed to be equal to this water depth plus the rainfall depth minus the infiltration losses as presented by Philip (1969).

Smith et al. model (1993) enable us to make a substantial advance in representing the basic features of point infiltration associated with erratic rainfall patterns. However, the Smith model did not provide for all situations of practical interest. Corrado (1994) developed a formulation that may represent infiltration for any time evolution of rainfall rate, regardless of the production of surface natural saturation in any period. The new model provided a conceptual representation of infiltration during complex storms in soils with a negligible hysteresis loop.

Serrano (2001) presented a new solution built with a decomposition series of the implicit Green and Ampt equation (Serrano, 1997;2001) for an introduction to decomposition of nonlinear equations with examples. It was noted that a few terms in the series provided an accurate simple solution for practical applications. However, as with any asymptotic series, the decomposition expansion is not universally convergent. Sometimes the values of the parameters are such that the series is inaccurate over a portion of the time simulations. Later Sergio (2003) expanded on the results by providing an improved expression that includes more terms in the series, while remaining of simple application. Sergio also establishes a simple criterion for convergence that allows the practicing hydrologist the determination of conditions of error.

Most theoretical analyses of infiltration (Rubin, 1966; Smith and Parlange, 1978) have used the equation for vertical flow through a simple soil profile with a planar, unvegetated surface. The results illuminate the effects of soil texture and initial moisture content on infiltration commonly observed in field measurements. Effects of soil

structure on infiltration received less theoretical attention until the advent of interest in macropore flow (Beven and Germann, 1981, 1982). Several authors have combined Monte Carlo simulations of the distributions of soil properties with physically based models of percolation and sheet flow. Smith and Hebbert (1979) analyzed the effect on overland flow of random vibrations superimposed on a deterministic trend of infiltration properties along the surface flow path. Later Freeze (1980) introduced stochastic components into several parameters of a rainfall-runoff model and illustrated that the variability of saturated hydraulic conductivity had a strong influence on predicted hydrographs.

Smmith and Leopold (1942) and Dortignac and Love (1961) discovered there is simple relationship between vegetation cover density and infiltration capacity measured with infiltrationmeters, they also documented large changes in infiltration with only moistest changes in vegetation density. Thomas Dunne (1991) presented a alternate theory to observe the effects of vegetation density, temporal and special variance on the runoff.

This research focuses on simpler loss models than a rigorous solution to the Richards equations. A generally accepted principle in engineering hydrologic modeling is that each component should exhibit similar complexity. More precisely, a model should not be more complex than necessary to achieve its purpose; it should not include more than the essential details to describe the system being modeled. Thus a very detailed infiltration modeling approach would be inconsistent with a lumped-parameter, highly simplified unit hydrograph model.

The loss models included in this study are the fractional loss model, a simplified Green-Ampt infiltration model, and the initial abstraction constant loss model. These three are selected because of their relative simplicity -- these models are at about the same conceptual complexity as the unit hydrograph model.

3.4 Fractional Loss Model (FRAC)

The fractional loss model (FRAC) assumes that the watershed immediately converts a constant fraction of each rainfall input into an excess rainfall fraction that subsequently contributes to runoff (McCuen, 1998). The constant runoff fraction is a runoff coefficient. The FRAC model is attractive for automated processing because of its simplicity and because it preserves the correct runoff volume without iteration. The FRAC loss model is expressed in Equations 3.10 and 1.11 as:

$$L(t) = (1 - C_r)P(t) \qquad if \int_0^t P(\tau)d\tau > I_a \qquad (3.10)$$

$$L(t) = P(t) \qquad if \int_0^t P(\tau)d\tau < I_a \qquad (3.11)$$

Where L(t) is the loss rate as a function of time. P(t) is the observed rainfall rate as a function of time. C_r is a runoff coefficient (proportion of rainfall that becomes runoff). I_a is an initial abstraction term (has dimension of length).

This model implicitly assumes that the rainfall loss is a watershed property and is independent of storm history. Additional details of the data preparation, separation techniques, and rainfall loss models are reported in He (2004). In this work both zero and non-zero initial abstractions were examined.

3.5 Initial Abstraction Constant Loss Model (IACL)

The initial-abstraction, constant-loss model (IACL) assumes that after rainfall a certain portion is initially stored, infiltrated, or otherwise removed from the system and never appears as runoff.

After the initial abstraction is satisfied, the loss rate is some constant value. The difference between input rainfall rate and this constant loss rate is the excess rainfall rate. The IACL loss model is expressed in Equations 3.12 and 3.13 as:

$$L(t) = C \qquad if \quad \int_0^t P(\tau)d\tau \; > I_a \tag{3.12}$$

$$L(t) = P(t) \qquad if \quad \int_0^t P(\tau)d\tau \; < I_a \tag{3.13}$$

3.6 Simplified Green-Ampt Infiltration (GAIN) Loss Model

The Green-Ampt Infiltration (GAIN) model in this study is a simplification of the original Green-Ampt infiltration model. The GAIN model assumes that the watershed has some capacity to absorb rainfall and runoff occurs only when the rainfall input rate exceeds the absorption rate. The model is developed using the infiltration theory of Polubarinova-Kochina (1962), but the model is structurally identical to the independently developed Green-Ampt model, with some minor conceptual differences. It has been shown that Green-Ampt equation predicts infiltration and the resulting surface runoff from natural rainfall events more accurately than the Soil Conservation Service's (SCS) curve number method, both for small plots and watershed-size areas (Rawls and Brakensiek 1988; Van Mullem 1991).

The GAIN assumes that an infiltration front propogates into the watershed soils according to Darcy's law and the water content change across the front is equal to the soil

porosity. The front propogates into the soil without moisture redistribution; excess rainfall is the difference between the actual rainfall and the loss as the event progresses.

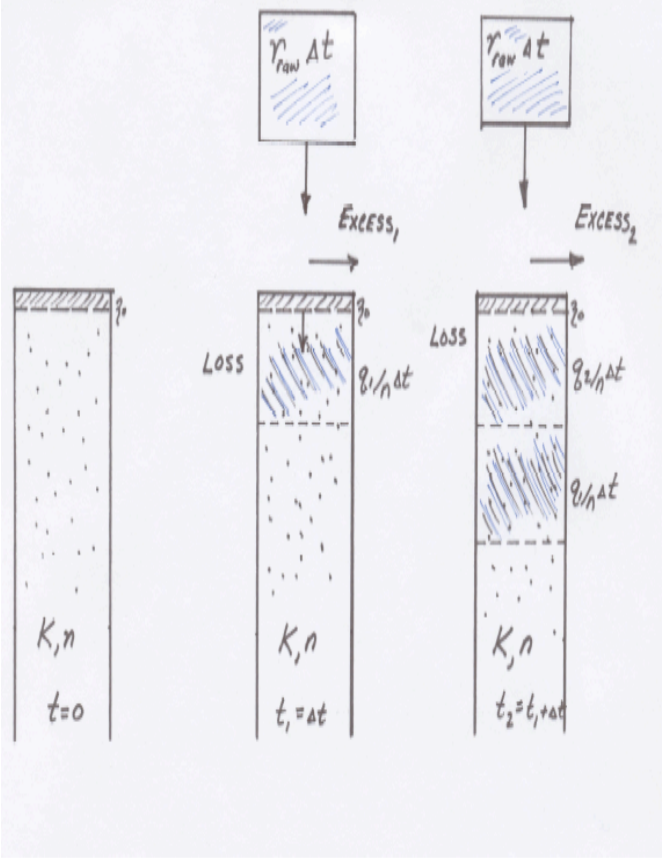

Figure 3.1: Schematic of Infiltration

Figure 3.1 is a schematic of the infiltration model. The three soil profiles represent the infiltration at different times, the left most profile is before the event begins. In that image the initial wetting position should be at the land surface, but a small depth is assumed into the soil to prevent an infinite gradient when computing the flux. The middle image is after a pulse of rainfall occurs. The rainfall volume input is represented by the block above the soil column. After the infiltration for that time interval is calculated this portion (possibly all the rainfall) is allowed to infiltrate into the soil, any remainder is labeled the excess and becomes runoff. The next (right most) image is one

time interval later. This image depicts how the infiltration depths are stacked into the soil sequentially advancing the wetting front.

$$\frac{\partial z}{\partial t} = \frac{q}{n} \qquad (3.14)$$

The wetting front velocity depicted in the figure (the right two soil profiles) is expressed in Equation 3.14; q, n, and z are the potential infiltration rate, the soil porosity, and the infiltration front position at time t. Equation 3.15 is an expression of Darcy's law relating the potential rate to the front position as:

$$q = K\frac{H + h_c + z}{z} \qquad (3.15)$$

The variables H and h_c are the ponding depth and suction potential. Substition of the second equation into the first provides a model for infiltration and hence a tool to estimate rainfall losses as expressed in Equation 3.16.

$$n\frac{\partial z}{\partial t} = K\frac{H + h_c + z}{z} \qquad (3.16)$$

The computation proceeds in light of the following additional simplifications: H is taken to be zero, consistent with other authors (Charbeneau, 2000). The suction potential reflects current soil moisture conditions. For a dry clay soil it could be quite large, but would reduce to some minimum rather quickly. In this work we assumed a fixed value because the time scale of our problems is large enough that this term becomes irrelevant quickly and after the initial absorption of rainfall, the system behaves as nearly unit-gradient throughout each event. The initial gradient into a dry soil would be quite large as the wetting depth is also zero so a small nonzero value was also assumed. The resulting model is then expresses as in Equation 3.17.

$$n\frac{\partial z}{\partial t} = K\frac{h_c + z + \varsigma_0}{\varsigma_0} \qquad (3.17)$$

Where, $h_c = 0.10$, $\zeta_0 = 0.01$, and K and n, are adjustable parameters both of which can be related to soil descriptions. The numerical values for suction potential and initial wetting position are strictly ad-hoc and no systematic approach was used in their specification. For most geologic media where infiltration may occur, the value of n will range from 10% to 50% with 35% probably being a typical value. K can range over several orders of magnitude for different materials, but is restricted in this study to range between literature values for sand to silty-clay.

The algorithm to compute loss and the excess precipitation is as follows:

1. Time-difference computations are used to extract rainfall rates from the observed cumulative rainfall depths, these rates are the raw rainfall rates, P(t).
2. $q_t = K\frac{h_c + z_t}{z_t}$ is used to compute the potential infiltration rate for the time increment.
3. If the potential rate is greater than or equal to the raw rate, all the rainfall infiltrates (L(t) = P(t)) , and the net infiltration depth for that time increment is computed from $z_{t+\Delta t} = z_t + \frac{P(t)}{n}$.
4. If the potential rate is smaller than the raw rate, the excess rainfall is the difference of the raw rate and the potential infiltration (L(t) = q_t), and the net infiltration for that time increment is $z_{t+\Delta t} = z_t + \frac{q(t)}{n}$.
5. All the time indexes are incremented by one and the procedure returns to item 2.

This approach assumes that the rainfall loss model is a watershed property (and is related to soil properties).

CHAPTER 4

CONVENTIONAL APPROACH TO UNIT HYDROGRAPH PARAMETERIZATION

This chapter briefly describes the conventional approach used in this research for unit hydrograph and loss model parameter identification and presents performance results as well as regionalization results for the central Texas watersheds.

4.1 Methods

The conventional approach relies on a set of custom-written FORTRAN programs to de-convolve the observed rainfall and runoff data and construct the hydrograph and loss parameters. Once parameters are determined regionalization methods are used to develop prediction equations for practical applications. The analysis is based on the method used by Weaver (2003) and described by O'Donnell (1960), where each rainfall increment is treated as an individual storm and the runoff from these individual storms are convolved using a unit hydrograph to produce the model of the observed storm.

The analysis required that both the rainfall and runoff data were converted through linear interpolation to a 1-minute interval. The 1-minute interval was selected because it was a small finite interval that approximated the limiting behavior of an instantaneous unit hydrograph (IUH).

The IUH is conceptualized from a finite interval unit hydrograph as

$$q_T(t) = \frac{S(t) - S(t-T)}{T} \qquad (4.1)$$

Where $q_T(t)$ is the depth per time T at some elapsed time t. T is some finite time interval,

and *S(t)* is the S-hydrograph (a cumulative hydrograph). The *S*-hydrograph was inferred from the cumulative runoff data for each station in the database. The basis for linear interpolation was the range between the observed runoff values for *T*. The limiting case as the duration vanishes is by definition the IUH

$$q_T(t) = \lim_{T \to 0} \frac{S(t) - S(t-T)}{T} = \frac{d}{dt}[S(t)] \qquad (4.2)$$

In this research, *T* is 1 minute and was selected as being a good approximation to the limiting value, and is a realistic time interval over which rainfall might be reported (very little rainfall data are ever reported at 1-minute increments, 5-minute intervals are uncommon, and even 15-minute intervals are sparse); hence the results in this dissertation are 1-minute unit hydrographs that are assumed to be valid representations of the instantaneous unit hydrographs.

This assumption was tested by analyzing five storms for station 08057320 using both 1-minute and 5-minute durations. The resulting estimated hydrographs are indistinguishable for all practical purposes. Further, even at an interval of 15 minutes, the resulting modeled hydrographs are not distinguishable. Other durations for the IUH approach are not elaborated on further in this dissertation.

Leinhard (1964) derived a unit hydrograph model using a statistical-mechanical analysis and two important assumptions. The first is that the travel time taken by an excess raindrop on the watershed to the outlet is proportional to the path-line distance the excess raindrop must travel. The second assumption is that the area swept by any characteristic distance is proportional to some power of that characteristic distance. The Leinhard hydrograph model was selected both for its adjustable shape and because

Leinhard's derivation gives meaningful physical insight into the resulting parameter values.

The Leinhard hydrograph distribution is a generalized gamma distribution (Leinhard, 1964;1967) and is expressed as,

$$f(t) = \frac{\beta}{\Gamma(n/\beta)}\left(\frac{n}{\beta}\right)^{n/\beta}\frac{1}{t_{rm\beta}}\left(\frac{t}{t_{rm\beta}}\right)^{n-1}\exp\left[-\frac{n}{\beta}\left(\frac{t}{t_{rm\beta}}\right)^{\beta}\right] \qquad (4.3)$$

The parameters n and $t_{rm\beta}$ in the distribution have physical significance: $t_{rm\beta}$, is a mean residence time of an excess raindrop on the watershed, conceptually similar to the conventional term of time to peak (but numerically different); n, is an accessibility number roughly equal to the exponent on the distance-area relationship (a shape parameter). β, is the degree of the moment of the residence time, $\beta=1$ would be the arithmetic mean, and the distribution becomes the gamma hydrograph distribution that has been used extensively in hydrology, while for $\beta=2$ the residence time is a root-mean-square time, and the distribution becomes a different gamma distribution. The Rayleigh hydrograph distribution (Cleveland and others, 2003; He, 2004) is a special case of the generalized gamma distribution, and for integral values of the ratio n/β the distribution is a Weibull distribution. This distribution is the IUH that is used throughout this research. $\beta=2$ was selected to be faithful to the Leinhard's original derivation.

Equation 4.3 can also be expressed as a dimensionless hydrograph using the following transformations (Leinhard, 1972) to express the distribution in conventional dimensionless form:

$$t_{rm\beta} = \left(\frac{n}{n-1}\right)^{1/\beta} T_p \qquad (4.4)$$

$$Q_p = f(T_p) \qquad (4.5)$$

Expressed as a dimensionless hydrograph distribution equation 4.3 becomes,

$$\frac{Q}{Q_p} = \left(\frac{t}{T_p}\right)^{n-1} \exp\left[-\frac{n-1}{\beta}\left(\left(\frac{t}{T_p}\right)^{\beta} - 1\right)\right] \qquad (4.6)$$

Figure 4.1 is a plot of the NRCS dimensionless unit hydrograph and the Leinhard unit hydrograph for two particular values of n. β in this figure is two. The figures illustrates that the dimensionless hydrograph, Equation 4.6, mimics the behavior of the NRCS-DUH.

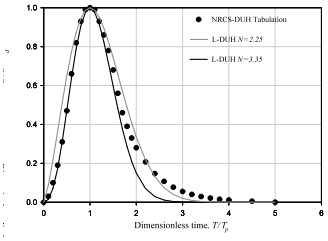

Figure 4.1. Comparison of NRCS DUH and Leinhard Hydrograph with various shape parameters. (from Cleveland, and others. 2006)

The IUH becomes increasingly symmetrical for larger values of n, and therefore, unlike the shape of many right skewed (longer recession limb) observed hydrographs. As a result, large values (greater than about 5) for are not anticipated. Leinhard (1972) suggested that large values have limited physical interpretation from arguments of statistical mechanics.

4.2 Finding UH and Loss Parameters

To implement the IUH, a rainfall loss model is required. In this section the three loss models were used, in part to see if model choice provided any advantages, and in anticipation of relating to soil properties, impervious fraction, or other similar properties readily available for engineering studies. While the models differ, there use in the estimation procedure is the same.

The storm-optimum loss parameters for each model and corresponding storm-optimum UH parameters are determined by a sequential semi-constrained search technique similar to, but modified from the search techniques used earlier in the research. The search technique uses a coarse grid of loss model parameters combined with the grid resolution for the unit-hydrograph in Cleveland and others (2006). The results of these initial searches are used in the refinement search that assumes the search has identified results that are close to a storm-optimal result and uses a differential search from these ordered quadrupules. There is no guarantee that the results are optimal in the Kuhn-Tucker sense but the procedure allows monitoring of the progress of the parameter estimation as well as limited adaptive control of the search ranges during the computations. The computational effort is not trivial and a purpose built cluster computer (Cleveland and Smith, 2004) is used to increase the computation throughput.

Using one of the three loss models, the excess rainfall hyetograph was computed. The excess rainfall hyetograph is convolved using a FORTRAN program to generate simulated streamflow hydrographs in the database for each watershed.

Using a second FORTRAN program the hydrograph parameters for each storm are systematically adjusted until the maximum absolute deviation at peak discharge (Q_pMAX) is minimized—a merit function. The merit function is

$$Q_p MAX = \left| Q_m(t_p) - Q_o(t_p) \right| \qquad (4.7)$$

where Q is the discharge (cubic length per time), the subscripts m and o represent model and observed discharge, respectively, t_p is the actual time in the observations when the observed peak discharge occurs. Although a peak time is expressed, the nomenclature of t_p is different from T_p to distinguish between observed peak of the storm (t_p) and time-to-peak of a unit hydrograph model (T_p). The merit function is designed to favor matching the peak discharge magnitude with little regard for the rest of the hydrograph.

A search technique was used instead of more elegant or adaptive methods such as reduced gradient minimization or simplex minimization, principally to ensure a result. The search systematically computes the value of a merit function using every permutation of model parameters as listed in Table 4.1

Table 4.1. Search ranges and increments for three loss models.

FRAC Model				
Parameter Name	Low Value	High Value	Search Increment	Units
C_r	$\int Q(t)dt / \int P(t)dt$	--	--	--
t_{rms}	1.0	720.0	1.0	minutes
N	1.0	12.0	0.01	none
IACL Model				
Parameter Name	Low Value	High Value	Search Increment	Units
Ia	0.0	2.0	0.005	inches
C_L	0.0	0.036	0.0001	inches/minute
t_{rms}	1.0	720.0	1.0	minutes
N	1.0	12.0	0.01	none
GAIN Model				
Parameter Name	Low Value	High Value	Search Increment	Units
ϕ	0.1	0.8	0.001	none
K	0.0	0.036	0.0001	inches/minute
T_{rms}	1.0	720.0	1.0	minutes
N	1.0	12.0	0.01	none

Fractions of a minute were ignored and sub *0.01* resolution in the shape parameter was considered unnecessary. The set of parameters that produces the smallest value of the merit function is retained as the optimal set for a storm. This approach, although computationally expensive, is robust. The n and $t_{rm\beta}$ parameters were computed using a purpose-built Linux cluster computer constructed from discarded PCs to speed up the computational throughput.

This procedure produces an n and $t_{rm\beta}$ value for each storm. These results are called "storm optimal" values. The mean values for n and $t_{rm\beta}$ for each watershed are computed from the storms recorded on each watershed. Then Q_p and T_p are computed, and provide the basis for statistical analysis to generate regression models to estimate hydrograph parameters for similar Texas watersheds.

Several observations on the approach are useful. First, the approach reported here was designed to be entirely automated. Once the database is prepared, the computations are run without analyst intervention in contrast to other approaches (Asquith and others, 2005). Second, some of the storms were pathologically unsuitable (peak rainfall rate after peak runoff rate); however, because of program robustness the program still produces a result. These storms were manually removed when detected by graphical data analysis. Third, each storm is analyzed in its entirety; multiple peaks in a storm that could potentially serve as sub-set storms and analyzed independently are not used.

4.3 Results and Exploratory Analysis

A summary analysis for all storms studied for each of the three loss models is presented on Figure 4.2. The figure contains six panels organized from top to bottom as

the total runoff volume (volume is normalized by each watershed's area, thus the dimension is a length), the peak discharge rate (discharge is normalized by each watershed's area, thus the dimension is length/time), and the time of the peak discharge. The left panels are scatterplots of these measures with an equal value line to indicate the ideal performance, the right panels are boxplots of the distributions of the various measures. In addition to these graphics, Table 4.2 tabulates the essential information displayed in the boxplots.

Table 4.2**.** Storm summary statistics, three loss models.

Runoff Depth	1st - Quartile	Median	3rd - Quartile	Units
Observed	0.277	0.603	1.140	Inches
FRAC	0.276	0.595	1.130	Inches
GAIN	0.244	0.496	0.982	Inches
IACL	0.220	0.478	0.950	Inches
Peak Flow	1st - Quartile	Median	3^{rd} - Quartile	Units
Observed	1.4E-3	3.8E-3	8.2E-3	inches/minute
FRAC	8.7E-4	2.4E-3	5.6E-3	inches/minute
GAIN	9.8E-4	2.7E-3	6.4E-3	inches/minute
IACL	9.3E-4	2.6E-3	5.0E-3	inches/minute
Time of Peak	1st - Quartile	Median	3^{rd} - Quartile	Units
Observed	646	1140	1460	Minutes
FRAC	641	1120	1460	Minutes
GAIN	636	1120	1450	Minutes
IACL	654	1150	1490	Minutes

The scatterplot of the observed runoff volume and the model runoff volume for about 1500 storms (upper left panel) in the database using the three different loss models illustrates that there are differences in results between the three models. The FRAC model is the only model that was forced to match volume and thus agrees well with the equal volume line in the volume plot. The other two models, GAIN and IACL were not forced to match volume and have an additional degree of freedom; a consequence of a need to keep the grid-search selection algorithm unchanged for different loss models.

This panel illustrates that these loss models (GAIN and IACL) exhibit more variability.

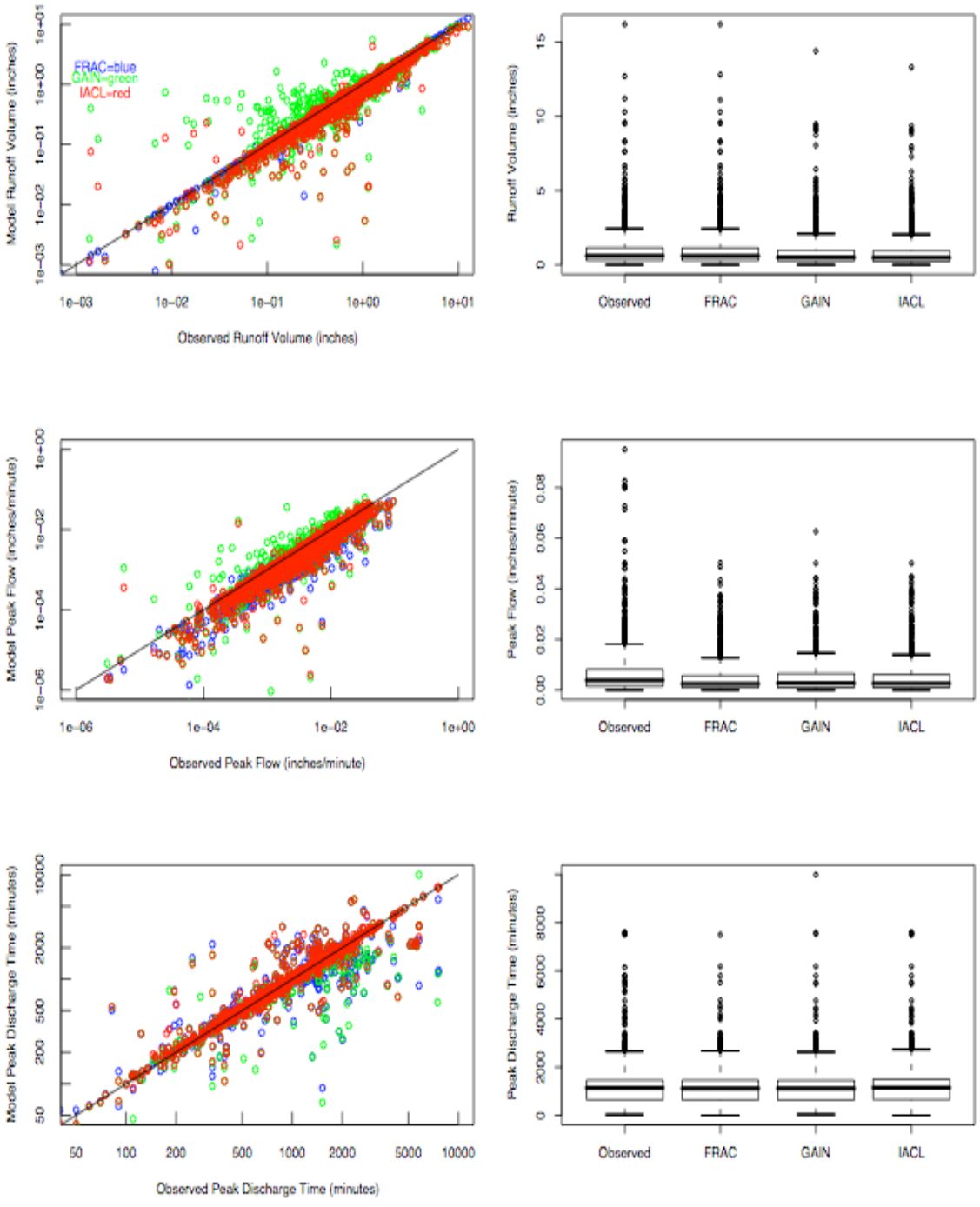

Figure 4.2. Relationship of observed and modeled runoff volume, peak discharge, and time of peak discharge for three loss models.

The boxplot of the observed runoff volume and the model runoff volume for the same results (upper right panel) further illustrates differences. The FRAC model distribution is essentially identical to the observed distribution; a result anticipated as the FRAC model is forced to match the observations. The two other models are biased low, meaning that the computed runoff depth is less than observed. The differences in the medians for all three models are significant as compared to the observed results, even for the FRAC model. This finding (FRAC not exactly same as observed) is attributed to an handful of storms with pathological errors (in the analysis program). The difference in medians between the FRAC and other two loss models are also significant, but the differences between the GAIN and IACL model are not significant. This result is interpreted as either of these models are equivalent when computing total runoff volume. The author speculates that further refinement to force a volume match would produce performance comparable to the FRAC model.

The scatterplot of the observed peak discharge and the model peak discharge (left middle panel) illustrates that all the model results exhibit a low bias relative to the equal value line. The bias is attributed to the nature of the merit function selected in the grid search algorithm, which will de-emphasize peak value in an attempt to match the hydrograph shape. The associated boxplot of the distribution of the peak discharges for the different loss models illustrates this bias; more importantly the differences in the medians are significant as compared to the observed results. The difference in medians between the models are not significant, this result is interpreted to mean that any of the loss models perform roughly the same with respect to the computation of peak discharge.

The scatterplot of the observed time of the observed peak discharge and the model time of the model peak discharge (left lower panel) illustrates that all three loss models qualitatively perform the same. The associated boxplot as well as non-parametric tests (Wilcox) indicate that the three distributions have no statistically significant differences. This result is interpreted to mean that the loss models have little impact on the computed response time of the study watersheds. This particular finding is important in that it supports the concept that the timing estimates can be de-coupled from the loss estimates with little impact on the resulting the unit hydrograph; such de-coupling is a principal step in the Asquith and Roussel (2007) approach.

4.4 Hydrograph Parameters

This section presents an analysis of the resulting loss model parameters from the station mean values from the set of storms for each station. Figure 4.3 is a scatterplot of the empirical cumulative frequency distribution of the runoff coefficient for the stations, categorized by development factor. The basin development factor and other watershed soil and land-use-related properties are listed in Appendix 1, Table 3.

In the figure the difference between developed and undeveloped watersheds is apparent. Undeveloped watersheds in general have a smaller runoff coefficient than developed watersheds. The difference is preserved even if watershed size is considered. The principal interpretation of this figure is that a developed watershed will, on average, convert more rainfall into excess rainfall than an undeveloped watershed.

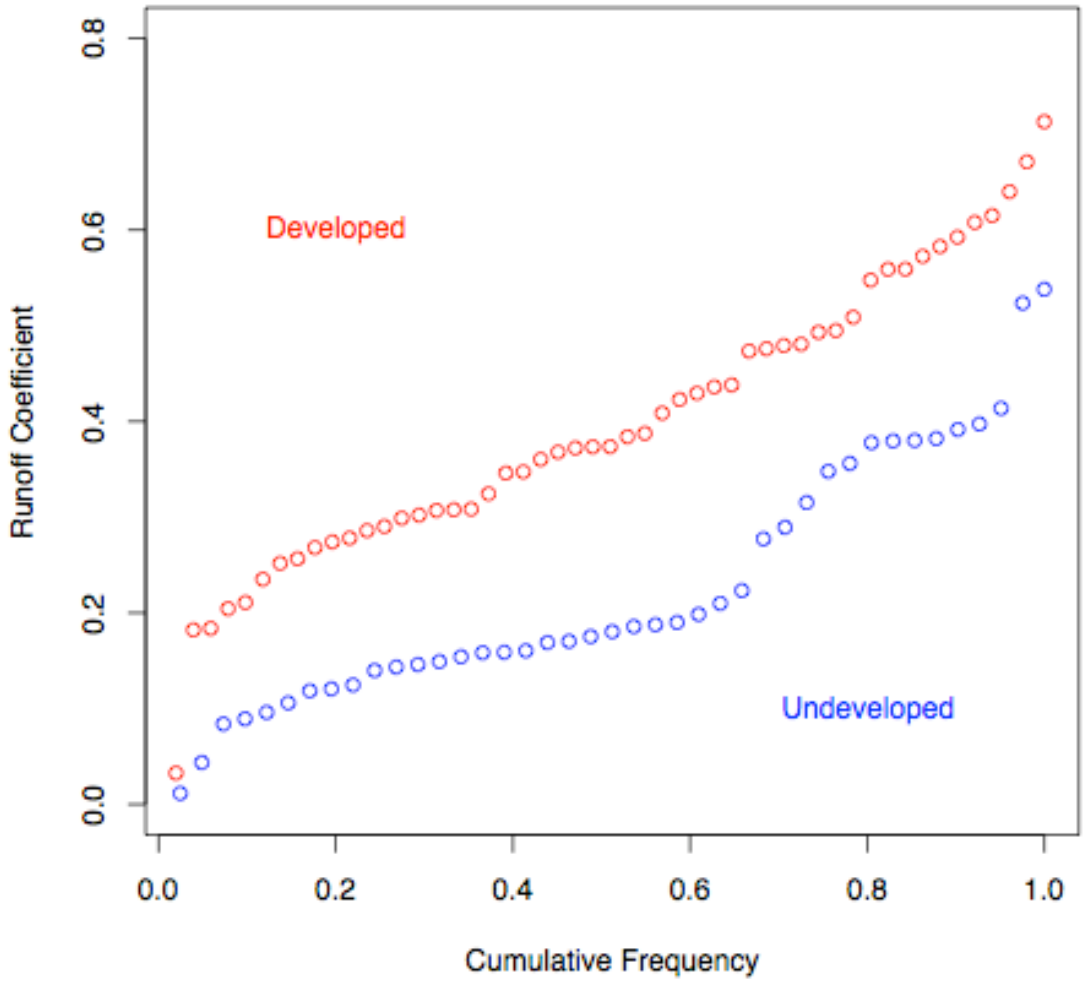

Figure 4.3. Comparison of station mean values of Cr for developed and undeveloped watersheds, FRAC loss model.

Figure 4.4 is a similar plot for the characteristic time based on the FRAC model. In this figure the characteristic time is significantly smaller for developed watersheds than for undeveloped watersheds. The interpretation of this figure is that a developed watershed will redistribute the excess rainfall to the outlet faster than an undeveloped watershed. Of importance is the time scale is logarithmic, the differences in this figure

are quite significant. So according to the FRAC model, which produces reasonable estimates, a developed watershed will not only convert more rainfall into runoff in a volumetric sense, it will also transfer that rainfall to the outlet faster, resulting in comparatively higher peak discharges that for an undeveloped watershed.

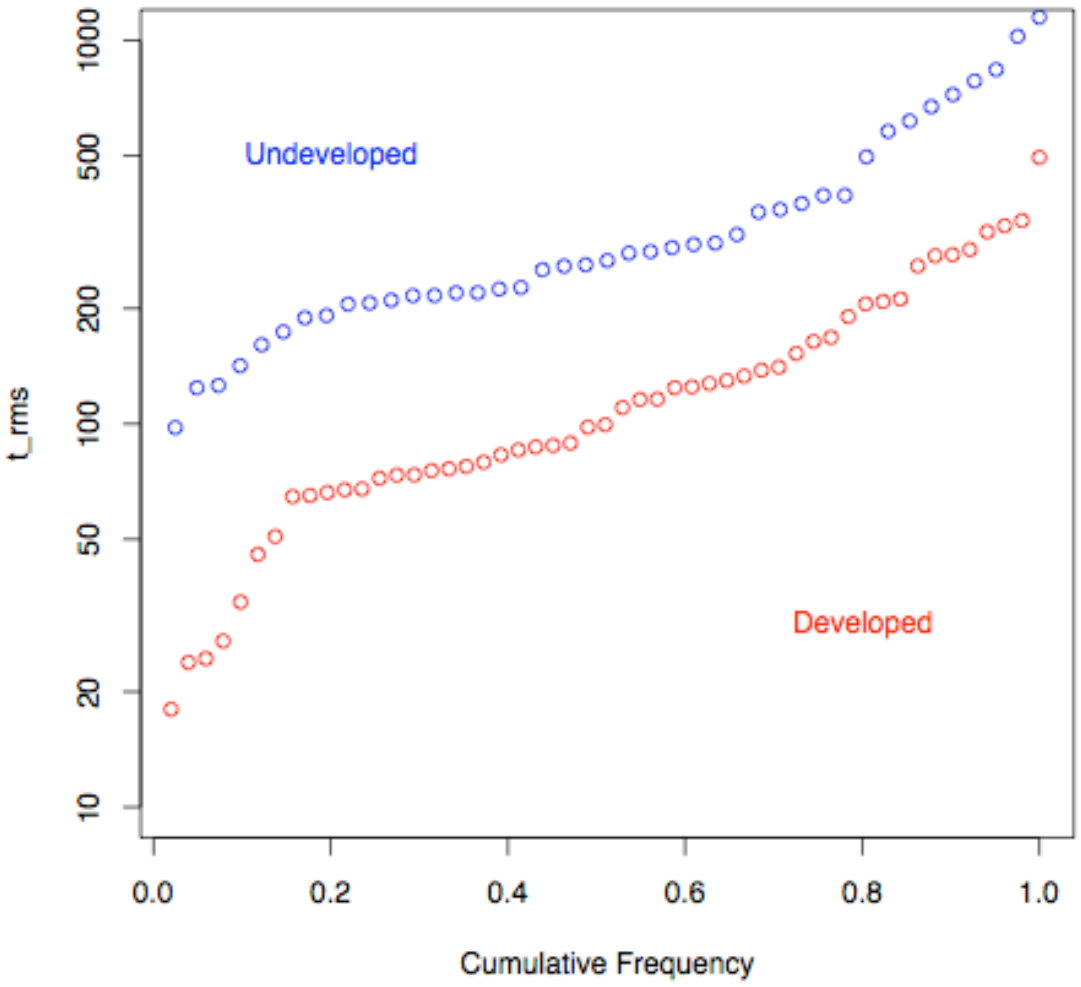

Figure 4. 4. Comparison of station mean characteristic time for undeveloped and developed watersheds, FRAC loss model.

Figure 4.5 is a scatterplot of the empirical cumulative frequency distribution of the initial abstraction depth for the stations, categorized by development factor, for the IACL model (a two-parameter loss model).

In the figure the difference between developed and undeveloped watersheds is apparent, and the difference is statistically significant. The median values are 0.56 and 0.82 inches for a developed and undeveloped watershed, respectively. Undeveloped watersheds in general have a larger initial abstraction than the developed watersheds. Interpreting the initial abstraction as a surrogate for storage the undeveloped watersheds in the study on average store almost fifty percent more depth than a developed watershed, so smaller storms that will produce runoff on a developed watershed may not produce runoff on an undeveloped watershed.

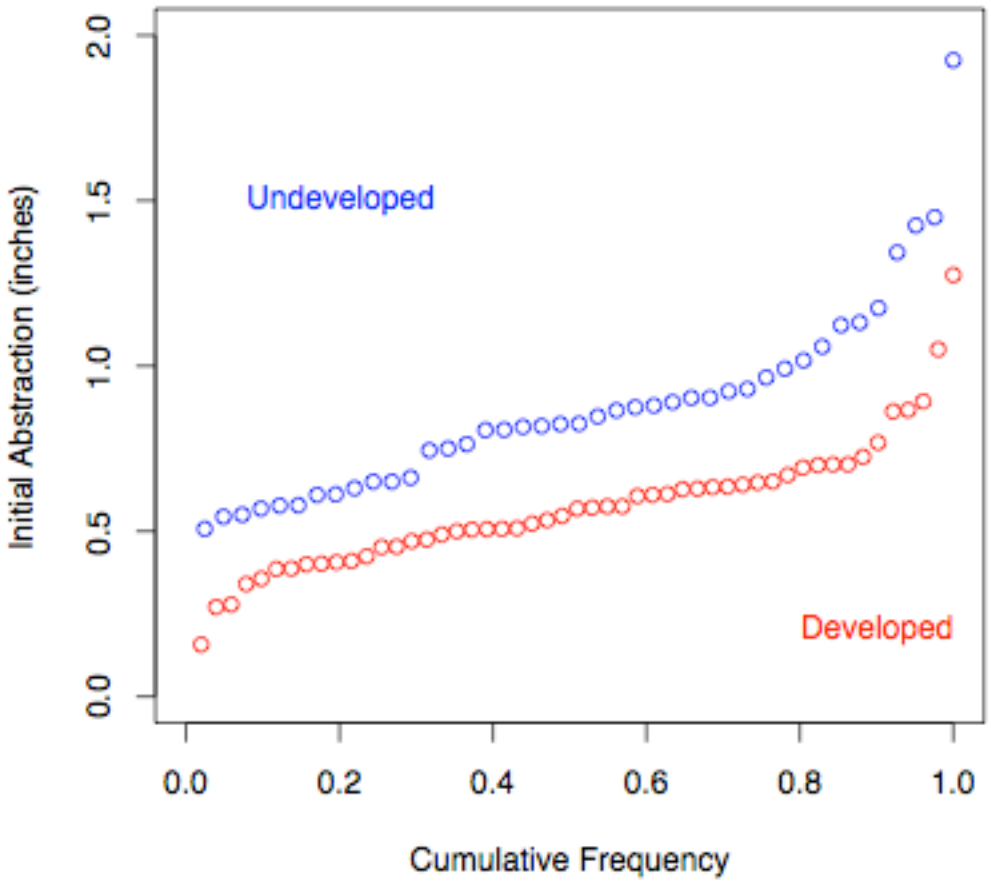

Figure 4.5. Comparison of station mean values of Ia for developed and undeveloped watersheds, IACL loss model.

Figure 4.6 is an equivalent plot of the constant loss rate, CL for the study watersheds. The median values of CL for undeveloped and developed study watersheds are 0.91 inches per hour and 0.76 inches per hour, and the difference in these values is significant. Undeveloped watersheds exhibit a loss rate about fifteen percent greater on average than does a developed watershed. So in addition to storing more incoming rainfall, undeveloped watersheds other losses reduce the magnitude of the remaining runoff signal considerably.

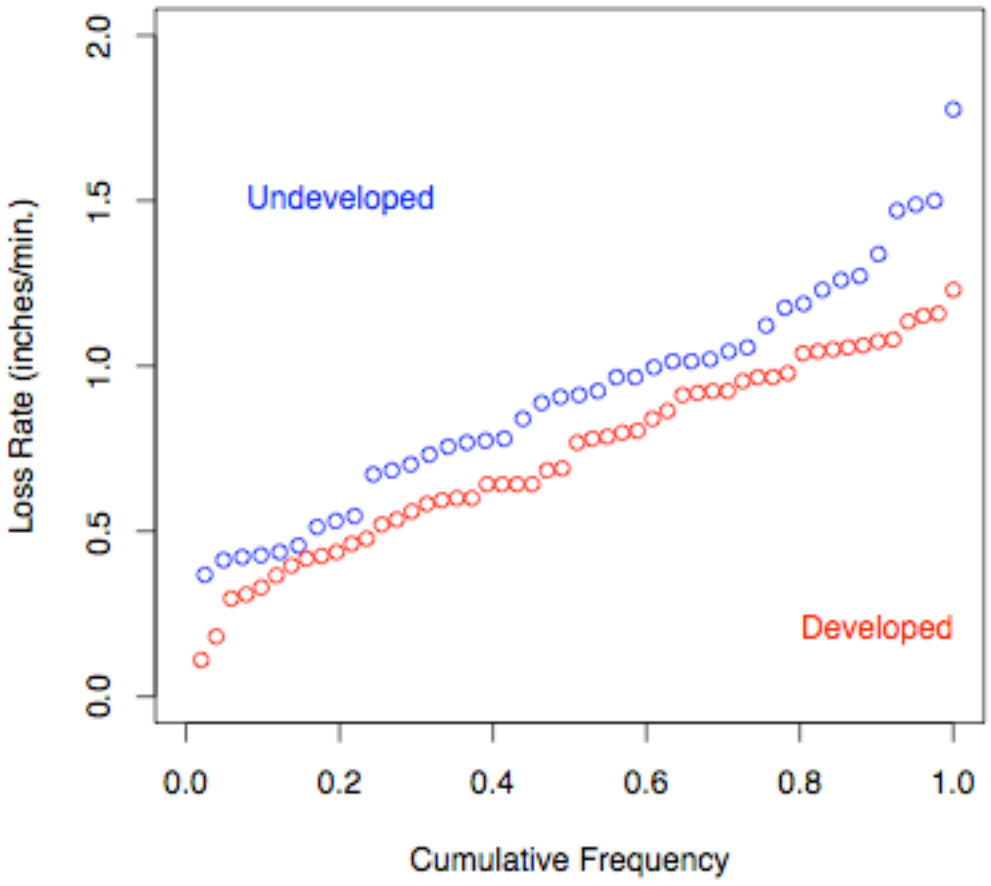

Figure 4.6. Comparison of station mean values of CL
for developed and undeveloped watersheds, IACL loss model.

Figure 4.7 is a similar plot for the characteristic time based on the IACL model. In this figure the characteristic time is significantly smaller for developed watersheds than for undeveloped watersheds. As with the FRAC model, the interpretation of this figure is that a developed watershed will redistribute the excess rainfall to the outlet faster than an undeveloped watershed. Also, as was observed with the FRAC model, the IACL model which produces reasonable estimates (but does not match volume as well), a developed watershed not only converts more rainfall into runoff in a volumetric sense, it

will also transfer that rainfall to the outlet faster, resulting in comparatively higher peak discharges that for an undeveloped watershed. The consistent interpretation is both expected and reassuring.

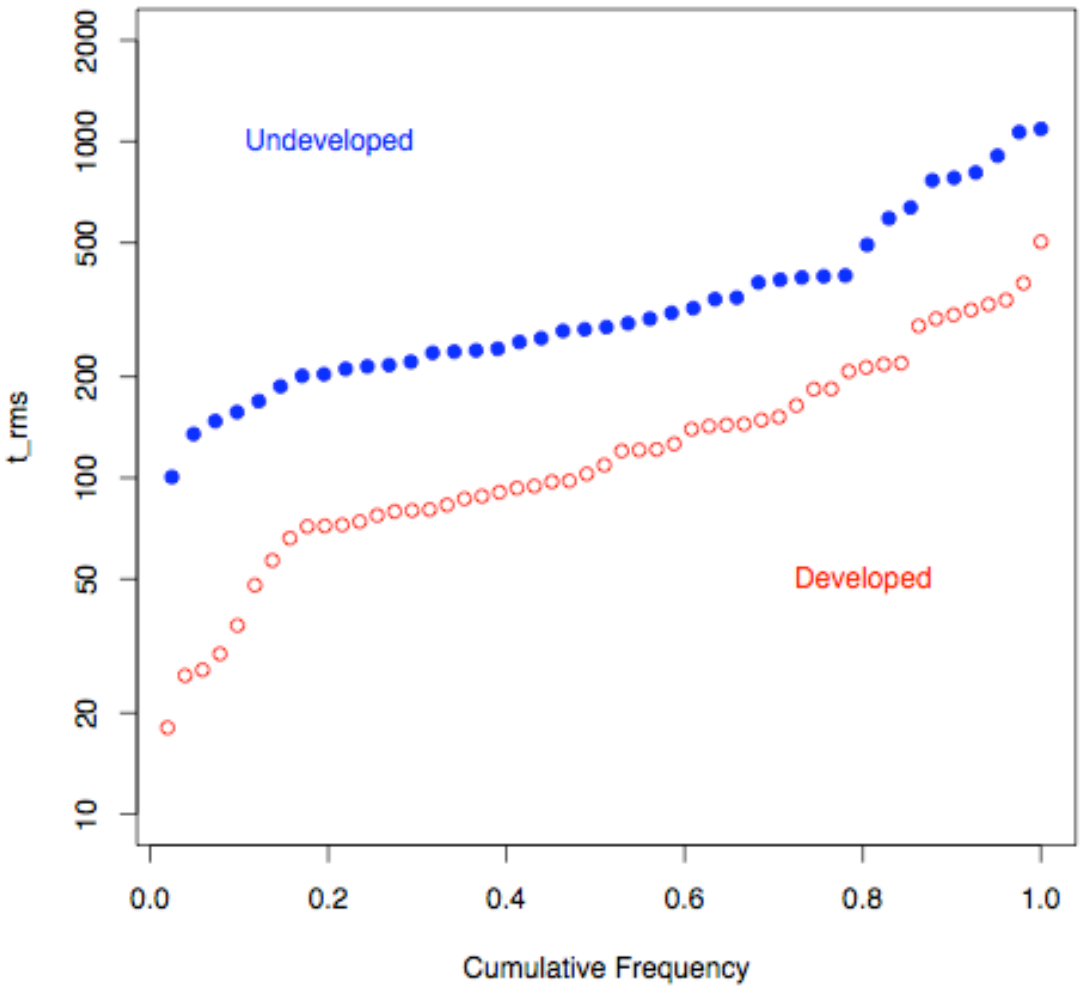

Figure 4.7. Comparison of station mean timing parameter values for undeveloped and developed watersheds, IACL loss model.

Figure 4.8 is a scatterplot of the empirical cumulative frequency distribution of the change in water content across the wetting front (a porosity) for the stations, categorized by development factor, for the GAIN model (a two-parameter loss model).

In the figure the differences between developed and undeveloped watersheds is small, and essentially indistinguishable. Interpreting the porosity as reflective of either moisture conditions or soil properties, the author concludes that undeveloped watersheds and developed watersheds are essentially the same with regards to ability to store infiltrated water – this result is a concern because the GAIN model was investigated for its promise to be parameterized independently of observations (from soil descriptions, etc.).

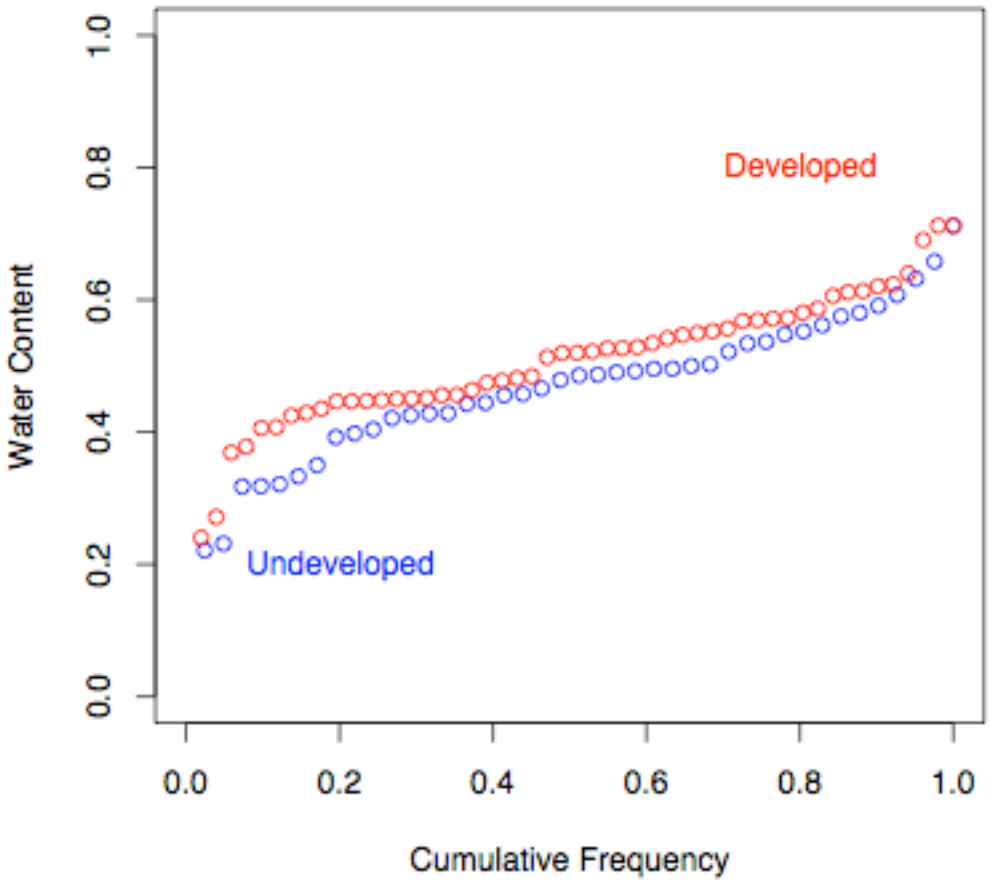

Figure 4.8. Comparisons of station mean values for water content change (porosity) for developed and undeveloped watersheds, GAIN loss model.

Figure 4.9 is an equivalent plot of the hydraulic conductivity (permeability), for the study watersheds. Undeveloped watersheds exhibit a higher conductivity than a developed watershed, so although the soils on either type of watershed can store about the same depth of water the undeveloped watersheds can fill this storage faster.

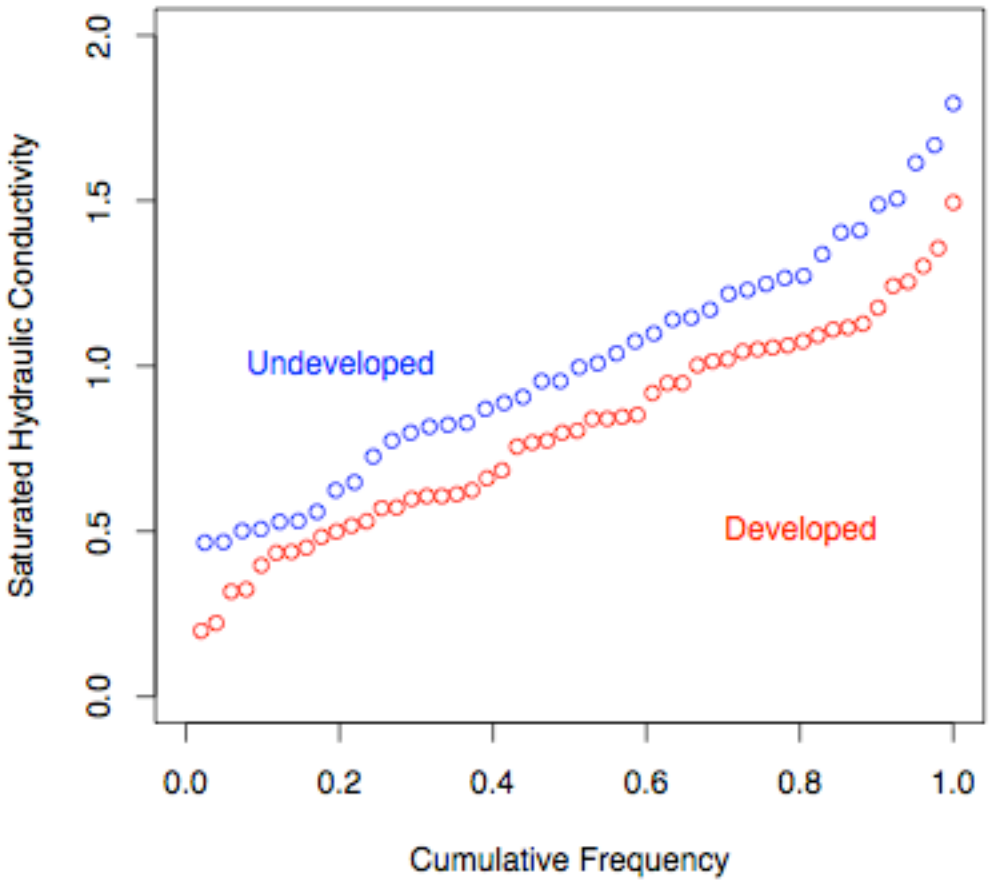

Figure 4.9. Comparisons of station mean values of Ksat for developed and undeveloped watersheds, GAIN loss model.

Figure 4.10 is a similar plot for the characteristic time based on the GAIN model. In this figure the characteristic time is significantly smaller for developed watersheds than for undeveloped watersheds. As with the other models, the interpretation of this

figure is that a developed watershed will redistribute the excess rainfall to the outlet faster than an undeveloped watershed. Also, as was observed with the other models, the GAIN model, which produces reasonable estimates (but does not match volume as well), a developed watershed not only converts more rainfall into runoff in a volumetric sense, it will also transfer that rainfall to the outlet faster, resulting in comparatively higher peak discharges that for an undeveloped watershed.

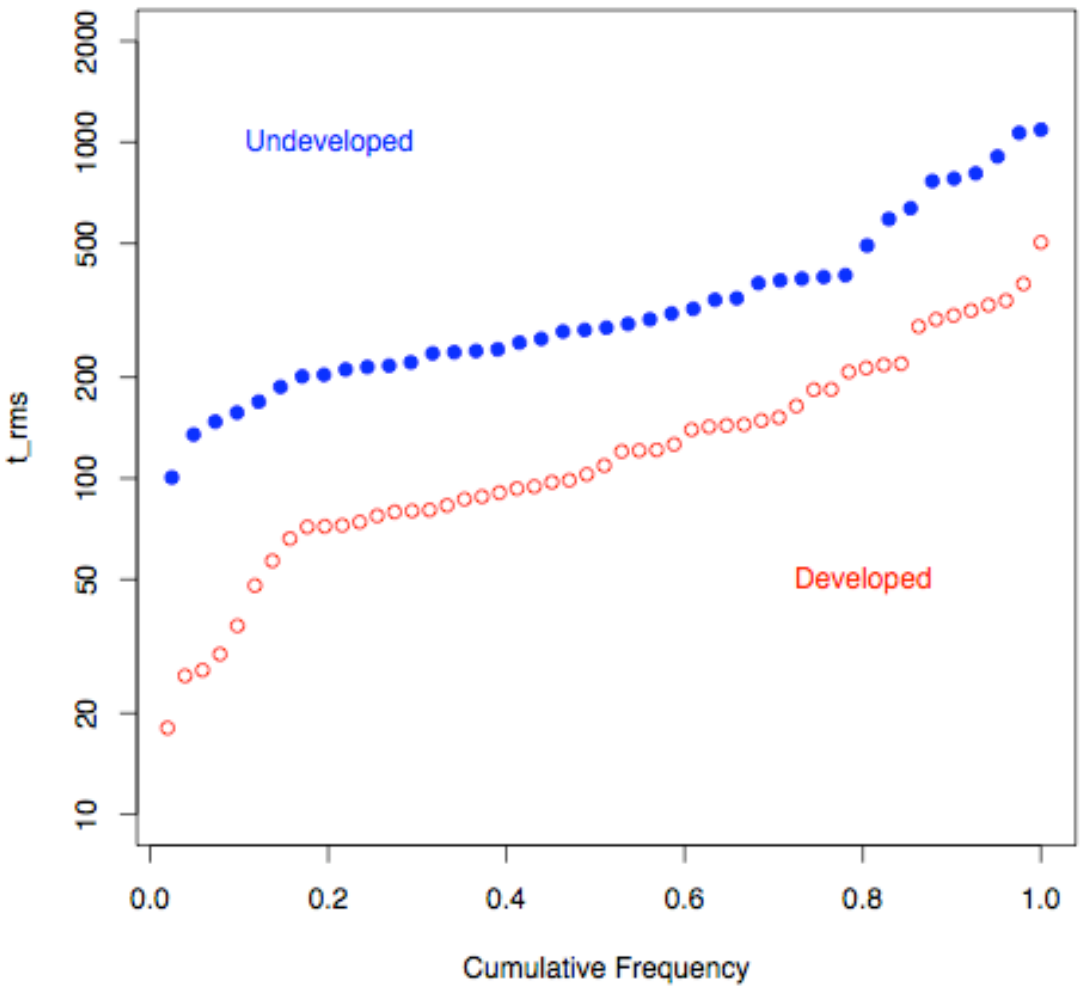

Figure 4.10. Comparisons of characteristic time for undeveloped and developed watersheds, GAIN loss model.

Interpretation of the results presented in this section are that all the models perform about the same when compared to observations. The FRAC model preserves volume better because it is constrained to do so, the other two models were not optimized to the point where they matched volume as well, because of computational constraints and the desire to keep the underlying programs internally consistent.

The station mean values for the principal model parameters are correlated with development factor with the exception of porosity in the GAIN model.

4.5 Regionalization of the Results

Regression equations to allow estimation of hydrograph model parameters from physical descriptions of the watersheds are developed in this section. For practical application, estimation of FRAC, IACL, or GAIN model parameters (and the associated hydrograph parameters) is needed for application on ungaged or unmonitored watersheds. This estimation ability can be provided by regression between the model parameters (each a regressor variable) and selected watershed characteristics (explainatory variables).

Several distinct watershed characteristics were evaluated as candidates for estimation of model parameters for ungaged watersheds. Favorable candidates are judged in part by the statistical significance within the regression equations; statistical significance (p-value_10) is measured by p-value_0.05. The watershed characteristics for each of the 92 watersheds were obtained from Asquith and others (2005) or determined (or computed) as necessary. Each of the candidate characteristics are listed in Appendix 1, Table 3. Briefly the characteristics are:

1. Values for contributing drainage area TDA for each watershed were obtained from Asquith and others (2005, Table 2). Preliminary analysis showed that TDA has similar predictive properties as MCL. A contributing reason for the similarity is the statistically significant relation between MCL and TDA. The author decided not to use TDA for final regression computations in part because prior experience with FRAC model results showed that a ratio variable of MCL/MCS was a good explainatory variable for the timing parameter that not only captured the effects of watershed size, but also its slope.
2. Values for main channel length MCL were obtained from Asquith and others (2005, Table 2). The MCL is defined as the length in miles of the longest defined channel by a 30-meter digital elevation model from the approximate watershed headwaters to the outlet. L is statistically significant for estimation of IA and CL and is used in the final regression computations.
3. Values for dimensionless main channel slope MCS were obtained from Asquith and others (2005, Table 2). The MCS is defined as the change in elevation in feet between the two end points of MCL divided by MCL. A 30-meter digital elevation model was used to compute S for this report.
4. National Resources Conservation Service (National Resources Conservation Service, 2006) curve numbers (CN) were obtained by standard lookup tables and ancillary tools. The CNs for each of the 92 watersheds are listed to three significant figures, which reflects the value used in the analyses. However, the author acknowledges that for a typical watershed CN likely has measurable resolution no better than a couple of integer values. The CN is a parameter used

to estimate the maximum potential retention of rainfall in a watershed (National Resources Conservation Service, 2006); the CN reportedly accounts for differences between soil types, land cover classifications, and other hydrologic conditions of the land surface that affect watershed storage of rainfall. The CN method generally represents a non-time distributed, watershed loss model. The CN method likely is the most common rainfall and runoff model for typical hydrologic-engineering circumstances. Because the CN is well known, represents an overall capacity of a watershed to absorb rainfall, and is statistically significant for estimation of the loss model parameters, CN is used for final regression computations.

5. Soil types and textures were obtained from U.S. Geological Survey (2006). Exploratory analysis of the relations between loss model parameters and soil types and textures indicated that various measures (sand, silt, clay, loam, hydraulic conductivity, and others) were inferior to the CN in terms of predictive capabilities. The author decided not to use soil types and textures for final regression computations. This exploratory analysis was especially disappointing with regards to the GAIN model, which is directly related to soil properties that are correlated with textural properties.
6. The binary classification of watershed development D was considered. Values for D were obtained from Asquith and others (2005, Table 1). The D factor (Asquith and others, 2005, Table 1) is a state variable representing a binary classification of the state of development in a watershed (undeveloped and developed). The classification scheme parallels and accommodates the disparate discussion and

conceptualization seen in over 220 reports that provided the original data for the rainfall and runoff database (Asquith, and others, 2004). D is statistically significant for estimation of loss and timing parameters and is used in final regression computations.

7. Another binary classification considered was whether the watershed is characteristized by rock-dominated terrain and thin soils, rock channels, and karstic features, such as the limestone watersheds in and around the Austin and San Antonio areas. The rock classification factor (R) was obtained through local knowledge and geologic and soil data for the watersheds. The R (ROCK) for each of the 92 watersheds is listed in Appendix 1, Table 3. R is statistically significant for estimation of IA and CL and is used in final regression computations.

In summary, of the eight candidate watershed characteristics, the four characteristics of MCL/S, D, R, and CN were used in the final stages of linear regression (equation) analysis.

For each model (FRAC, IACL, GAIN) four regression equations were determined that relate the watershed properties to the model parameters, these regression equations represent the conventional approach to unit hydrograph application on un-gaged or unmonitored watersheds.

For FRAC loss model, the regression equation of runoff coefficient Cr. shows below:

$$Cr = 10^{(-6.38+0.13D-0.22R)} * (MCL/MCS)^{0.005} * (CN)^{3.1} \quad R^2 = 0.51$$

IACL loss model, the regression equations about I_a and Cr are:

$$Ia = 10^{(1.3-0.13D+0.12R)} * (MCL/MCS)^{-0.006} * (CN)^{-0.76} \quad R^2 = 0.51$$
$$Cr = 10^{(0.4-0.06D+0.18R)} * (MCL/MCS)^{-0.15} * (CN)^{-1.01} \quad R^2 = 0.42$$

GAIN loss model, the regression equations about ϕ(n) and K are:

$$\phi(n) = 10^{(-0.97+0.03D+0.04R)} * (MCL/MCS)^{-0.04} * (CN)^{0.39} \quad R^2 = 0.56$$
$$K = 10^{(-1.32-0.09D+0.2R)} * (MCL/MCS)^{-0.1} * (CN)^{-0.15} \quad R^2 = 0.45$$

CHAPTER 5

DTRM APPROACH TO UNIT HYDROGRAPH PARAMETERIZATION

5.1 Introduction

Generating an excess rainfall arrival time distribution at the watershed outlet was addressed by placing a computational particle on each cell of a DEM grid, computing the direction this particle would move from an 8-cell pour point model (O'Calligan and Mark, 1984), and computing the speed of the particle according to a uniform flow equation whose velocity term is determined by the slope along the particle path at the particle's current position. A short interval of time is allowed to pass, and the particle's new position is calculated and the entire computational process is repeated.

In this chapter a variation on these basic concepts was applied to produce a response function at the outlet with *S*-curve hydrograph properties. This empirical *S*-curve hydrograph is a residence time distribution of rainfall on the watershed and thus this distribution must contain information equivalent to the time-area histogram. A particle-tracking code originally developed by Cleveland (1991) and subsequently used in numerical dye-tracing of the confluence of two streams in Houston, Texas (Wang and others, 1991 and 1996) was modified to perform the grid arithmetic. This research code tracks the position of particles and records the exit time from the watershed of each particle and the cumulative exit times for all particles (the *S*-curve). This program is referred to as the Digital Terrain Runoff Model (DTRM). Specification of how the particles move in response to their position on the watershed elevation grid determines the specific shape of the S-curve and ultimately the estimates for T_p and T_c.

5.2 Motion Equations

Figure 5.1 depicts the watershed that drains past USGS gaging station 08057320. This watershed is referred to as the Ash Creek watershed in the remains of this thesis. This station is selected because the small size of the watershed is fast to get the test run results. In the figure the solid curve represents the path that a raindrop would follow from the northeast part of the watershed to the outlet located in the southwest corner of the watershed. This curve is called the pathline. Any point in the watershed can be represented by its Cartesian coordinates, x and y. A particle at any point in the watershed will lie on its pathline (determined by the particle's initial position relative to the outlet). The particle at any position will have an x-component and y-component of velocity, and these two components can be resolved into a pathline component of velocity. The relationship between the pathline system and the Cartesian system is depicted in Figure 5.1 as the two velocity vector systems on the Eastern side of the figure, near the peak of a hill. In the analysis, both coordinate systems were used. The pathline system was used to determine pathline velocities then these were converted into Cartesian velocities for the displacement steps. The reason for this seemingly duplicate effort was in anticipation of incorporating more complex kinematics in the future. The Universal Transverse Mercator (UTM) coordinate system used on the 30-meters DEM maps here is a grid-based method of specifying locations on the surface of the Earth and the units are in kilometers.

Figure 5. 1. Shaded relief map of watershed associated with USGS gaging station 08057320. A particle pathline, pathline and Cartesian velocities are depicted for a single rainfall particle.

Over a short time interval, the particle will move according to ordinary mechanics a distance determined by the product of the appropriate component velocities and the time interval. In the Cartesian coordinates, the set of trajectory equations for a particle is

$$\begin{aligned} x_p(t+\Delta t) &= x_p(t) + u_p(x_p(t), y_p(t), t)\Delta t \\ y_p(t+\Delta t) &= y_p(t) + v_p(x_p(t), y_p(t), t)\Delta t \end{aligned} \tag{5.1}$$

In equation 5.1, x and y are spatial locations, u and v are x-, and y- components of velocity at a location, t is time, and the subscript p is a particle index (i.e. the p-th particle). The equation, as written, represents a first-order Euler model to integrate the displacement rates of the particles. The equations require specification of the velocity of a particle at any location. In addition to these requirements, the specification of direction is critical. Either a Cartesian system (as above) or a path-line system can be used.

The principle advantage of a path-line system (if the pathlines are straightforward to compute) is that the kinematic equations reduce into a single spatial dimension (distance along the path). In the case of the constant, linear, and quadratic flux law models a pathline system is feasible and convenient.

There are three conventional simplified-physics approaches to velocity specification. The first is to assume velocity is a constant, and assign velocity independent of topographic relief (slope). Travel time is proportional to the path-line distance from the particle's initial placement to the outlet. This approach appears to be the method used by Kull and Feldman (1998), although they do acknowledge more complicated methods involving estimating overland and channel flow times. In the constant velocity approach a very flat watershed and a very steep watershed would have identical particle travel speeds.

The second approach is to assume velocity is proportional to watershed slope, and compute the velocity field based on the particle positions. Operationally one would compute velocities for each grid cell, and assign these velocities to particles residing in the cell until they exit that cell and enter another. This assumption is a potential flow approach where the watershed elevation is the flow potential. Equation 5.2 represents

the formula in a path line coordinate system used to determine the velocity at any location in the watershed. In practice we only have elevations at discrete grid points so a difference equation is used to determine the local watershed slopes.

$$u(\xi) = k * \left| \frac{dz}{d\xi} \Big|_{(\xi)} \right| \tag{5.2}$$

The value of k represents the velocity of the particle on a unit slope. These unit velocities could be estimated from classical overland flow equations or tabulations in use in current hydrology methods (e.g. NRCS). This motion equation is similar to time-area methods of Laurenson (1964), and Muzik (1996).

The third approach is to assume the square of velocity is proportional to watershed slope, and compute the velocity field dependent on the particle positions. This assumption is essentially a potential flow approach where the watershed elevation is the square-root of flow potential. Equation 5.3 represents the formula in a path line coordinate system used to determine the velocity at any location in the watershed.

$$u(\xi) \cdot |u(\xi)| = k^2 * \left| \frac{dz}{d\xi} \Big|_{(\xi)} \right| \tag{5.3}$$

The value of k^2 represents the square of velocity of the particle on a unit slope. The absolute value formulation is used so that the numerical method preserves correct directional information (flow is always downslope). This approach is similar to existing NRCS methods, but makes no distinction between channel and overland flow. All the results in this chapter are based on this kinematic model, and the procedure here could be interpreted as a modified NRCS-velocity method.

In the present work we have adopted the following structure for k (British unit)

$$k^2 = (\frac{1.5}{n} d^{\frac{2}{3}})^2 \tag{5.4}$$

Where n is a frictional term (an adjustable parameter) that is conceptually analogous but not numerically equal to Manning's n, d is a mean flow depth (an adjustable parameter).

Thus the combination of equations 5.3 and 5.4 is

$$u(\xi) = \frac{1.5}{n} d^{\frac{2}{3}} (\left| \frac{dz}{d\xi} \right|_{(\xi)} \Bigg|)^{\frac{1}{2}} \tag{5.5}$$

Equation 5.5 is intended to look like a Manning's equation (the last term is the local slope of the watershed at the particle location). This particular structure is selected to make the procedure look like Manning's type physics is incorporated. The resulting particle kinematics are analogs to Woodings (1965) kinematic wave analysis for overland flow and similar to the isochrone derivation technique of Sagafian and Julien (1995) who adapted the kinematic wave theory for distributed rainfall-runoff modeling and presented an example (Saghafian and others, 2002) for a watershed in West Africa.

The applicability of the velocity model is subject to an important consideration regarding the backwater effect from downstream. In this work we have implicitly assumed that there is no backwater effect, but the Houston watersheds are known to have backwater effects at the gaging stations as well as tidal influence. Additionally the Houston data have slopes one order of magnitude smaller than the remaining watersheds and the applicability of kinematic-wave type flow is questionable.

5.3 Direction and Slope in DTRM

Unit runoff in the model moves downhill according to the Manning's-like formula (Equation 5.5). Downhill direction in the model coordinates is determined by the relationship of the index (current cell) and the 8-cells surrounding it (O' Calligan and Mark, 1984). Figure 5.2 is a diagram of an index cell and its surrounding cells.

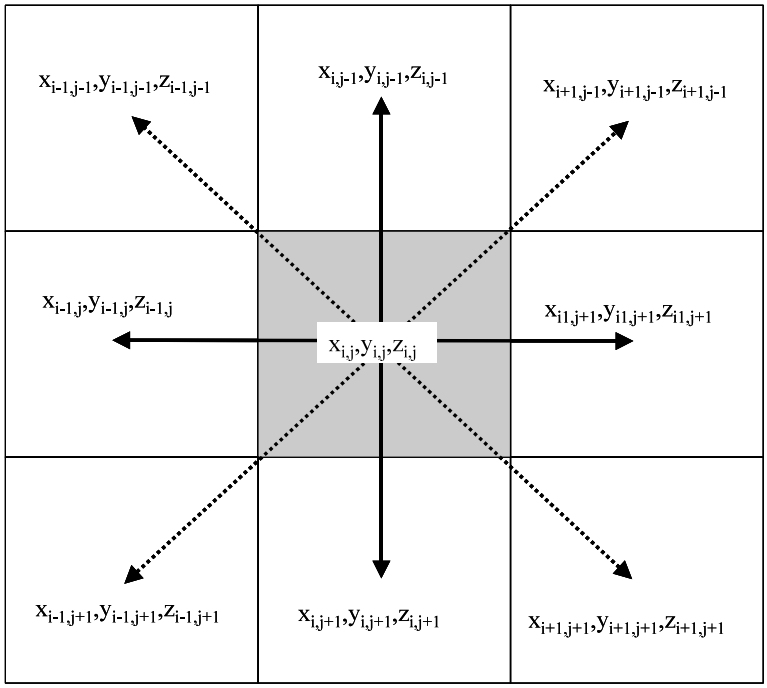

Figure 5.2. Cell pour-point model used to determine downhill direction and slopes for particle kinematics.

Downhill is determined in the following fashion: The elevation differences between the index cell and the 8 surrounding cells are computed (z-values in figure 5.2). This computation produces 8 different elevation differences. Of the 8 differences the largest positive value is chosen as the downhill direction (negative differences are uphill relative to the index cell). This direction is stored in a direction map array. It represents the direction a water parcel will move if it resides anywhere in the index cell.

Furthermore this direction map also defines the pathline system for the index cell. If there is no downhill direction the cell is labeled as a sink and treated separately below. The slope is computed using the selected difference value (from the direction finding step), and dividing by the travel distance from cell-to-cell. Once the speed is known, the time to travel from cell-to-cell can be determined from the ratio of cell-to-cell distance along the travel path and the speed just calculated, or the particle can simply be allowed to move downhill for a specified time interval.

For example in Figure 5.1, the marker where the velocity vectors originate is located approximately at elevation 577 feet in the digital map array. The eight cells surrounding the marker starting directly North and moving clockwise are at elevations 580, 581, 581, 579, 578, 576, 577, and 579 feet. Only 576 feet is lower in elevation than the reference cell of 577 feet so the direction that the particle could move is to the South-West. The difference in elevation between the two cells is 1 foot of elevation. The distance from the two cell centers is $\sqrt{2} \times 30$ meters = 138 feet. Thus the dimensionless slope in the cell is computed to be 1/138 = 0.007. The travel speed of the particle in this cell is $u(\xi) = (1.5/n)d^{0.67}(0.007)^{0.5}$. The numerical values of n and d were determined by trial-and-error for a single storm.

5.4 Pits and Channel Flow

Sinks (pits) in the elevation grid are treated separately. In the data for station 08057320, Ash Creek at Highland Road, Dallas, Texas it was observed that the sinks occurred at or near locations where there was an obvious channel in the relief map, so it was subsequently assumed that sinks (in this model) represent locations where channel

flow begins. Rather than smooth the watershed elevation map as was done by many other researchers, it was decided to force the particle to move from the sink towards the outlet. The flow direction is directly from a sink to the single watershed outlet. For example, Figure 5.3 is a rendering of the Ash Creek watershed looking from the West. The location of a sink is depicted on the figure, there are other sinks, but the one in the figure is most apparent. The flow path is the Euclidian path from the sink to the outlet. This path is indicated by the dashed line on Figure 5.3. Slope is determined from the elevation difference between the sink and the outlet and this straight-line flow distance. Speed and time of travel are then computed as above.

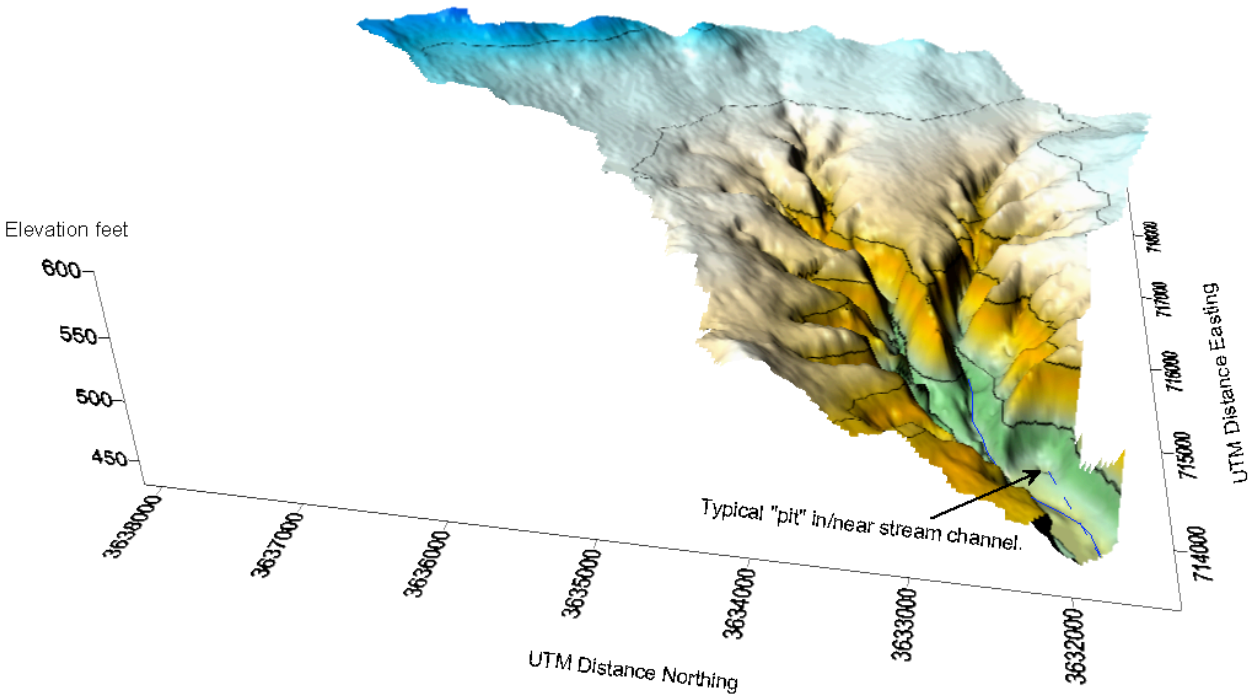

Figure 5.3. Surface rendering of watershed associated with USGS gaging station 08057320 (Units in KM) showing a sink and the assumed flow path from sink to the outlet.

This ad-hoc treatment of pits is a significant departure from previous studies, but replaces the need to carefully identify channel paths, and eliminates a smoothing step thus preserving the elevation array intact.

5.5 Hydrograph Timing Parameters

Watershed representation.

All time-area methods require some kind of information about the spatial distribution of watershed elevation. This information can be obtained manually from USGS topographical maps, by engineering survey, or from USGS digital elevation models (DEM). Regardless of the original source, the representation will eventually be a grid whose horizontal and vertical elements will represent locations on the surface of the Earth, and whose entries will represent elevation above some datum. The results reported here are based on USGS 30-meter DEM maps downloaded from the Internet.

Once the DEM is constructed, the file is converted into a format for the particle-tracking model. Essentially this step adds the location of the outlet to the file, some simulation control instructions, and the values of n and d. One file for each watershed was prepared in this manner. In addition the Ash Creek watershed was constructed entirely manually (using elevations read from paper maps) at a lower resolution to demonstrate the generality of the procedure.

Particle position maps

The computation of the trajectory of each individual particle produces a "cloud" of particles distributed on the watershed at any simulation time. These particle maps

have some value in determining how the particles traverse the watershed and when channel-like flow begins (i.e. all particles confined to narrow curvilinear features). Figure 5.4 is an example of the particle maps for the Ash Creek watershed using manually entered elevations. In the figure the positions of particles still in the watershed are plotted at different times. In Figure 5.4 one can see the general outline of the watershed is illustrated at time zero. As time evolves the particle "cloud" moves downslope toward the outlet. At about 30 simulated minutes (white triangles) the channel structure is apparent. It is noted that the elevation array in Figure 5.4 was manually prepared from paper-based maps and is at a much different resolution (~190 meters) than in Figures 5.1 and 5.3. It is also noted that Figure 5.4 is distorted with respect to vertical and horizontal distances.

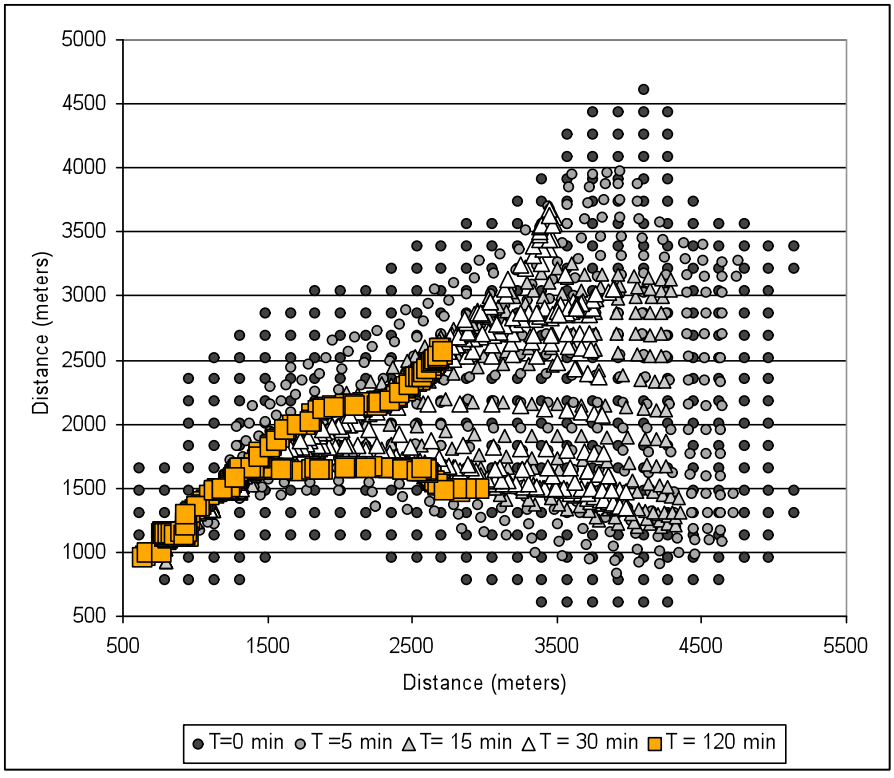

Figure 5.4 Particle positions at various times: Ash Creek watershed.

Particle map images (Figure 5.4) are illustrative of what is going on in the calculations, but are not particularly useful for unit hydrograph analysis. Instead the cumulative arrival time distribution of particles at the outlet is more important.

Generating the *S*-Curve Hydrograph

Figure 5.5 is a plot of the normalized arrival time distribution for the simulation in Figure 5.4 and represents the *S*-curve hydrograph for the watershed. Counting particles as they exit the computational domain and recording their exit time thus generates a cumulative arrival time distribution. The *S*-curve outlet hydrograph is derived from this arrival time distribution.

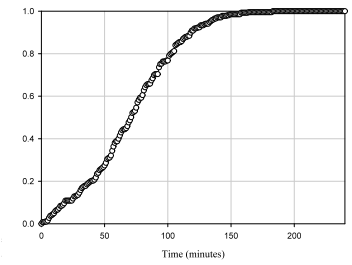

Figure 5.5. Empirical S-curve hydrograph.

The cumulative arrival time distribution is normalized by dividing the arrival time distribution (number of particles arrived at a given time) by the total number of particles

placed on the watershed. This normalized distribution (Figure 5.5) is used in the next step to fit an equivalent curvilinear unit hydrograph model and from that model extract the timing values.

On the illustrated watershed, using a 30-meter resolution DEM, 20,639 paths were identified (one of each grid cell on the approximately 7 square mile watershed) that drain the outlet located in the lower left corner of the figure. On some of the larger watersheds, over 500,000 paths were identified. Each path is defined by an individual particle's starting point, and each particle follows its own unique path. Equation 5.5 is evaluated at least once for each path, and multiple times for paths that traverse long distances across the watershed as particles move down-slope towards the outlet. The entire ensemble of the particles is moved contemporaneously and the arrival times of individual particles at the watershed outlet are recorded. The cumulative arrival time distribution of the particle ensemble is the residence time distribution of excess rainfall on the watershed and contains information equivalent to an S-curve hydrograph. Alternatively, one could compute the total travel time along each path and rank order these arrival times to construct the arrival time distribution. By fitting a unit hydrograph model to this empirical S-curve, unit hydrograph parameters are recovered. Figure 5.5 is one such cumulative arrival time distribution for the Ash Creek Watershed in Dallas, TX.

The computational burden is extreme, even though the approach as presented is highly parallel (the particles do not interact). A purpose-built cluster computer (Cleveland and Smith, 2004) was used to speed the computational throughput, by distributing the particle position computations among multiple processors. Despite

taking advantage of the parallel structure of the problem, it still takes considerable time to complete the description of even a single watershed.

Generating the Curvilinear Model

The output from the DTRM program is a time series that represents the empirical cumulative hydrograph. This cumulative hydrograph is shown on Figure 5.6 as the open circles. It is monotonically increasing towards its asymptotic value of unity as expected with a cumulative hydrograph. A curvilinear function is fit to the cumulative hydrograph so that we can use the curvilinear model for simulation of the direct runoff hydrograph.

The unit hydrograph model selected for this research is a generalized gamma distribution (Leinhard, 1964; 1967) and is expressed as

$$f(t) = \frac{\beta}{\Gamma(n/\beta)}\left(\frac{n}{\beta}\right)^{n/\beta}\frac{1}{t_{rm\beta}}\left(\frac{1}{t_{rm\beta}}\right)^{n-1}\exp\left[-\frac{n}{\beta}\left(\frac{t}{t_{rm\beta}}\right)^{\beta}\right] \tag{5.6}$$

The distribution parameters n and $t_{rm\beta}$ have physical significance in that $t_{rm\beta}$, is a mean residence time of a raindrop on the watershed, and n, is an accessibility number, roughly equal to the exponent on the distance-area relationship (a shape parameter). β is the degree of the moment of the residence time; $\beta=1$ would be the arithmetic mean, while for $\beta=2$ the residence time is a root-mean-square time. $\beta=2$ is used throughout this work. Unit hydrograph function can also be expressed as a dimensionless hydrograph using the following transformations (Leinhard, 1972) to express the distribution in conventional dimensionless form.

$$t_{rm\beta} = \left(\frac{n}{n-1}\right)^{1/\beta} T_p \tag{5.7}$$

$$Q_p = f(T_p) \tag{5.8}$$

Expressed as a dimensionless hydrograph distribution, then it becomes

$$\frac{Q}{Q_p} = \left(\frac{t}{T_p}\right)^{n-1} \exp\left[-\frac{n-1}{\beta}\left(\left(\frac{t}{T_p}\right)^{\beta} - 1\right)\right] \tag{5.9}$$

The cumulative distribution function is determined by integrating Equation 5.6 and this cumulative distribution is fit to the empirical S-curve hydrograph using a least square error minimization criterion. Once the distribution parameters, n and $t_{rm\beta}$ are recovered, they are then converted into conventional hydrograph parameters using Equation 5.7 and 5.8. Figure 5.6 shows that the cumulative arrival time distribution for Ash Creek Watershed also displays the "fitted" Leinhard unit hydrograph, which is the source of the timing parameters for subsequent rainfall-runoff modeling.

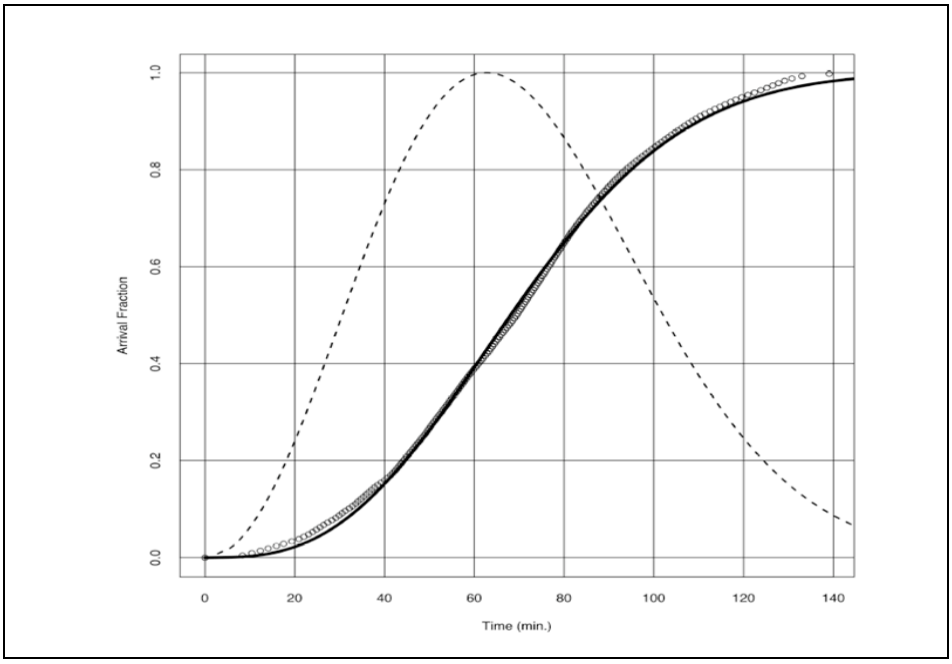

Figure 5.6. Fitting curvilinear hydrograph model to empirical S-curve.
Empirical cumulative arrival time distribution (open circle)
and fitted cumulative unit hydrograph distribution(solid line).
The dashed line is the dimensionless unit hydrograph for this watershed.

The solid *S*-curve is the cumulative distribution function based on the unit hydrograph function (Equation 5.6 above). It is "fit" to the empirical cumulative distribution function generated by the particle-tracking model using a least square error criterion and a reduced gradient method to minimize the error.

In principle, the time of concentration, T_c, should be the time at which the cumulative hydrograph is unity, but the cumulative hydrograph approaches unity asymptotically. T_c was selected as the time when the cumulative hydrograph obtained a value 0.98, a fraction of the total distribution. The choice of the value 0.98 is strictly ad hoc, and no rigorous selection method was applied.

The result is that the values of n and $t_{rm\beta}$ are determined from a terrain model, which is conceptually equivalent to determining unit hydrograph parameters from physical watershed characteristics (for example: main channel length, slope, etc.), except this work considers the ensemble of characteristics (all the potential flow paths, all the slopes along these paths, etc.).

The DTRM was applied to the entire set of watersheds using 30-meter digital elevation data. The watersheds were classified into "developed" and "undeveloped" watersheds. Representatives of each classification existed in all the database modules, thus the classification does not reflect a particular geographic location. The values used in equation 5.5 for generating the cumulative hydrographs for developed watersheds are n=0.04 and d=0.2. These values were determined by trial-and-error using the Ash Creek watershed (a developed watershed) and the June 3, 1973 storm to calibrate the particle-tracking model. These two values were applied to all developed watersheds regardless of size and location. The values used in equation 5.5 for generating the cumulative

hydrographs for undeveloped watersheds are n=0.08 and d=0.2, and were determined by a single-storm trial and error "calibration" of the Little Elm watershed. These two values were applied to all underdeveloped watersheds regardless of size and location.

For each watershed, DTRM was run once using the appropriate n_f and d values and a single Leinhard hydrograph, with two parameters, n and $t_{rm\beta,}$ is generated for each watershed. These two values are determined entirely from topographic data and the assumed n_f and d; no actual rainfall-runoff data is used by the DTRM.

In appendix Table 2 is a list of the estimated watershed parameter values for each watershed successfully analyzed. The list is a composite of manual and automated results in an effort to extend the number of successful analysis.

5.6 Application of DTRM

For each watershed DRTM was run once and a single Rayleigh hydrograph, with two parameters, a residence time, and a reservoir number, are generated (i.e. two values for each watershed). These two values are determined entirely from topographic data and the assumed friction coefficient.

The rainfall loss models using here are Initial Abstraction Constant Loss model (IACL), Fractional Loss Model (FRAC), and Green-Ampt Infiltration (GAIN) model. Therefore DTRM model is running three times based on different loss models.

Figure 5.7 is a representative example of output from this testing. The observed hydrograph is the dashed line with the step-wise changes in value, while the smooth curve is the model result using the same hyetograph (input rainfall).

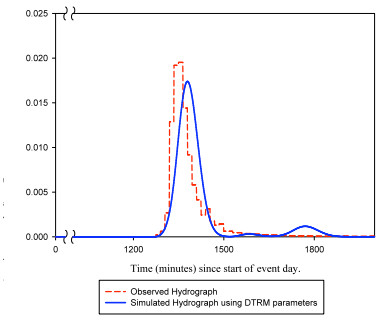

Figure 5.7. Model (based on DTRM parameters) and observed hydrographs for Ash Creek for May 27, 1975 storm.

The plot in Figure 5.7 is typical, but not all storms were reproduced equally well, especially on the larger watersheds. Despite this current limitation, the analysis suggests that the topographic information alone is sufficient to produce qualitatively acceptable hydrographs.

136 storms are randomly selected to measure the "fit" of the hydrographs between observed and modeled runoff. The measurements are the average mean value of the residuals (MEAN), median value of residuals (MEDIAN), standard deviation of residuals (SD) and the inter-quartile range of residuals (IQR). These values represent how much

the “difference” between the curves of the hydrographs. IQR is a measure of the spread of or dispersion within a data set, it is calculated by taking the difference between the upper and the lower quartiles. It is the width of an interval, which contains the middle of 50% of the sample. So it is smaller than the range and its value is less affected by outliers. The results are listed in Table 5.1. Figure 5.8 shows the plots of these measurements over the selected 136 storms. FRAC has an ideal close to zero MEAN and MEDIAN values, and has an acceptable SD value in a small range up to 0.01. IACL and GAIN models have very similar results in these measurements, which is as expected because IACL can always be looked as a special case of GAIN models.

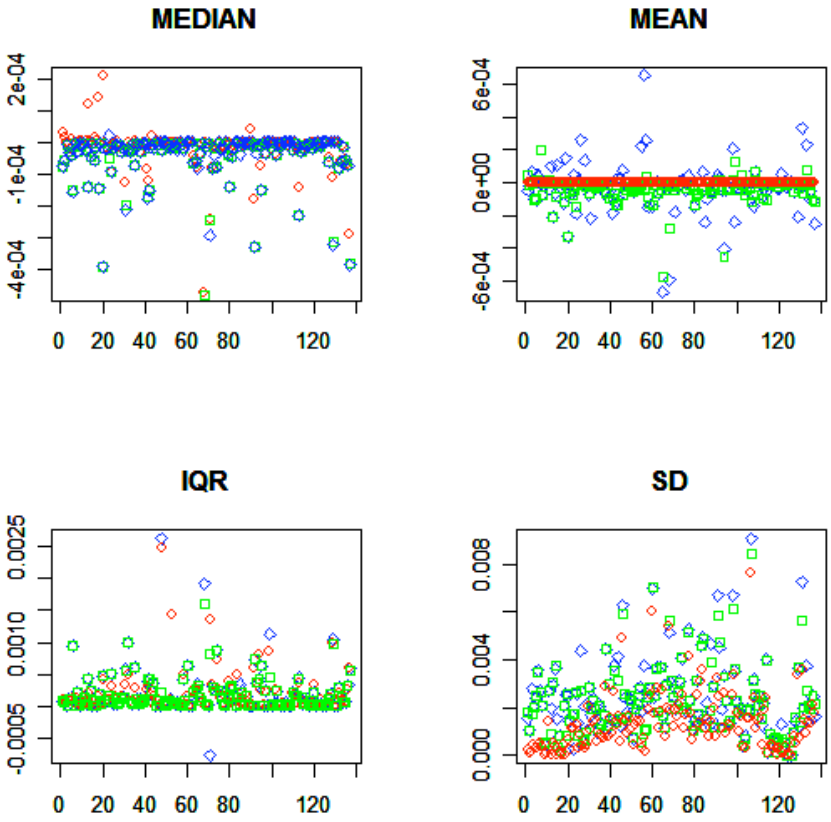

Figure 5.8: The plots of runoff hydrograph "fits" measurements, where Red circle=FRAC, Green square=IACL, Blue diamond=GAIN.

The results of DTRM model will be evaluated by comparing with conventional analysis of unit hydrograph, which developed directly from the observed data (Cleveland, 2006). Figure 5.9 is a set of plots that qualitatively illustrate the performance of the approach on over 2200 storms. The left panels are the results when the unit hydrographs are generated using the DTRM procedure using FRAC loss model, the right panels are the same storms, except the hydrograph parameters were determined by conventional analysis (i.e. rainfall and runoff data are used, no knowledge of watershed physical characteristics is used). The upper plots are the observed peak discharge and simulated peak discharge for individual storms. An equal-value line is plotted that represents an ideal result. The variability of the DTRM procedure is larger, and the DTRM result is more symmetric around the equal value line. The increased variability is anticipated as the method has no access to rainfall data to estimate hydrologic response.

The lower plots are the time when the peak discharge occurred in either the observations or the simulations. As in the upper plots, the variability for the DTRM procedure is larger. The median values of the peak discharge or time of peak discharge (for roughly 2200 storms) are similar regardless of classification (observed, simulated-DTRM, simulated-Conventional). A Kruskal-Wallis test supports this conclusion – there is no evidence to reject the null hypothesis that the median values do not differ for either method when compared to each other or to the observations at a level of significance of $\alpha = 0.05$.

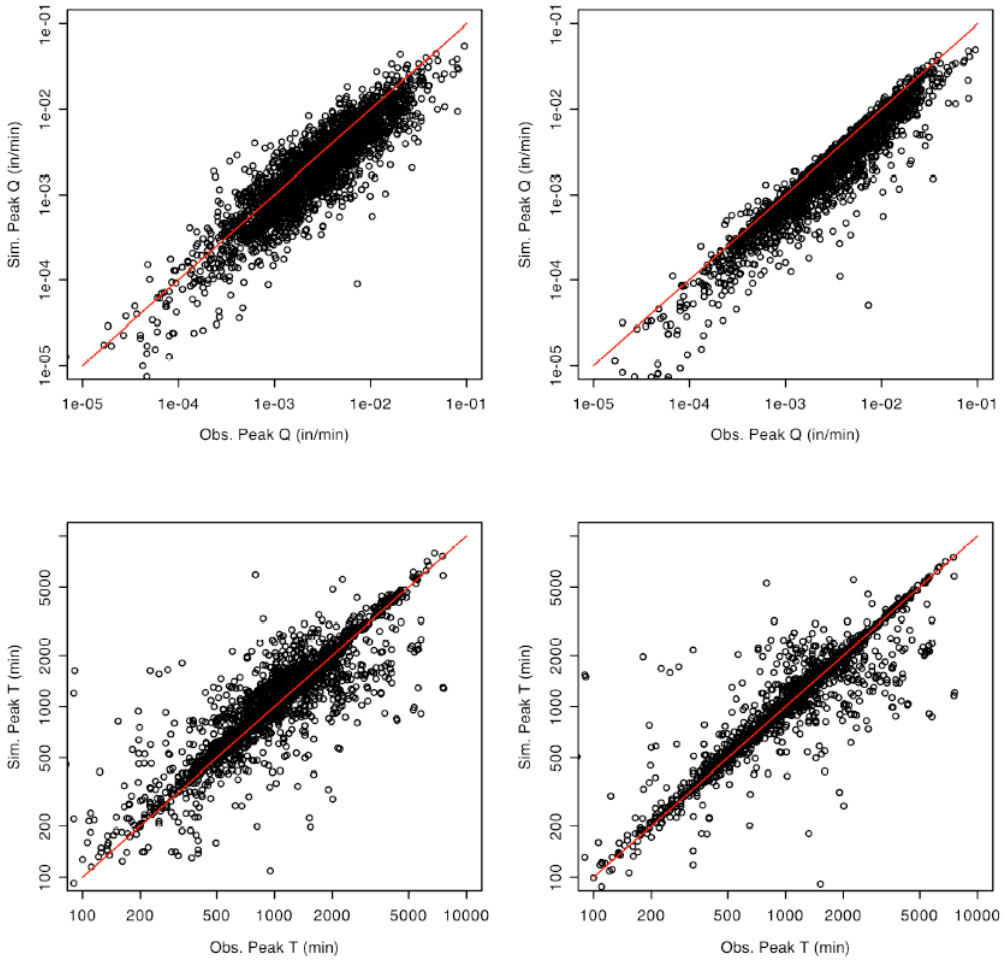

Figure 5.9: Relationship of simulated and observed peak flows (Q) and time of peak flows (T) for storms using particle tracking model (left images) and conventional hydrograph analysis (right images)

Further analysis is performed on other two loss models. Figure 5.10 and Figure 5.11 are a set of plots comparing the DTRM model with the observed data using three loss models on over 1600 storms. GAIN model has a bigger variability than the other two loss models in both T_p and Q_p predictions, however most of the points are clouded around equal-vale lines.

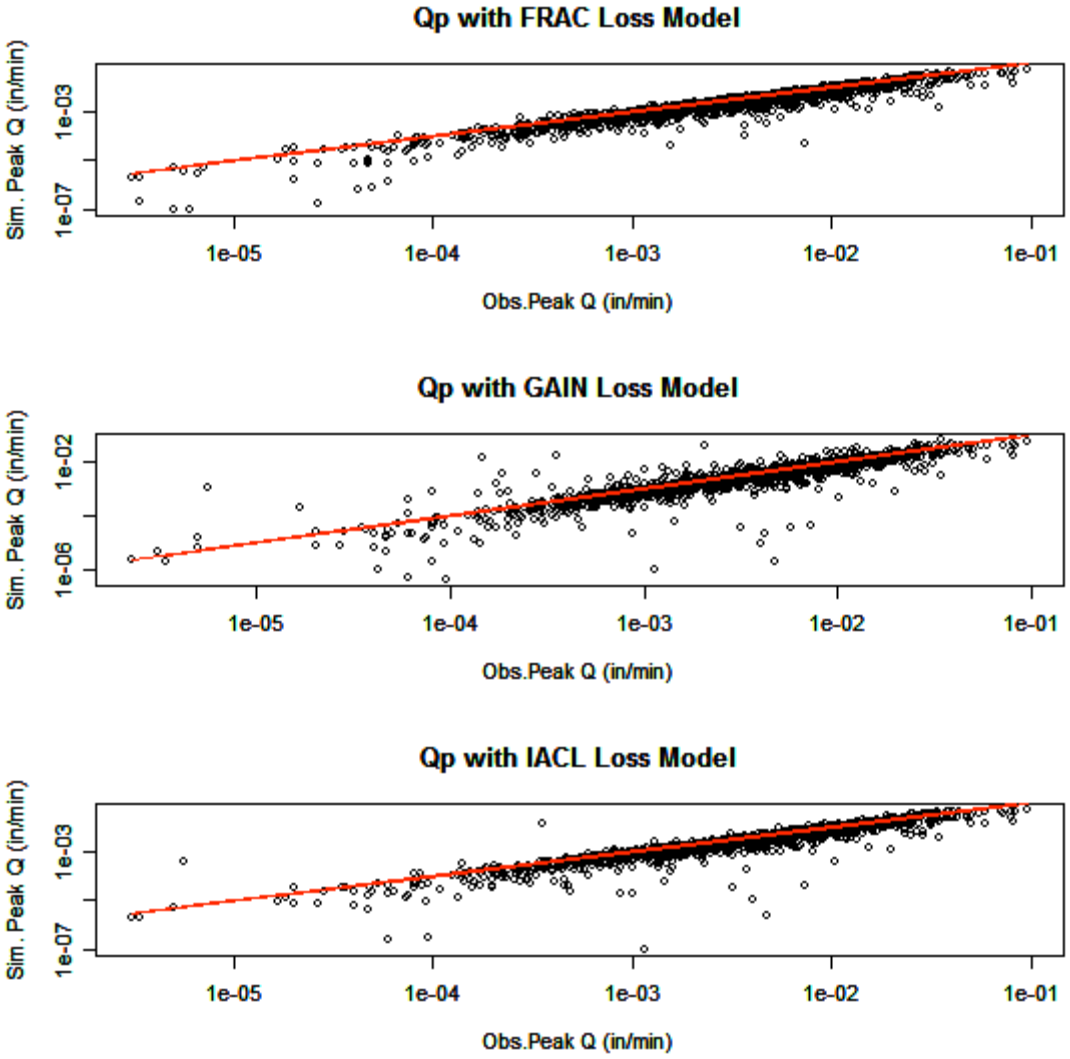

Figure 5.10 : Relationship of simulated and observed peak flows (Q)

for over 1600 storms using three loss models.

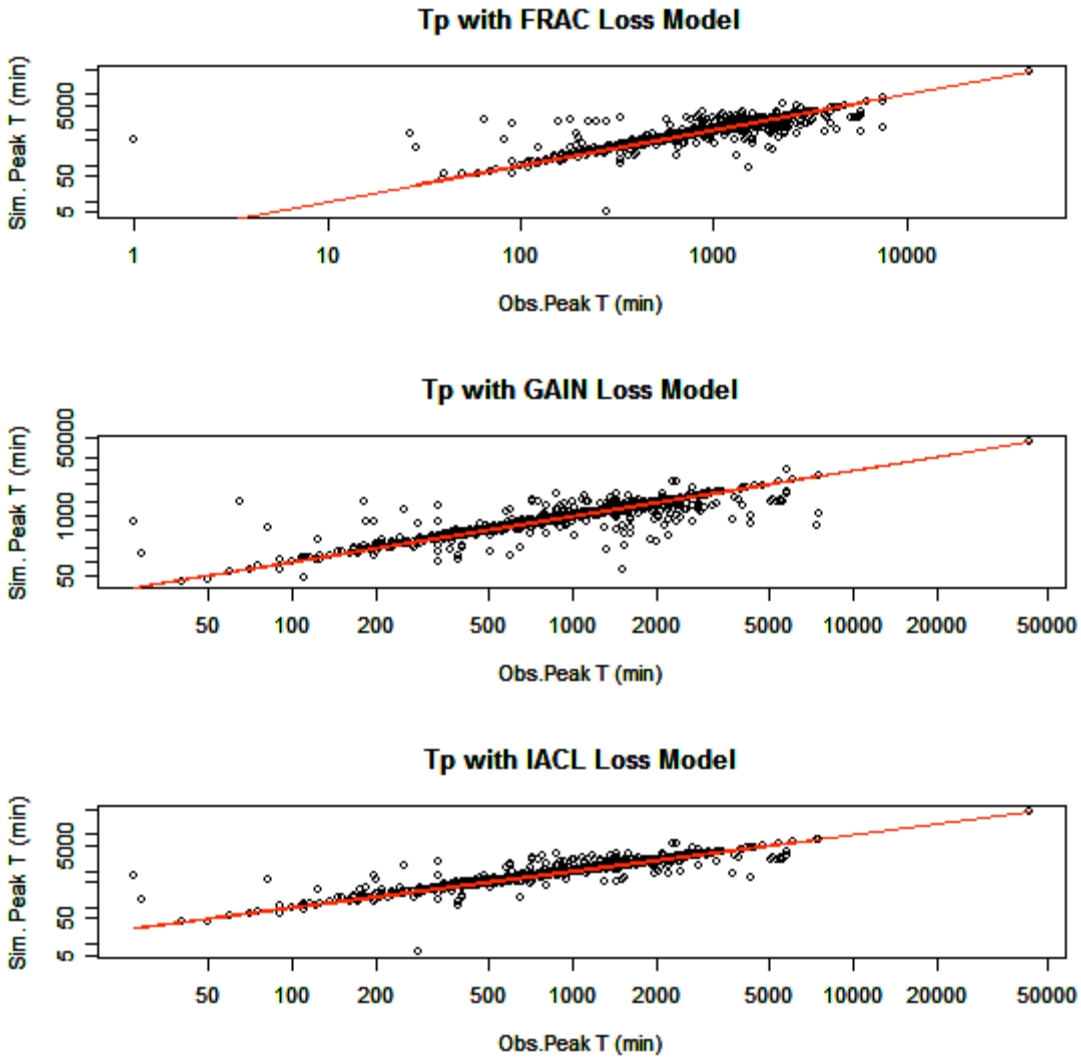

Figure 5.11 : Relationship of simulated and observed peak time (T)

for over 1600 storms using three loss models.

These results qualitatively demonstrate that a terrain-based runoff model can produce acceptable direct runoff hydrographs with minimal calibration using only elevation data to generate a unit hydrograph. Combined with the rainfall loss model the approach can simulate episodic behavior at about the same order of magnitude in terms of peak discharge and temporal bias.

CHAPTER 6

CONCLUSIONS

The unit hydrograph is defined as a direct runoff hydrograph resulting from a unit pulse of excess rainfall generated uniformly over the watershed at a constant rate for an effective duration. The unit hydrograph method is a well-known hydrologic-engineering technique for estimation of the runoff hydrograph given an excess rainfall hyetograph. Methods to estimate the unit hydrograph for ungaged watersheds using common watershed characteristics and topographic information of watershed is useful to hydrologic engineers. A synthetic unit hydrograph method is proposed here, based on a digital elevation model. A large database of more than 2200 storms with both rainfall and runoff data for 126 watersheds in Texas is used for unit hydrograph investigation approaches.

The terrain-based runoff model can generate qualitatively acceptable direct runoff hydrographs from minimal physical detail of the watershed. Only elevation data and assumptions about travel velocities are required to predict watershed response. The requisite elevation data are freely available on the Internet, or can be hand-prepared from paper-based maps.

No attempt was made to optimize the friction terms in the DTRM model to account for different land-uses, etc., yet combined with an appropriate rainfall loss model the approach has simulated episodic behavior at about the same order of magnitude as

observed behavior in terms of peak discharge and temporal bias. Thus, for the small watersheds studied in this research, topography is a significant factor controlling runoff behavior (more so than land-use and other descriptive considerations) and consequently the timing parameters common in all hydrologic models.

Three loss models are chosen for the study, they are Initial Abstraction Loss Model (IACL), Fractional Loss Model (FRAC) and Green-Ampt Infiltration (GAIN) Loss Model. The results didn't come with too much difference compared for these three loss models, although the IACL model and GAIN model did come with more similar results. And this is expected because IACL model can be looked as a special case of GAIN. Also the loss models have little impact on the timing parameters of the study watersheds.

The DTRM is related to existing NRCS methods, and could be considered to be a modified NRCS velocity approach where the analysis is completely automated and the kinematics are performed within the model without analyst interaction. The method ignored distinctions between channel flow and overland flow yet produced estimates within +/- two standard deviations of other methods. The similarity of the results to the other methods both increases confidence in the other methods, and indicates that the other methods, while overtly empirical, incorporate similar simplified-physics as does DTRM.

The final comparison of the DTRM model with the observed runoff data gave a sound prediction for the peak discharge and the time to peak. Also for the selected storms, a good "fit" results can be seen for the modeled and observed runoff curve.

Future suggestions

Since we make no difference on particle's travel velocity over the while watershed, the local slope is highly related to the travel time. And for the urban city area like Houston or other more "flat" watersheds, the DTRM model cannot perform well compared with observed runoff data. This is because in the real situation, the particle's velocity also depends on the channel depth while we made the constant depth assumption. Also the runoff prediction runs good for single storm event. But for the multiple storms, the loss model and the unit hygrograph's assumption may be totally changed.

REFERENCES

Appleby, V.C. (1970), "Recession and the Base Flow Problem", *Water Resources Research*, Vol. 6., No. 5, pp 1398-1403.

Asquith, W.H., and R. M. Slade, (1997), "Regional Regression Equations for Estimation of Peak Streamflow Frequency for Natural Basins in Texas.", *U.S. Geological Survey Water Resources Investigations Report 1996-4307*, 68p.

Asquith, W. H., Thompson, D. B., Cleveland T. G. and X. Fang. (2004), "Synthesis of Rainfall and Runoff Data used for Texas Department of Transportation Research Projects O-4193 and O-4194" *U.S. Geological Survey , Open File Report 2004-103*, p 50.

Bahram Saghafian, Pierre Y. Julien and H. Rajaie (2002), "Runoff Hydrograph Simulation Based on Time Variable Isochrone Technique", *Journal of Hydrology*, 261, 193-203.

Barnes , B. S. 1959. "Consistency in Unitgraphs". *Journal of the Hydraulics Division,* 85(HY8)**,** 39-61.

Bates, B., and Davies, P.K.(1988), "Effect of Base Flow Separation on Surface Runoff Models.", *J. of. Hydrology*, v103, pp 309-322.

Bell, F. C., and S. O. Kar. (1969), "Characteristic Response Times in Design Flood Estimation". *Journal of Hydrology,* 8, 173-196.

Bedient, P., Huber, W. (1948), "Hydrology and Flood Plain Analysis", *Addison-Wesley Publishing Company.*

Bender, Donald L. and Roberson, John A.(1961), "The Use of a Dimensionless Unit Hydrograph to Derive Unit Hydrographs for Some Pacific Northwest Basins", *Journal of Geophysical Research*, 66(2), pp 521-527.

Blank, D., Delleur, W., and A. Giorgini.(1971), "Oscillatory Kernel Functions in Linear Hydrologic Models." *Water Resour. Res., Vol. 7, No. 5*, pp 1102-1117.

Boufadel, Michel C.(1998), "Unit Hydrographs Derived from the Nash Model", *Journal of the American Water Resources Association*, 34(1).

Bree, T. (1978), "The Stability of Parameter Estimation in the General Linear Model." *J. Hydrology, Vol 37., No. 1*, pp 47-66.

Brent M. Troutman and Michael R. Karlinger (1985), "Unit Hydrograph Approximations Assuming Linear Flow through Topologically Random Channel Networks", *Water Resources Research*, Vol. 21, No.5, p 743-754.

Brown, J.R., Ulery, R.L., and Parcher, J.W. (2000), "Creating a Standardized Watersheds Database for the Lower Rio Grande/Rio Bravo, Texas." *U.S. Geological Survey Open-File Report 2000-065*, 13p.

Bruce N. Wilson and J. William Brown (1992), "Development and Evaluation of A Dimensionless Unit Hydrograph", *Water Resources Bulletin*, Vol. 28, No. 2 p: 297-408.

Bruen, M. and Dooge, J.C.I.(1992), "Unit Hydrograph Estimation With Multiple Events and Prior Information: I. Theory and a Computer Program", *Hydrological Sciences Journal*, 37(5), pp 429-443.

Canavos, G. C. (1984), "Applied Probability and Statistical Methods" Little, Brown and Company, Boston, Massachusetts, 1984, pp. 149-153.

Capece, J. C., K. L. Campbell, and L. B. Baldwin. (1986), "Estimation of runoff peak rates and volumes from flatwoods watersheds." *Agricultural Engineering Department, Institute of Flood and Agricultural Sciences, University of Florida, Gainesville, Florida.*

Charbenau, R.J. (2000), "Groundwater Hydraulics and Pollutant Transport", *Prentice Hall, New Jersey,* 593p.

Chow, V. T., (1964). "Handbook of Applied Hydrology", *McGraw Hill*, *New York.* Sec. 14.

Chutha, P., and J. C. I. Dooge, "The Shape Parameters of the Geomorphologic Unit Hydrograph", *J. of Hydrology*, 117, 81-97.

Clark C. O. (1945), "Storage and the Unit Hydrograph", *Tran. Am. Soc. Civ. Engrs*, 110, 1419-1488.

Cleveland, T.G., (1991), "A Comparison of Sampling Design Criterion Using a Lagrangian Particle Tracking Model for Transport in Porous Media", *Final Report to Houston Advanced Research Center, Woodlands, Texas.* 54p.

Cleveland, T.G., Thompson, D., Fang,X. (2003), "Instantaneous Unit Hydrographs for Central Texas", *Proceedings of Texas Section Spring 2003 Meeting, Corpus Christi, Texas. Data @* http://129.7.204.231/Texas_Hydrology/texas_paired_data.html

Cleveland, T.G., X. He., Asquith, W.H., Fang, X., and Thompson, D.B., (2006), "Instantaneous Unit Hydrograph Selection for Rainfall-runoff Modeling of Small Watersheds in North and South Central Texas." *J. Irrigation and Drainage Engineering*, *ASCE* , Vol 132, No 5, pp 479-485.

Collins, W.T., (1939), "Runoff Distribution Graphs from Precipitation Occurring in More Than One Time Unit", *Civil Engineering*, 9(9), pp 559-561.

Commons, G. G..(1942), "Flood Hydrographs", *Civil Engineering*, 12(10), pp 571-572.

Croley II, Thomas E. (1980), "Gamma Synthetic Hydrographs," *Journal of Hydrology*, 47, pp. 41-52.

Daniel W. Kull and Arlen D. Feldman (1998), "Evolution of Clark's Unit Graph Method to Spatially Distributed Runoff", *Journal of Hydrologic Engineering,* Vol.3 No. 1.

Dooge, J.C.I. (1973), "Linear Theory of Hydrologic Systems." *U.S. Dept. of Agriculture, Technical Bulletin 1468.*

Dooge, J.C.I. (1959), "A General Theory of the Unit Hydrograph", *Journal of Geophysical Research*, 64(2), pp. 241-256.

Dooge, J.C.I. and Bruen, Michael (1989), "Unit Hydrograph Stability and Linear Algebra", *Journal of Hydrology*, 111, pp 377-390.

Eagleson, P. S. (1962), "Unit Hydrograph Characteristics for Sewered Areas." *Journal of the Hydraulics Division,* 88(HY 2)**,** 1-25.

Eagleson, P. S., Mejia-R, R., and March, F., (1966), "Computation of Optimum Realizable Unit Hydrographs", *Water Resources Research*, 2(4), pp 755-764.

Edson, C. G. (1951), "Parameters for Relating Unit Hydrograph to Watershed Characteristics", *Trans. Am. Geophys. Union*, 32(4), pp 591-596

Epsey, W. H., and C. W. Morgan. (1966), "A Study of Some Effects of Urbanization on Storm Runoff from a Small Watershed*." Report No.3. Texas Water Development Board Austin, TX.*

Espey, W. h., and D.G. Altman. (1978), "Nomographs for Ten Minute Unit Hydrographs for Small Urban Watersheds." Epa-600/9-78-035. Environmental protection Agency Washington D.C.

Fang, X., and S. Dehui. (2003), “Estimating Traveling Time of Flat Terrain by 2-dimensional Overland Flow Model.” The international symposium on shallow flows, Delft University of Technology, The Netherlands June 16-18.

Fang, X. Cleveland, T. G., Garcia, C. A., Thompson, D. B., and R. Malla. (2005), “Literature Review on Time Parameters for Hydrographs.” *Texas Department of Transportation Research Report 0-4696-1. Lamar University,* 82 p.

Francis R. Hall (1968), “Base-Flow Recessions-A Review”, *Water Resources Research*, Vol. 4 No. 5. 973-983.

Gaddi Ngirane-Katashaya and Robert Cowen (1999), “Modeling of A Dimensionless Synthetic Unit Hydrograph”, *Water S. A*., Vol. 25. No. 1 p 25-32.

Garg, S. K. (2001), “Irrigation Engineering and Hydraulic Structures.” *Khanna Publishers.*

Gert Aron and Elizabeth L. White (1982), “Fitting a Gamma Distribution Over A Synthetic Unit Hydrograph”, *Water Resources Bulletin*, Vol. 18, No. 1 p:95-98.

Gray, D. M. (1961), “Synthetic Unit Hydrographs for Small Watersheds”. *Journal of the Hydraulics Division***,** 87(HY4)**,** 33-54.

Haan, C. T., B.J. Barfield, and J.C. Hayes (1994), “Design Hydrology and Sedimentology for Small Catchment”, *Academic Press, New York.*

Haktanir, T., and N. Sezen. (1990), “Suitability of Two-parameter Gamma and Three–parameter Beta Distributions as Synthetic Unit Hydrographs in Anatolia.” *Hydrological Sciences,* 35(2)**,** 167-184.

Holtan H. N.(1961) , “A Concept for Infiltration Estimates in Watershed Engineering”, *USDA Bull*. P 41-51.

Holtan, H. N. and Overton, D. E. (1963), “Analyses and Application of Simple Hydrographs”, *Journal of Hydrology*, 1(3), pp 250-264.

Horner, W. W., and F. L. Flynt., (1936), “Relation between rainfall and runoff from small urban areas.”, *Trans. ASCE,* 101(140-206).

Horton, R. E., (1940), “An Approach toward a Physical Interpretation of Infiltration-Capacity,” *Soil Sci. Soc. Am. J.* vol. 5, pp. 399-417.

Huber, W. C. (1984), “Discussion of "Estimating Urban Time of Concentration". 122-124.

Hydrologic Engineering Center (HEC), (2000), “Hydrologic Modeling System”, HECHMS, *Technical Reference Manual*, 149 p.

I. Muzik (1996), “Flood Modeling with GIS-Derived Distributed Unit Hydrographs”, *Hydrological Processes*, Vol. 10, 1401-1409.

Izzard, C. F., (1946), “Hydraulics of Runoff from Developed Surfaces.”, *26th Annual Meetings of the Highway Research Board*.

J. A. Mawdsley and A. F. Tagg (1981), “Identification of Unit Hydrographs From Multi-event Analysis”, *Journal of Hydrology*, Vol. 49(1981) 315-327.

James, W. P., P.W. Winsor, and J.R. Williams. ,(1987), “Synthetic Unit Hydrographs”. *Journal of Water Resources,* 113(1)**,** 70-81.

J.A.Van Mullem, Member, ASCE (1991), “Precipitation Distributions and Green-Ampt Runoff”, *Journal of Irrigation and Drainage Enineering*, Vol.117. No.6.p:944-959.

J.E. Nelson and N.L. Jones (1995), “Reducing Elevation Runoff Error in Digital Elevation Data”, *Journal of Hydrology*, 169, 37-49.

Jin C., “A Deterministic Gamma-type Geomorphologic Instantaneous Unit Hydrograph Based on Path Types”, *Wat. Resour. Res.*, 28(2), 479-486, 1992.

Kent, K. M. (1972). “Travel time, Time of Concentration and Lag.” Chapter 15, the section 4 “Hydrology” of the National Engineering Handbook.

Kerby, W. S. (1959), “Time of Concentration for Overland Flow”, *Civil Engineering,* 29(3)**,** 174.

Kirpich, Z. P. (1940), “Time of Concentration of Small Agricultural Watersheds.”, *Civil Engineering, ASCE,* 10(6)**,** 362.

Khanal, P. C. (2004). ,“Development of Regional Synthetic Unit Hydrograph for Texas Watersheds.” Master Thesis. Lamar University.

Kreyszig, E. (1979), “Advanced Engineering Mathematics”, Wiley, New York, 939p.

Krishna P Jonnalagadda (2003 Feb). “Determination of Instantaneous Unit Hydrographs for Small Watersheds of Central Texas” University of Houston.

Kumar A., Bellam, N.K, and A. Sud.(1999), “Performance of an Industrial Source

Complex Model: Predicting Long-term Concentrations in an Urban Area." *Environmental Progress*, Vol. 18., No. 2, pp 93-100.

Kull, D. W., and Feldman, A. D., (1998), "Evolution of Clarks Unit Graph Method to Spatially Distributed Runoff." *J. Hydrologic Engineering*, ASCE 3(1), p. 9-19.

Langbein, W. B. (1947), "Topographic Characteristics of Drainage Basins", 968C. U.S. Geological Survey.

Lars Bengtsson and Janusz Niemczynowicz (1998), "Using the Rational Method for Design in Complex Urban Basins", *Nordic Hydrology*, 29, 73-90.

Laurenson, E.M. (1964). "A Catchment Storage Model for Runoff Routing." *J. Hydrology.* 2, 141-163.

]Laurenson, E.M., and O'Donnell, T. (1969), "Data Error Effects in Unit Hydrograph Derivation." *J. Hyd. Div. Proc. ASCE. 95 (HY6),* pp 1899-1917.

Lazarescu, Ioana, (2003 May) "Correlation of Geometric Properties of Small Watersheds in Central Texas with Observed Instantaneous Unit Hydrograph" University of Houston.

Leinhard, J. H., (1964), "A Statistical Mechanical Prediction of the Dimensionless Unit Hydrograph", *Journal of Geophysical Research*, Vol 69. No. 24., p. 5231-5238.

Lienhard, J. H., and Meyer P. L., (1967), "A Physical Basis for the Generalized Gamma Distribution", *Quarterly of Applied Math*. Vol 25, No. 3. p. 330-334.

Leinhard, J.H. (1972), "Prediction of the Dimensionless Unit Hydrograph." *Nordic Hydrology, 3*, pp 107-109.

Linsley, R. K., M. A. Kohler, and J. L. H. Paulhus (1958), "Hydrology for Engineer", McGraw - Hill Publications., New York.

L.M. Tallaksen (1995), "A review of Baseflow Recession Analysis", *Journal of Hydrology*, 165, 349-370.

Lopez, O. G. (1973), "Response Time in Urban Colorado Basins", Master Thesis. Colorado State University.

Maidment, D. R. (1993), "Developing a Spatially Distributed Unit Hydrograph by Using GIS", *Proceedings of Hydro* HIS93, IAHS Pub. No. 211.

Mawdsley, J. A. and Tagg, A. F. (1981), "Identification of Unit Hydrographs from

Multi-event Analysis," *Journal of Hydrology*, 49, pp 315-327.

Marco Franchini and Michele Pacciani (1991), "Comparative Analysis of Several Conceptual Rainfall-Runoff Models", *Journal of Hydrology*, Vol. 122 (1991) 161-219.

Mays, Larry W. and Coles, Lynn (1980), "Optimization of Unit Hydrograph Determination," *Journal of the Hydraulics Division*, 106(HY1), ASCE, pp 85-97.

Mays, Larry W. and Taur, Cheng-Kang (1982), "Unit Hydrographs via Nonlinear Programming", *Water Resources Research*, 18(4), pp 744-752.

McCuen, Richard H. and Bondelid, Timothy R.(1983), "Estimating Unit Hydrograph Peak Rate Factors", *Journal of the Irrigation and Drainage Division*, 109(2), ASCE, pp 238-249.

McCuen, R. H., S.L. Wong and W.J. Rawls. (1984), "Estimating Urban Time of Concentration." *Journal of Hydraulic Engineering,* 110(7)**,** 887-904.

McCuen, R.H. (1998), "Hydrologic Analysis and Design" (2nd ed.), Prentice Hall, Saddle River, N.J.

Meadows, M. E., and G. E. Blandford. (1983), "Improved Methods and Guidelines for
Modeling Stormwater Runoff from Surface Coal Mined Lands." 147. *Water Resources Research Institute Lexington, Kentucky.*

Meadows, M. E., and E. W. Ramsey. (1991). "South Carolina Regional Synthetic Unit Hydrograph Study: Methodology and Results." *U.S. Geological Survey Reston*,VASeptember.

Mikio Hino and Kazuo Nadaoka (1979), "Mathematical Derivation of Linear and Nonlinear Runoff Kernels", *Water Resources Research*, Vol. 15, No. 4. p918-928.

M. H. Diskin and A. Boneh (1975), "Determination of an Optimal IUH for Linear, Time Invariant Systems from Multi-Storm Records", *Journal of Hydrology*, Vol.24 (1975) 57-76.

M. M. Kshirsagar, Balaji Rajagopalan and Upmanu Lall (1995), "Optimal Parameter Estimation for Muskingum Routing with Ungauged Lateral Inflow", *Journal of Hydrology*, Vol. 169, 25-35.

Mockus, V. (1957), "Use of Storm and Watershed Characteristics in Synthetic Hydrograph Analysis and Application." , *U.S. Department of Agriculture, Soil Conservation Service.*

Morgali, J. R. a. R. K. L. (1965), “Computer Analysis of Overland Flow.”, *Journal of Hydraulics Division.,* (HY3).

Muzik, I. (1996), “Lumped Modeling and GIS in Flood Predictions”, In Singh, V.P. (Ed.) *Geographical Information Systems in Hydrology*, Kulwer Academic Publishers, The Netherlands.

Nash, J. E. (1957), “The form of Instantaneous Unit Hydrograph.”, 3. IASH Publ. No.45.

Nash, J.E. (1958), “The Form of the Instantaneous Unit Hydrograph”. *Intl. Assoc. Sci. Hydrology*, Pub 42, Cont. Rend. 3 114-118.

Nash, J. E., (1959), “Systematic Determination of Unit Hydrograph Parameters”, *Journal of Geophysical Research*, 64(1), pp 111-115.

Nathan, R.J., and T.A. McMahon, (1990), “Evaluation of Automated Base Flow and Recession Analyses.” *Water Resources Research*, Vol. 26. No. 7, pp 1465-1473.

Nauman, E.B., and Buffham B.A. (1983), “Mixing in Continuous Flow Systems”, Wiley Interscience, New York.

National Resources Conservation Service(NRCS), “National Engineering Handbook” http://www.nrcs.usda.gov/technical/ENG/neh.html

Nelder, J.A., and R. Mead. (1965), “A Simplex Method for Function Minimization.” *Computer J.,* 7, pp 308-313.

O’ Calligan, J.F., and Mark, D.M. (1984), “Extraction of Drainage Networks from Digital Elevation Data.” Computer Vision, Graphics, and Image Processing, No. 28, pp. 323-344.

Olcay, Unver and Larry W. Mays (1984), “Optimal Determination of Loss Rate Functions and Unit Hydrographs”, *Water Resources Research*, Vol. 20, No. 2, p 203-214.

Olivera, F. and Maidment, D., (1999), “Geographic Information Systems (GIS)-based Spatially Distributed Model for Runoff Routing”, *Water Resour. Res*. 35(4), p. 1135-1164.

Overton, D. E. (1971), “Estimation of Surface Water Lag Time from the Kinematic Wave Equations.” *Water Resources Bulletin,* 7(3)**,** 428-440.

Overton, D. E., and M. E. Meadows (1976), “Stormwater Modelling.”, Academic Press INC.**,** 358.

P. Buchanan, K. W. Savigny and J. De Vries (1990), “A Method for Modeling Water Tables at Debris Avalanche Headscarps”, *Journal of Hydrology*, Vol 113 (1990) 61-88.

Peter S. Eagleson, Richardo Mejia-R and Frederic March (1966), “Computation of Optimum Realizable Unit Hydrographs”, *Water Resources Research*, Vol. 2, No.4, pp.755-764.

Polubarinova-Kochina, (1962), “Theory of Ground Water Movement” Translated from the Russian by J. M. Roger De Weist, *Princeton University Press, New Jersey*.

Powell, M. J. D. (1964), “An Efficient Method for Finding the Minimum of a Function of Several Variables without Calculating Derivatives.” *Computer J.*, 6, pp 155-162.

Prasad, R. (1970), “Numerical Method of Computing Flow Profiles.”, *Journal of the Hydraulics division,* 96(HY 1)**,** 75-86.

Press, W.H., Flannery, B.P., Teukolsky, S.A., Vetterling, W.T. (1989), “Numerical Recipes – The Art of Scientific Computing”, Cambridge University Press. 818p.

Ragan, R. M., and J. O. Duru. (1972), “ Kinematic Wave Nomograph for Time of Concentration.”, *Journal of the Hydraulics Division,* 98(HY10)**,** 1765-1771.

Ramser, C. E. (1927), “Runoff from Small Agricultural Areas”. *Journal of Agricultural Res.,* 34(9)**,** 797-823.

Rao, A. R., J.W. Delleur and P.B.S. Sarama. (1972), “Conceptual Hydrologic Models for Urbanising Basins.”, *Journal of Hydraulic Division,* 98(HY7)**,** 1205-1220.

Rao, A. R., and J. W. Delleur. (1974), “Instantaneous Unit Hydrograph, Peak Discharges, and Time Lags in Urban Areas.”, *Hydrological Sciences Bulletin,* 19(2)**,** 185-198.

R. A. Wooding (1965), “A Hydraulic Model for The Catchment-Stream Problem. I. Kinematic-Wave Theory”, *Journal of Hydrology*, Vol. 3 (1965) 254-267.

R. A. Wooding (1965), “A Hydraulic Model for The Catchment-Stream Problem. II. Numerical Solutions”, *Journal of Hydrology*, Vol. 3 (1965) 268-282.

Reich, B. M. (1962), “Design Hydrographs for Very Small Watershed from Rainfall.”

CER62BMR41. Dept. of Civil Engineering, Colorado State University Fort Collins, Colorado.

Rodriquez-Iturbe, I., and J. B. Valdes (1979), "The Geomorphologic Structure of Hydrologic Response", *Wat. Resour. Res.,* 15(6), 1409-1420.

Roussel, M. C., Thompson, D. B., Fang, X., Cleveland, T. G., and Garcia, A. C., (2005), "Timing Parameter Estimation for Applicable Texas Watersheds", Texas Department of Transportation Research Report 0-4696- 2.

Saghafian, B. and Julien, P. Y., (1995), "Time to Equilibrium for Spatially Variable Watersheds", *J. of Hydrology*, 172, p. 231-245.

Saghafian, B., Julien, P. Y., and Rajaie, H., (2002), "Runoff Hydrograph Simulation Based on Time Variable Isochrone Technique", *J. of Hydrology*. 261, p. 193-203.

Sauer, V. B., Thomas, W.O. Jr., Stricker, V.A., and Wilson, K.V. (1981), "Magnitude and Frequency of Floods in the United States.", U.S. Geological Survey Reston, VA.

S.Birikundavyi and J.Roussele (1997), "Use of Partial Duration Series for Single-Station and Regional Analysis of Floods", *Journal of Hydrologic Engineering*, Vol. 2, No. 2 April p:68-75.

Schulz, E. F., and O.G. Lopez. (1974), "Determination of Urban Watershed Response Time.", Colorado State University, Fort Collins, CO.

Shamseldin, A. Y., and J. E. Nash (1998), "The Geomorphological Unit Hydrograph - A Critical Review", *Hydrology and Earth Syst. Sci.*, 2(1), 1-8.

Sherman, L. K.(1932), "Stream Flow from Rainfall by Unit-graph Method", *Engineering News-Record*, 108(14), pp: 501-506.

Shih-Min Chiang, Ting-Kuei Tasy, and Stephan J. Nix (2002), "Hydrologic Regionalization of Watersheds. I: Methodology Development", *Journal of Water Resources Planning and Management*, Vol. 128, No. 1 January pp: 3-11.

Shih-Min Chiang, Ting-Kuei Tasy, and Stephan J. Nix (2002), "Hydrologic Regionalization of Watersheds. II: Applications", *Journal of Water Resources Planning and Management*, Vol. 128, No. 1 January pp:12-20.

Singh, S. K. (2000), "Transmuting Synthetic Unit Hydrograph into Gamma Function.", *Journal of Hydrologic engineering,* 5(4)**,** 380-385.

Skaggs, R. W., and R. Khaleel (1982), "Infiltration" in C. T. Haan, ed., *Hydrologic*

Modeling of Small Watersheds, Monograph 5, American Society of Agricultural Engineers, St. Joseph, Mich., pp:4-166.

Snyder, F. F. (1938), "Synthetic Unit Hydrograph.", *Trans. Amer. Geophysical Union,* 19, 447-454.

Snyder, W. M.(1956), "Hydrograph Analysis by the Method of Least Squares", *Proceedings, American Society of Civil Engineers*, 81, pp 793-1—793-25.

Soil Conservation Service (now NRCS) (1972), "National Engineering Handbook", Chapter 4, U.S.D.A., Washington D.C.

S. Shukla, S.Mostaghimi, B. Petrauskas, and M. Al-Smadi (2000), "Multivariate Technique for Base Flow Separation Using Water Quality Data", *Journal of Hydrologic Engineering,* Vol.5 No. 2 p:172-179.

Suhil K. Singh (2000), "Transmuting Synthetic Unit Hydrographs Into Gamma Distribution", *Journal of Hydrologic Engineering*, Vol 5 No. 4 October p: 380-385
Saghafian, B. and P.Y. Julien. 1995. "Time to equilibrium for spatially variable watersheds." J. of Hydrology. 172, pp. 231-245.

S. Yue and M. Hashino (2000), "Unit Hydrographs to Model Quick and Slow Runoff Components of Stream Flow", *Journal of Hydrology*, Vol. 227(2000) 195-206.

Taylor, A. B., and H.E. Schwarz. (1952), "Unit Hydrograph Lag and Peak Flow Related to Basin Characteristics.", *Transactions, American geophysical Union*.

U.S. Department of Agriculture (1973), "Linear Theory of Hydrologic Systems", *Technical Bulletin No.1468, Agricultural Research Service*, Washington D.C.

Unver, Olcay and Mays, Larry W.(1984), "Optimal Determination of Loss-rate Function and Unit Hydrographs", *Water Resources Research*, 20(2), pp 203-214.

Usul, N., Tezcan, B. (1995), "Determining Synthetic Unit Hydrographs and Parameters for Four Turkish Basins", *Journal of Soil and Water Conservation*, Vol. 50, pp.170-173.

Viessman, W., and G.L. Lewis (2003), "Introduction to Hydrology.", 5 ed., 1. 1 vols. Pearson Education**,** 612.

Vijay K. Gupta, Ed Waymire and C. T. Wang (1980), "A Representation of an Instantaneous Unit Hydrograph From Geomorphology", *Water Resources Research*, vol. 16, No. 5, p. 855-862

Wang, K.H., T.G. Cleveland, J.R. Rogers, and X. Ren, (1991), "A Three Dimensional

Hydrodynamic Model of the Confluence of White Oak and Buffalo Bayou in Houston, Texas - Theory, Numerical Implementation, and Results.", Final report to Harris County Flood Control District, UH-CEE-91-7, Vol 1., 105p.; Vol 2., 287 p.

Wang, KH, Cleveland, T.G., Fitzgerald, S. , and X. Ren, (1996)., "Hydrodynamic Flow Model at the Confluence of Two Streams." *American Society of Civil Engineers*, *Journal of Engineering Mechanics,* Vol. 122, No. 10, pp 994-1002.

Walton, W. C., and T. A. Prickett. (1963), "Hydrogeologic Electric Analog Computers.", *Journals of Hydraulics Division,* 4567.

Williams, J. R., and R. W. J. Hann. (1973), "HYMO: Problem Oriented Computer Language for Building Hydrologic Models.", *Water Resources Res.,* 8(1)**,** 79-86.

Wilson, W. A. (1972). "Unit Hydrograph Response Times." Master thesis. Colorado State University.

Wong, T. S. W. (1996), "Time of Concentration and Peak Discharge Formulas for Planes in Series.", *Journal of Irrigation and Drainage Engineering,* 122(4)**,** 256-258.

Wu, I.-P. (1963), "Design Hydrographs for Small Watersheds in Indiana.", *Journal of the Hydraulics Division,* 89(HY6)**,** 36-65.

Zhao, Bing and Tung, Yeou-Koung (1994), "Determination of Optimal Unit Hydrographs by Linear Programming", *Water Resources Management*, 8, pp 101-119.

Zoch, R.T. (1934), "On the Relation Between Rainfall and Stream Flow.", *U.S. Dept. Commerce, Monthly Weather Review, Part I, v. 62*, pp 315-322.

APPENDICES

Appendix 1, Table 1. U.S. Geological Survey Stream-Gaging Stations Studied.

[STATION_ID is USGS Station identifier, STATION NAME is the USGS common name for the station, LATITUDE in DD()MM'SS" North; LONGITUDE in DD()MM"SS" West. Adapted from Asquith and others (2004), and Liscum (1998)].

STATION_ID	STATION NAME	LATITUDE	LONGITUDE
08042650	North Creek sub. 28A near Jermyn, Tex.	33()14'52"	98()19'19"
08042700	North Creek near Jacksboro, Tex.	33()16'57"	98()17'53"
08048520	Sycamore Creek at IH 35W, Fort Worth, Tex.	32()39'55"	97()19'16"
08048530	Sycamore Creek Trib. above Seminary South Shopping Center, Fort Worth, Tex.	32()41'08"	97()19'44"
08048540	Sycamore Creek tributary at IH 35W, Fort Worth, Tex.	32()41'18"	97()19'11"
08048550	Dry Branch at Blandin Street, Fort Worth, Tex.	32()47'19"	97()18'22"
08048600	Dry Branch at Fain Street, Fort Worth, Tex.	32()46'34"	97()17'18"
08048820	Little Fossil Creek at IH 820, Fort Worth, Tex.	32()50'22"	97()19'22"
08048850	Little Fossil Creek at Mesquite Street, Fort Worth, Tex.	32()48'33"	97()17'28"
08050200	Elm Fork Trinity River sub. 6 near Muenster, Tex.	33()37'13"	97()24'15"
08052630	Little Elm Creek sub. 10 near Gunter, Tex.	33()24'33"	96()48'41"
08052700	Little Elm Creek near Aubrey, Tex.	33()17'00"	96()53'33"
08055580	Joes Creek at Royal Lane, Dallas, Tex.	32()53'43"	96()41'36"
08055600	Joes Creek at Dallas, Tex.	32()51'41"	96()52'27"
08055700	Bachman Branch at Dallas, Tex.	32()51'26"	96()50'12"
08056500	Turtle Creek at Dallas, Tex.	32()48'26"	96()48'08"
08057020	Coombs Creek at Sylvan Ave, Dallas, Tex.	32()46'01"	96()50'07"
08057050	Cedar Creek at Bonnieview Road, Dallas, Tex.	32()44'50"	96()47'44"
08057120	McKamey Creek at Preston Road, Dallas, Tex.	32()57'58"	96()48'11"
08057130	Rush Branch at Arapaho Road, Dallas, Tex.	32()57'45"	96()47'44"
08057140	Cottonwood Creek at Forest Lane, Dallas, Tex.	32()54'33"	96()45'54"
08057160	Floyd Branch at Forest Lane, Dallas, Tex.	32()54'33"	96()45'34"
08057320	Ash Creek at Highland Road, Dallas, Tex.	32()48'18"	96()43'04"
08057415	Elam Creek at Seco Boulevard, Dallas, Tex.	32()44'14"	96()41'36"
08057418	Fivemile Creek at Kiest Boulevard, Dallas, Tex.	32()42'19"	96()51'32"
08057420	Fivemile Creek at US Highway 77W, Dallas, Tex.	32()41'15"	96()49'22"
08057425	Woody Branch at IH 625, Dallas, Tex.	32()40'58"	96()49'22"

STATION_ID	STATION NAME	LATITUDE	LONGITUDE
08057435	Newton Creek at IH 635, Dallas, Tex.	32()39'19"	96()44'41"
08057440	Whites Branch at IH 625, Dallas, Tex.	32()29'26"	96()44'25"
08057445	Prarie Creek at US Highway 175, Dallas, Tex.	32()42'17"	96()40'11"
08057500	Honey Creek sub. 11 near McKinney, Tex.	33()18'12"	96()41'22"
08058000	Honey Creek sub.12 near McKinney, Tex.	33()18'20"	96()40'12"
08061620	Duck Creek at Buckingham Road, Garland, Tex.	32()55'53"	96()39'55"
08061920	South Mesquite Creek at SH 352, Mesquite, Tex.	32()46'09"	96()37'18"
08061950	South Mesquite Creek at Mercury Road, Mesquite, Tex.	32()43'32"	96()34'12"
08063200	Pin Oak Creek near Hubbard, Tex.	31()48'01"	96()43'02"
08068400	Panther Branch near Conroe, Tex.	30()11'34"	95()29'09"
08068438	Swale No.8 at Woodlands, Tex.	30()08'38"	95()28'09"
08068440	Lake Harrison at drop inlet at Woodlands, Tex.	30()08'24"	95()28'33"
08068450	Panther Branch near Spring, Tex.	30()08'04"	95()28'38"
08073630	Bettina Street Ditch at Houston, Tex.	29()46'32"	95()32'23"
08073750	Stoney Brook Street Ditch at Houston, Tex.	29()44'05"	95()30'22"
08073800	Bering Ditch at Woodway Drive, Houston, Tex.	29()45'22"	95()29'44"
08074100	Cole Creek at Guhn Rd. at Houston, Tex.	29()51'24"	95()30'55"
08074145	Bingle Road Storm Sewer at Houston, Tex.	29()51'31"	95()29'09"
08074150	Cole Creek at Deihl Road, Houston, Tex.	29()51'04"	95()29'16"
08074200	Brickhouse Gully at Clarblak St., Houston, Tex.	29()49'53"	95()31'42"
08074250	Brickhouse Gully at Costa Rica St., Houston,Tex.	29()49'40"	95()28'09"
08074400	Lazybrook Street Storm Sewer at Houston, Tex.	29()48'15"	95()26'04"
08074500	Whiteoak Bayou at Houston, Tex.	29()46'30"	95()23'49"
08074540	Little Whiteoak Bayou at Trimble St., Houston, Tex.	29()47'33"	95()22'06"
08074750	Brays Bayou at Addicks-Clodine Rd., Houston,Tex.	29()43'11"	95()39'37"
08074760	Brays Bayou at Alief Road, Alief, Tex.	29()42'39"	95()35'13"
08074780	Keegans Bayou at Keegan Road near Houston, Tex.	29()39'55"	95()35'42"
08074800	Keegans Bayou at Roark Road near Houston, Tex.	29()39'23"	95()33'43"
08074810	Brays Bayou at Gessner Drive, Houston, Tex .	29()40'21"	95()31'41"
08074850	Bintliff Ditch at Bissonnet at Houston, Tex.	29()41'16"	95()30'20"

STATION_ID	STATION NAME	LATITUDE	LONGITUDE
08074900	Willow Waterhole Bayou at Landsdowne St., Houston, Tex.	29()39'01"	95()29'11"
08074910	Hummingbird Street Ditch at Houston, Tex.	29()39'44"	95()29'11"
08075000	Brays Bayou at Houston, Tex.	29()41'49"	95()24'43"
08075300	Sims Bayou at Carlsbad Street Houston, Tex.	29()37'33"	95()29'56"
08075400	Sims Bayou at Hiram Clarke Street, Houston,Tex.	29()37'07"	95()26'45"
08075470	Sims Bayou at MLK Blvd., Houston, Tex.	29()38'42"	95()20'13"
08075500	Sims Bayou at Houston, Tex Yes	29()40'27"	95()17'21"
08075550	Berry Bayou at Gilpin Street at Houston, Tex.	29()38'32"	95()13'22"
08075600	Berry Bayou Trib. at Globe St., Houston, Tex.	29()39'00"	95()14'18"
08075650	Berry Bayou at Forest Oaks Street, Houston, Tex.	29()40'35"	95()14'37"
08075700	Berry Creek at Galveston Rd. at Houston, Tex.	29()21'05"	95()15'11"
08075730	Vince Bayou at Pasadena, Tex.	29()41'40"	95()12'58"
08075750	Hunting Bayou Trib. at Cavalcade St., Houston, Tex.	29()48'00"	95()20'02"
08075760	Hunting Bayou at Falls St. at Houston, Tex.	29()48'22"	95()19'50"
08075770	Hunting Bayou at IH-610, Houston, Tex.	29()47'35"	95()16'04"
08075780	Greens Bayou at Cutten Road near Houston, Tex.	29()56'56"	95()31'10"
08075900	Greens Bayou at U.S. Hwy 75 near Houston, Tex.	29()57'22"	95()24'57"
08076000	Greens Bayou near Houston, Tex.	29()55'05"	95()18'24"
08076200	Halls Bayou at Deertrail St. at Houston, Tex.	29()54'07"	95()25'21"
08076500	Halls Bayou at Houston, Tex.	29()51'42"	95()20'05"
08076700	Greens Bayou at Ley Road, Houston, Tex.	29()50'13"	95()13'59"
08077100	Clear Creek Trib. at Hall Rd., Houston, Tex.	29()36'09"	95()16'41"
08094000	Green Creek sub. 1 near Dublin, Tex.	32()10'00"	98()20'30"
08096800	Cow Bayou sub. 4 near Bruceville, Tex.	31()19'59"	97()16'02"
08098300	Little Pond Creek near Burlington, Tex.	31()01'35"	96()59'17"
08108200	North Elm Creek near Cameron, Tex.	30()55'52"	97()01'13"
08111025	Burton Creek at Villa Maria Road, Bryan, Texas	30()38'48"	96()20'57"
08111050	Hudson Creek near Bryan, Texas	30()39'38"	96()17'59"
08136900	Mukewater Creek sub. 10A near Trickham, Tex.	31()39'01"	99()13'30"
08137000	Mukewater Creek sub. 9 near Trickham, Tex.	31()41'40"	99()12'18"
08137500	Mukewater Creek at Trickham, Tex.	31()35'24"	99()13'36"
08139000	Deep Creek sub. 3 near Placid,Tex.	31()17'25"	99()08'13"
08140000	Deep Creek sub. 8 near Mercury, Tex.	31()24'09"	99()08'13"

STATION_ID	STATION NAME	LATITUDE	LONGITUDE
08154700	Bull Creek at Loop 360, Austin, Tex.	30()22'19"	97()47'04"
08155200	Barton Creek at SH 71, Oak Hill, Tex.	30()17'46"	97()55'31"
08155300	Barton Creek at Loop 360, Austin, Tex.	30()14'40"	97()48'07"
08155550	West Bouldin Creek at Riverside Drive, Austin, Tex.	30()15'49"	97()45'17"
08156650	Shoal Creek at Steck Avenue, Austin, Tex.	30()21'55"	97()44'11"
08156700	Shoal Creek at Northwest Park, Austin, Tex.	30()20'50"	97()44'41"
08156750	Shoal Creek at White Rock Drive, Austin, Tex.	30()20'21"	97()44'50"
08156800	Shoal Creek at 12th Street, Austin, Tex.	30()16'35"	97()45'00"
08157000	Waller Creek at 38th Street, Austin, Tex.	30()17'49"	97()43'36"
08157500	Waller Creek at 23rd Street, Austin, Tex.	30()17'08"	97()44'01"
08158050	Boggy Creek at US 183, Austin, Tex.	30()15'47"	97()40'20"
08158100	Walnut Creek at FM 1325, Austin, Tex.	30()24'35"	97()42'41"
08158200	Walnut Creek at Dessau Road, Austin, Tex.	30()22'30"	97()39'37"
08158380	Little Walnut Creek at Georgian Drive Austin, Tex.	30()21'15"	97()41'52"
08158400	Little Walnut Creek at IH 35, Austin, Tex.	30()20'57"	97()41'34"
08158500	Little Walnut Creek at Manor Road, Austin, Tex.	30()18'34"	97()40'04"
08158600	Walnut Creek at Webberville Road, Austin, Tex.	30()16'59"	97()39'17"
08158700	Onion Creek near Driftwood, Tex.	30()04'59"	97()00'29"
08158800	Onion Creek at Buda, Tex.	30()05'09"	97()50'52"
08158810	Bear Creek below FM 1826, Driftwood, Tex.	30()09'19"	97()56'23"
08158820	Bear Creek at FM 1626, Manchaca, Tex.	30()08'25"	97()50'50"
08158825	Little Bear Creek at FM 1626, Manchaca, Tex.	30()07'31"	97()51'43"
08158840	Slaughter Creek at FM 1826, Austin, Tex.	30()12'32"	97()54'11"
08158860	Slaughter Creek at FM 2304, Austin, Tex.	30()09'43"	97()49'55"
08158880	Boggy Creek (south) at Circle S Road, Austin, Tex.	30()10'50"	97()46'55"
08158920	Williamson Creek at Oak Hill, Tex.	30()14'06"	97()51'36"
08158930	Williamson Creek at Manchaca Road, Austin, Tex.	30()13'16"	97()47'36"
08158970	Williamson Creek at Jimmy Clay Road, Austin, Tex.	30()11'21"	97()43'56"
08159150	Wilbarger Creek near Pflugerville, Tex.	30()27'16"	97()36'02"
08177600	Olmos Creek tributary at FM 1535, Shavano Park, Tex.	29()34'35"	98()32'45"
08177700	Olmos Creek at Dresden Drive, San Antonio, Tex.	29()29'56"	98()30'36"

STATION_ID	STATION NAME	LATITUDE	LONGITUDE
08178300	Alazan Creek at St. Cloud Street, San Antonio, Tex.	29()27'29"	98()32'59"
08178555	Harlendale Creek at West Harding Street, San Antonio, Tex.	29()21'05"	98()29'32"
08178600	Panther Springs Creek at FM 2696 near San Antonio, Tex.	29()37'31"	98()31'06"
08178620	Lorence Creek at Thousand Oaks Boulevard, San Antonio, Tex.	29()35'24"	98()27'47"
08178640	West Elm Creek at San Antonio, Tex.	29()37'23"	98()26'29"
08178645	East Elm Creek at San Antonio, Tex.	29()37'04"	98()25'41"
08178690	Salado Creek tributary at Bitters Road, San Antonio, Tex.	29()31'36"	98()26'25"
08178736	Salado Creek tributary at Bee Street, San Antonio, Tex.	29()26'37"	98()27'13"
08181000	Leon Creek tributary at FM 1604, San Antonio, Tex.	29()35'14"	98()37'40"
08181400	Helotes Creek at Helotes, Tex.	29()34'42"	98()41'29"
08181450	Leon Creek tributary at Kelly Air Force Base, Tex.	29()23'12"	98()36'00"
08182400	Calaveras Creek sub. 6 near Elmendorf, Tex.	29()22'49"	98()17'33"
08187000	Escondido Creek sub. 1 near Kenedy, Tex.	28()46'41"	97()53'41"
08187900	Escondido Creek sub. 11 near Kenedy, Tex.	28()53'39"	97()53'41"

Appendix 1, Table 2. Selected Physical Characteristics for Study Watersheds.

[TDA, Total drainage area in square miles; BP, Basin perimeter in miles; MCL, main channel length in miles; BR; basin relief in feet; MCS, main channel slope in feet per mile; MCS2, alternate main channel slope in feet per mile; TDA, BP, MCL, BR, MCS are determined as in Brown and others (2000); MCS2 is determined as in Asquith and Slade (1997)].

Station no.	Latitude	Longitude	TDA	BP	MCL	BR	MCS	MCS2
08155200	30()17'46"	97()55'31"	89.6	67.7	28.5	752.2	19.1	25.6
08155300	30()14'40"	97()48'07"	116.6	91.2	45.1	983.0	15.3	21.3
08158810	30()09'19"	97()56'23"	12.3	19.7	6.3	374.1	49.1	58.5
08158820	30()08'25"	97()50'50"	24.5	37.1	14.8	590.6	28.5	39.4
08158825	30()07'31"	97()51'43"	21.0	29.1	12.5	443.6	27.4	35.1
08158050	30()15'47"	97()40'20"	12.6	20.8	7.4	309.8	39.3	41.8
08158880	30()10'50"	97()46'55"	3.6	12.5	4.4	265.7	43.2	59.5
08154700	30()22'19"	97()47'04"	22.8	31.6	10.0	568.3	36.3	56.5
08158380	30()21'15"	97()41'52"	5.3	13.0	4.0	155.8	32.2	36.9
08158700	30()04'59"	97()00'29"	123.7	78.8	33.3	794.6	16.3	23.8
08158800	30()05'09"	97()50'52"	167.3	106.1	48.9	1013.7	13.9	20.7
08156650	30()21'55"	97()44'11"	2.7	10.2	3.0	183.2	48.0	60.7
08156700	30()20'50"	97()44'41"	6.3	15.2	4.5	242.0	34.0	48.8
08156750	30()20'21"	97()44'50"	6.8	16.6	5.1	257.9	30.2	46.2
08156800	30()16'35"	97()45'00"	12.7	29.3	10.6	438.7	30.5	39.5
08158840	30()12'32"	97()54'11"	8.8	17.9	5.0	313.8	48.7	62.9
08158860	30()09'43"	97()49'55"	23.2	34.2	12.8	534.2	32.0	41.6
08157000	30()17'49"	97()43'36"	2.2	10.1	4.1	212.6	47.2	51.7
08157500	30()17'08"	97()44'01"	4.2	14.8	5.2	256.9	45.6	49.8
08158100	30()24'35"	97()42'41"	12.7	23.9	5.7	292.9	47.1	48.2
08158200	30()22'30"	97()39'37"	26.4	32.9	10.9	401.7	30.1	35.0
08158400	30()20'57"	97()41'34"	5.7	14.2	4.5	167.1	32.2	35.5
08158500	30()18'34"	97()40'04"	12.1	22.2	8.6	315.1	33.8	35.7
08158600	30()16'59"	97()39'17"	53.6	53.7	19.5	528.9	20.5	26.1
08155550	30()15'49"	97()45'17"	2.7	10.2	3.7	243.2	69.9	66.4
08159150	30()27'16"	97()36'02"	4.5	12.1	3.7	169.9	42.4	43.1
08158920	30()14'06"	97()51'36"	6.3	14.8	5.0	315.4	51.3	61.9
08158930	30()13'16"	97()47'36"	18.7	30.3	10.4	492.8	37.5	46.7
08158970	30()11'21"	97()43'56"	27.4	42.0	17.6	607.4	27.1	34.1
08057320	32()48'18"	96()43'04"	7.2	16.6	5.4	174.9	34.4	29.5
08055700	32()51'26"	96()50'12"	11.0	21.5	7.8	213.2	27.4	26.7
08057050	32()44'50"	96()47'44"	9.5	18.4	6.2	258.5	38.3	41.2
08057020	32()46'01"	96()50'07"	4.5	15.1	5.1	261.8	49.4	51.3
08057140	32()54'33"	96()45'54"	8.6	20.1	7.5	231.0	30.0	30.4
08061620	32()55'53"	96()39'55"	7.7	17.0	5.5	122.7	18.3	20.5
08057415	32()44'14"	96()41'36"	1.0	5.7	1.9	71.8	31.4	33.4
08057418	32()42'19"	96()51'32"	8.1	18.5	5.6	235.8	38.0	41.6

Station no.	Latitude	Longitude	TDA	BP	MCL	BR	MCS	MCS2
08057420	32()41'15"	96()49'22"	14.4	24.3	8.3	285.1	30.6	34.1
08057160	32()54'33"	96()45'34"	4.6	15.6	5.3	180.4	32.6	33.7
08055580	32()53'43"	96()41'36"	1.9	7.9	3.0	115.0	38.3	38.0
08055600	32()51'41"	96()52'27"	5.7	17.5	6.7	215.1	31.1	31.7
08057435	32()39'19"	96()44'41"	5.9	13.6	4.1	208.4	46.0	45.8
08057445	32()42'17"	96()40'11"	8.9	21.9	8.4	170.3	18.6	19.1
08057130	32()57'45"	96()47'44"	1.3	7.3	2.6	126.6	41.2	47.9
08061920	32()46'09"	96()37'18"	12.9	24.6	7.6	156.5	18.5	20.5
08061950	32()43'32"	96()34'12"	23.3	37.0	12.6	205.0	13.9	16.2
08057120	32()57'58"	96()48'11"	6.6	15.4	5.2	206.0	34.3	39.1
08056500	32()48'26"	96()48'08"	6.4	17.2	6.4	218.0	32.0	33.5
08057440	32()29'26"	96()44'25"	2.6	9.7	3.5	159.3	45.3	44.1
08057425	32()40'58"	96()49'22"	10.3	19.2	6.2	270.2	37.4	41.6
08048550	32()47'19"	97()18'22"	1.1	6.6	2.0	49.6	23.6	23.8
08048600	32()47'19"	97()18'22"	2.6	11.4	3.8	97.7	23.7	25.0
08048820	32()50'22"	97()19'22"	5.7	16.9	6.0	190.9	30.5	31.5
08048850	32()48'33"	97()17'28"	12.9	26.9	9.4	251.4	25.5	26.7
08048520	32()39'55"	97()19'16"	17.6	24.3	7.5	219.6	25.6	26.8
08048530	32()41'08"	97()19'44"	1.0	5.0	1.7	106.3	65.9	62.4
08048540	32()41'18"	97()19'11"	1.3	6.3	2.4	140.5	49.9	59.1
08178300	29()27'29"	98()32'59"	3.3	10.6	3.6	316.3	81.1	87.9
08181000	29()35'14"	98()37'40"	5.5	14.5	5.4	463.2	52.3	82.8
08181400	29()34'42"	98()41'29"	14.9	31.2	9.8	691.4	48.1	64.1
08181450	29()23'12"	98()36'00"	1.2	8.1	3.1	53.1	16.6	16.9
08177600	29()34'35"	98()32'45"	0.3	3.6	1.3	101.5	69.7	75.9
08177700	29()29'56"	98()30'36"	20.8	30.7	11.0	410.3	25.4	34.8
08178555	29()21'05"	98()29'32"	1.9	10.4	4.1	51.9	13.3	12.8
08178600	29()37'31"	98()31'06"	9.6	21.4	7.1	489.5	43.2	66.2
08178620	29()35'24"	98()27'47"	4.1	11.3	3.6	227.9	51.9	63.2
08178640	29()37'23"	98()26'29"	2.5	9.3	3.0	328.2	80.6	103.5
08178645	29()37'04"	98()25'41"	2.5	10.6	4.0	340.2	58.4	85.9
08178690	29()31'36"	98()26'25"	0.4	4.3	1.2	46.1	18.7	21.3
08178736	29()26'37"	98()27'13"	0.7	5.2	1.7	82.5	46.3	49.7
08096800	31()19'59"	97()16'02"	5.1	14.1	4.5	265.2	52.5	59.0
08094000	32()10'00"	98()20'30"	2.4	9.9	3.4	158.7	45.8	46.0
08098300	31()01'35"	96()59'17"	23.0	40.8	13.7	191.6	10.3	13.9
08108200	30()55'52"	97()01'13"	46.4	60.7	20.0	274.1	11.0	13.3
08139000	31()17'25"	99()08'13"	3.1	11.0	3.4	269.3	83.6	80.1
08140000	31()24'09"	99()08'13"	7.3	18.8	5.9	319.7	31.4	48.9
08136900	31()39'01"	99()13'30"	21.7	37.5	12.4	502.7	22.4	40.4
08137000	31()41'40"	99()12'18"	4.1	13.8	4.4	121.7	18.3	25.0
08137500	31()35'24"	99()13'36"	69.2	61.0	19.4	568.5	15.7	29.3
08182400	29()22'49"	98()17'33"	7.2	17.0	4.9	146.5	33.4	30.2
08187000	28()46'41"	97()53'41"	3.1	9.9	2.8	143.9	48.1	51.4
08187900	28()53'39"	97()53'41"	8.8	16.5	4.9	145.2	21.7	27.7

Station no.	Latitude	Longitude	TDA	BP	MCL	BR	MCS	MCS2
08050200	33()37'13"	97()24'15"	0.9	6.9	2.6	149.0	58.9	56.4
08057500	33()18'12"	96()41'22"	2.1	8.3	2.1	120.6	54.7	56.0
08058000	33()18'20"	96()40'12"	1.2	6.1	2.1	113.3	52.7	54.1
08052630	33()24'33"	96()48'41"	2.1	9.3	3.3	114.0	34.7	34.3
08052700	33()17'00"	96()53'33"	73.1	66.9	23.2	297.5	8.7	11.6
08042650	33()14'52"	98()19'19"	6.6	15.0	4.6	338.3	48.2	72.7
08042700	33()16'57"	98()17'53"	24.0	36.3	11.6	416.6	26.5	31.8
08063200	31()48'01"	96()43'02"	18.2	27.3	8.7	192.6	15.8	21.2

Appendix 1, Table 3. Selected Soil and Land-Use-Related Characteristics for Central Texas (Houston omitted) Study Watersheds.

[DEV is development factor (binary variable 0=undeveloped, 1=developed); IMP is percent impervious cover; S_TEX is surface soil texture; CN is NRCS curve number by standard look-up tables; D_TEX is descriptive soil texture; PERM is NRCS reported permeability for given soil texture; BSC is soil horizon code; ROCK is rock cover factor (binary variable 0= no rock cover, 1=rock cover). Values are obtained from NRCS (2006) and USGS EROS (2006)].

STATION_ID	DEV	IMP	S_TEX	CN	D_TEX	PERM	BSC	ROCK
8042650	0	0	ST-FSL	63.4	Sandy Loam	0.00347	B	0
8042700	0	0	ST-FSL	62.5	Sandy Loam	0.00347	B	0
8048520	1	26	C	82.3	Clay	0.000128	C	0
8048530	1	58	C	86.7	Clay	0.000128	C	0
8048540	1	71	C	88	Clay	0.000128	C	0
8048550	1	61	FSL	91.2	Sandy Loam	0.00347	B	0
8048600	1	58	FSL	84.3	Sandy Loam	0.00347	B	0
8048820	1	16	C	83.4	Clay	0.000128	C	0
8048850	1	16	C	83	Clay	0.000128	C	0
8050200	0	0	CL	79.6	Clay Loam	0.000245	C	0
8052630	0	0	FSL	85.4	Sandy Loam	0.00347	B	0
8052700	0	0	SICL	84.1	Silty Clay Loam	0.00017	S	0
8055580	1	74	SIC	85.2	Silty Clay	0.000103	S	0
8055600	1	63	C	86.1	Clay	0.000128	C	0
8055700	1	56	C	85.5	Clay	0.000128	C	0
8056500	1	65	FSL	85.8	Sandy Loam	0.00347	B	0
8057020	1	62	SIC	85.5	Silty Clay	0.000103	S	0
8057050	1	63	SIC	85.7	Silty Clay	0.000103	S	0
8057120	0	0	SIC	80.2	Silty Clay	0.000103	S	0
8057130	1	66	SIC	82.9	Silty Clay	0.000103	S	0
8057140	1	62	SICL	86.8	Silty Clay Loam	0.00017	S	0
8057160	1	62	SIC	90.3	Silty Clay	0.000103	S	0
8057320	1	63	C	85.7	Clay	0.000128	C	0
8057415	1	65	C	87.8	Clay	0.000128	C	0
8057418	1	34	C	79.1	Clay	0.000128	C	0
8057420	1	40	C	81	Clay	0.000128	C	0
8057425	1	40	SIC	82.9	Silty Clay	0.000103	S	0
8057435	1	11	SIC	81.1	Silty Clay	0.000103	S	0
8057440	1	1	C	79.1	Clay	0.000128	C	0
8057445	1	49	FSL	86.5	Sandy Loam	0.00347	B	0
8057500	0	0	SIC	78.2	Silty Clay	0.000103	S	0
8058000	0	0	SIC	80.1	Silty Clay	0.000103	S	0
8061620	1	67	SIC	85	Silty Clay	0.000103	S	0

STATION_ID	DEV	IMP	S_TEX	CN	D_TEX	PERM	BSC	ROCK
8061920	1	49	C	86	Clay	0.000128	C	0
8061950	1	39	C	85.3	Clay	0.000128	C	0
8063200	0	0	C	79.4	Clay	0.000128	C	0
8094000	0	0	FSL	78.4	Sandy Loam	0.00347	B	0
8096800	0	0	SIC	80	Silty Clay	0.000103	S	0
8098300	0	0	C	80.5	Clay	0.000128	C	0
8108200	0	0	C	79.9	Clay	0.000128	C	0
8111025	1	26	FSL	70	Sandy Loam	0.00347	B	0
8111050	0	0	FSL	70	Sandy Loam	0.00347	B	0
8136900	0	0	C	75.8	Clay	0.000128	C	0
8137000	0	0	FSL	74.5	Sandy Loam	0.00347	B	0
8137500	0	0	C	76.5	Clay	0.000128	C	0
8139000	0	0	FSL	74.6	Sandy Loam	0.00347	B	0
8140000	0	0	FSL	74.4	Sandy Loam	0.00347	B	0
8154700	0	18	CL	68.9	Clay Loam	0.000245	C	1
8155200	0	2	CL	70.7	Clay Loam	0.000245	C	1
8155300	0	4	CL	69.8	Clay Loam	0.000245	C	1
8155550	1	67	SIL	87.3	Silt Loam	0.00072	S	1
8156650	1	56	SIC	83.6	Silty Clay	0.000103	S	1
8156700	1	64	SIC	86.6	Silty Clay	0.000103	S	1
8156750	1	64	SIC	86.8	Silty Clay	0.000103	S	1
8156800	1	66	SIC	87	Silty Clay	0.000103	S	1
8157000	1	70	SIC	88.3	Silty Clay	0.000103	S	1
8157500	1	71	SIC	89.1	Silty Clay	0.000103	S	1
8158050	1	53	SIL	83.9	Silt Loam	0.00072	S	1
8158100	0	0	SIC	72.6	Silty Clay	0.000103	S	1
8158200	0	0	SIC	75.6	Silty Clay	0.000103	S	1
8158380	1	73	SIC	88.9	Silty Clay	0.000103	S	1
8158400	1	73	SIC	85.6	Silty Clay	0.000103	S	1
8158500	1	66	CL	76.7	Clay Loam	0.000245	C	1
8158600	1	34	CL	74.5	Clay Loam	0.000245	C	1
8158700	0	0	STX-C	73.3	Clay	0.000128	C	1
8158800	0	0	STX-C	69.8	Clay	0.000128	C	1
8158810	0	0	CL	67.9	Clay Loam	0.000245	C	1
8158820	0	0	STX-C	67.2	Clay	0.000128	C	1
8158825	0	0	STX-C	69.8	Clay	0.000128	C	1
8158840	0	11	CL	68	Clay Loam	0.000245	C	1
8158860	0	0	SIC	79.4	Silty Clay	0.000103	S	1
8158880	0	0	SIC	79.4	Silty Clay	0.000103	S	1
8158920	1	23	CL	77.5	Clay Loam	0.000245	C	1
8158930	1	27	SIC	75.2	Silty Clay	0.000103	S	1

STATION_ID	DEV	IMP	S_TEX	CN	D_TEX	PERM	BSC	ROCK
8158970	1	0	C	77.7	Clay	0.000128	C	1
8159150	0	35	SIC	78.8	Silty Clay	0.000103	S	1
8177600	1	32	STX-C	84.8	Clay	0.000128	C	1
8178300	1	68	C	85.7	Clay	0.000128	C	1
8178555	1	65	C	84.2	Clay	0.000128	C	1
8178600	0	1	STX-C	79.7	Clay	0.000128	C	1
8178620	1	28	STX-C	60	Clay	0.000128	C	1
8178640	0	16	STX-C	78.4	Clay	0.000128	C	1
8178645	0	0	STX-C	78.2	Clay	0.000128	C	1
8178690	1	72	C	84.4	Clay	0.000128	C	1
8178736	1	0	C	92.3	Clay	0.000128	C	1
8181000	0	3	STX-C	79.2	Clay	0.000128	C	1
8181400	0	3	CBV-C	79.8	Clay	0.000128	C	1
8181450	1	26	CL	87.3	Clay Loam	0.000245	C	1
8182400	0	0	FSL	80	Sandy Loam	0.00347	B	1
8187000	0	0	SCL	83.8	Sandy Clay Loam	0.00063	B	1
8187900	0	0	SCL	73.3	Sandy Clay Loam	0.00063	B	1